TAMPEREEN TEKNILLINEN YLIOPISTO
TAMPERE UNIVERSITY OF TECHNOLOGY

Tiiti Kellomäki

Effects of the Human Body on Single-Layer Wearable Antennas

Julkaisu 1025 • Publication 1025

Tampere 2012

Tampereen teknillinen yliopisto. Julkaisu 1025
Tampere University of Technology. Publication 1025

Tiiti Kellomäki

Effects of the Human Body on Single-Layer Wearable Antennas

Thesis for the degree of Doctor of Science in Technology to be presented with due permission for public examination and criticism in Tietotalo Building, Auditorium TB109, at Tampere University of Technology, on the 23rd of March 2012, at 12 noon.

Tampereen teknillinen yliopisto - Tampere University of Technology
Tampere 2012

ISBN 978-952-15-2778-4 (printed)
ISBN 978-952-15-2779-1 (PDF)
ISSN 1459-2045

Suomen Yliopistopaino Oy
UNIPRINT TTY
Tampere 2012

Abstract

The effect of the human body on wearable off-body communication antennas is studied in the frequency range from 100 MHz to 2.5 GHz. Special emphasis is on single-layer structures, with metallisation in one layer only. In particular, the effect of the antenna–body-separation distance is studied extensively. The results are based on measurements of fabricated antennas worn by human subjects, as well as measurement and simulation results available in the literature.

A transition region is found between 200 and 500 MHz. Below this region, the posture and size of the human body are the key parameters to determine the resonant frequency of the antenna. Because the body is thin compared to the penetration depth, the radiation pattern of a body-worn antenna can be omnidirectional since the body does not shadow the backwards radiation.

Above the transition region, the body size and posture and the placement of the antenna on the body do not affect the input impedance or the resonant frequency, but the key parameter to determine the performance is the antenna–body-separation. The radiation pattern always includes a deep null because the radiation cannot penetrate the body.

To ease the comparison of different wearable antenna structures, new figures of merit are proposed: Detuning percentage gives the relative difference of the centre frequencies between the body-worn and the free-space case. Usable bandwidth describes the frequency band that fulfills certain specifications in all use conditions. Crossover distance indicates the distance where the forward gain on-body equals the free-space gain–a small crossover distance indicates that the antenna is well suited for body-worn use.

As a rule of thumb, the user should be kept at a minimum distance of wavelength/(2π) from a wearable single-layer antenna. At this distance, the input impedance and forward gain equal their free-space values, and the body-worn efficiency is between 60% and 80%. The reflection from the body can be utilised to increase the forward gain especially above 2 GHz. Single-layer topologies with quickly decaying near-fields should be preferred to dipole-like structures.

It is concluded that, contrary to common belief, both single- and multi-layer antenna topologies are feasible as wearable antennas. Both approaches should be considered when the antenna topology for a wearable system is selected. Single-layer antennas are especially useful in situations where the size of the antenna is restricted.

Foreword

The research discussed in this thesis was carried out at Tampere University of Technology, Department of Electronics, between 2005 and 2011.

My path towards the dissertation begun early, in school, when I was introduced to the fascinating world of radio. Amateur radio has given me a chance to combine theory and practice. I wish to thank Hannu OH3NOB who first got me interested in radios and taught me the basics, and Pena OH3BK and Mikko OH3HEI who patiently guided me through decibels and superheterodyne receivers. I am also grateful to all the club members of OH3TR who always gave me practical points of view when I had dived too deep in the ocean of theory.

Professor Markku Kivikoski accepted me as a doctoral student, finding a perfect project for me to start. Later, the supervision task was handed over to professor Lauri Kettunen. Congratulations Markku, for getting me started, and Lauri, for getting me to finish!

I had the opportunity to work at the Department of Electronics and with the RF Electronics research group. Dr. Jouko Heikkinen and Dr. Riku Mäkinen were always there to help me with practical problems and give valuable comments to my papers and this manuscript. Dr. Jari Kangas was always ready to read and comment as well. Through the years, I felt at home at the department, being helped and being of help to many.

My test subjects deserve to be specially acknowledged. Harri Raittinen, Janne Kiilunen, Joel Salmi, Juha Lilja, Taavi Saviauk, and Timo Kellomäki patiently stood in awkward positions and held their breath for the sake of my thesis.

At my very first conference I was lucky to meet friendly people, especially Danes, who welcomed me as a part of the worldwide antennas and propagation community. You made me want to go to conferences, and thus, to write papers. Your ideas, questions, and encouraging attitude have supported me during the lengthy path towards the doctoral degree. I wish to mention Antti Räisänen, Arne Schmitz, Emmi Kaivanto, Erkki Salonen, Jiaying Zhang, Jussi Rahola, Kaj Bjarne Jakobsen, Luigi Vallozzi, Markus Berg, Niels Vesterdal Larsen, Olav Breinbjerg, Patrick Van Torre, Sergey Pivnenko, Tomasz Maleszka, Tommi Laitinen, Tonny Rubæk, and Will Whittow, while probably forgetting someone very special. Thanks to Janne Ilvonen who rescued us from EuCAP, Barcelona, when the ash cloud shut down the air traffic, and greetings to the Aalto university radio people who shared the bus trip! We were forced to meet people from our own country, and perhaps the benefits of networking will exceed the trouble in travelling.

My conference friends inspired me into attending a course at Technical University of Denmark (DTU). Though it was only three weeks, I managed to grasp the feeling of the big world: this is how things are done in other universities, and perhaps our own traditions are not the best and only ones. Many thanks to Sergey for helping me with my accommodation troubles, and even more thanks to Sergey and Olav for the superb teaching.

The pre-examiners, professor Peter S. Hall and docent, Dr. Jussi Rahola, are acknowledged for their valuable comments. I was very happy to have your experience and knowledge added to mine in the final thesis. Jussi has been there since the beginning of my doctoral studies, and I still remember his comment, "This is exactly the research we are interested in," after my presentation in a project meeting. Alan Thompson proofread the thesis. Thank you for your kind words, sir.

My work has been financially supported by the GETA Graduate school in electronics, telecommunication and automation, the Nokia foundation, HPY:n tutkimussäätiö, Emil Aaltosen säätiö, Ulla Tuomisen säätiö, and the Finnish Cultural Foundation, Pirkanmaa Regional fund. I am especially grateful for GETA, not only for the opportunity to work independently for four years, but also for recognising me as promising enough for the graduate school position. Each of the grants pushed my self-esteem a bit, stating that my research is important and interesting. Thank you!

Friends–many of you still struggling towards your M.S. degree–thank you for your support, your stupid questions, and admiration. You accepted that I

often had to work and was busy, but also insisted on me getting some rest and invited me for a cup of tea. Otto Martin proofread some of my papers, which is gratefully acknowledged.

My family has set me an example of doctorhood. They never told me to "get a real job," and none of them was too shy to ask how I was proceeding. The forthcoming birth of the firstborn son inspired me to finally write the manuscript. Thanks for supporting your mum, Teemu! My husband Timo often seemed to do all the housekeeping and even to practice my hobbies while I worked. He patiently listened to my ravings and read my papers. Timo, your support was invaluable–I might have chosen a completely wrong subject to study, if it wasn't for you!

Thank you for your attenuation.

Tampere, January 23, 2012

Tiiti Kellomäki

P.S. Do not rotate the female connector, ever!

Contents

Abstract i

Foreword iii

List of Publications xi

Author's Contribution to Publications xiii

Lists of Symbols and Abbreviations xv

1 Introduction 1

1.1 Structure of the Thesis 2

1.2 Scientific Contribution 3

2 Background for the Research 5

2.1 Why Wearable Antennas? 5

2.2 Previous Research 8

2.2.1 Traditional Antenna Parameters 9

2.2.2 Parameters for Wearable Antennas 10
2.3 The Human Body from the Electromagnetic Point of View . . 11
2.4 Research Methodology 13

3 Body Effect on Antenna Impedance 17
3.1 Input Impedance and the Near-Field 17
3.2 Body Effect on Impedance 19
3.3 Detuning by the Body 21
3.3.1 Detuning of Dipoles near 100 MHz 22
3.3.2 Detuning of Dipole near 866 MHz 25
3.3.3 Detuning of Various Antennas near 1575 MHz 27
3.4 Summary: Body Effect on Impedance 30

4 Body Effect on Radiation Properties 33
4.1 Reflection from Dielectric Interface 34
4.1.1 Modelling Choices 34
4.1.2 Model 35
4.1.3 Modelling Choices Revisited 38
4.1.4 Effect of Reflection on Circular Polarisation 41
4.2 Shape of the Radiation Pattern 42
4.2.1 Patterns of Dipoles near 100 MHz 43
4.2.2 Patterns of Antennas at 866 MHz and Above 46

4.3 Efficiency vs. Antenna–Body-Separation 47
4.4 Gain vs. Antenna–Body-Separation 50
4.5 Summary: Body Effect on Radiation Parameters 55

5 Specific Problems Associated with Wearable Antennas 57
5.1 Effect of the Human Body on Antennas 57
5.2 Other Problems that Arise from Wearability 59
5.3 New Parameters for Wearable Antennas 60

6 Single-Layer and Multilayer Antennas 63
6.1 Single-Layer Antennas 63
6.2 Two- and Multilayer Antennas 64
6.3 Benefits and Drawbacks of Single- and Multilayer... 66
6.3.1 Benefits of Single-Layer Antennas over Multilayer . . . 66
6.3.2 Benefits of Multilayer Antennas over Single-Layer . . . 68
6.3.3 Summary: How to Choose the Topology 69

7 Conclusion 75

Bibliography 79

List of Publications

[P1] T. Kellomaki, J. Heikkinen, and M. Kivikoski.
Wearable antennas for FM reception.
In *Proc. European Conf. on Antennas and Propagation*,
Nice, France, November 2006.
6 pages.

[P2] T. Kellomäki, T. Björninen, L. Ukkonen, and L. Sydänheimo.
Shirt collar tag for wearable UHF RFID systems.
In *Proc. European Conf. on Antennas and Propagation*,
Barcelona, Spain, April 2010.
5 pages.

[P3] T. Kellomäki.
On-body performance of a wearable single-layer RFID tag.
IEEE Antennas Wireless Propagat. Lett.
Vol. 11, 2012.
Pages 73–76.

[P4] T. Kellomaki, J. Heikkinen, and M. Kivikoski.
One-layer GPS antennas perform well near a human body.
In *Proc. European Conf. on Antennas and Propagation*,
Edinburgh, UK, November 2007.
6 pages.

[P5] T. Kellomäki, W. G. Whittow, J. Heikkinen, and L. Kettunen.
2.4 GHz plaster antennas for health monitoring.
In *Proc. European Conf. on Antennas and Propagation*,
Berlin, Germany, March 2009.
5 pages.

[P6] T. Kellomäki and W. G. Whittow.
Bendable plaster antenna for 2.45 GHz applications.
In *Proc. Loughborough antennas and propagation conf.*,
Loughborough, UK, November 2009.
4 pages.

[P7] T. Kellomäki, J. Heikkinen, and M. Kivikoski.
Effects of bending GPS antennas.
In *Proc. Asia-Pacific Microwave Conf. (APMC)*, pages 1597–1600,
Yokohama, Japan, December 2006.
4 pages.

[P8] T. Kellomäki.
Snap-on buttons in a coaxial-to-microstrip transition.
In *Proc. Loughborough antennas and propagation conf.*,
Loughborough, UK, November 2009.
4 pages.

[P9] T. Kellomäki and L. Ukkonen.
Design approaches for bodyworn RFID tags.
In *Proc. International Symp. on Applied Sciences in Biomedical and Communication Technologies*, Rome, Italy, November 2010.
5 pages.

Author's Contribution to Publications

The author designed, fabricated, and measured the antennas presented in [P1], *"Wearable antennas for FM reception,"* and wrote the manuscript with the help of the co-authors.

The author designed, fabricated, and measured the antenna in [P2], *"Shirt collar tag for wearable UHF RFID systems,"* and [P3], *"On-body performance of a wearable single-layer RFID tag,"* and wrote the manuscript with the help of the co-authors.

The author conducted the measurements and analysis for [P4], *"One-layer GPS antennas perform well near a human body,"* and wrote the manuscript with the help of the co-authors.

The author designed, manufactured, and measured the antennas presented in [P5], *"2.4 GHz plaster antennas for health monitoring,"* and [P6], *"Bendable plaster antenna for 2.45 GHz applications."* The author wrote the manuscripts, except the parts that cover SAR, which were written by Dr. W. G. Whittow.

The author conducted the measurements and analysis for [P7], *"Effects of bending GPS antennas,"* and wrote the manuscript with the help of the co-authors.

The author designed, simulated, fabricated, and measured the structure in [P8], *"Snap-on buttons in a coaxial-to-microstrip transition,"* and wrote the manuscript.

The author conducted the literature survey, and wrote the manuscript of [P9], *"Design approaches for bodyworn RFID tags,"* with the help of the co-author.

Lists of Symbols and Abbreviations

$\angle$	Phase angle of a complex number
B	Inverse of the front-to-back ratio of electric fields, a complex number
β	Wavenumber, $\beta = 2\pi/\lambda$
D	Directivity
d	The largest physical dimension of an antenna
δ_s	Penetration depth or skin depth, the distance through which the amplitude of a plane wave decreases by e^{-1} or 0.386 or –8.686 dB in a lossy medium
dB	Decibel
dBi	Decibels over isotropic, a pseudo-unit of antenna gain
$\bar{E}$	Electric field vector
EBG	Electromagnetic band-gap
ε	Permittivity of a medium, $\varepsilon = \varepsilon_\mathrm{r}\varepsilon_0$
ε_0	Permittivity of vacuum, $\varepsilon_0 = 8.85 \cdot 10^{-12}$ F/m
ε_r	Dielectric constant, also known as relative permittivity
η_0	Wave impedance in vacuum, $\eta_0 = \sqrt{\mu_0/\varepsilon_0}$
η_ant	Antenna efficiency, $\eta_\mathrm{ant} = \eta_\mathrm{rad}M$
$\eta_\mathrm{ant}^\mathrm{body\text{-}worn}$	Antenna efficiency of the body-worn antenna
$\eta_\mathrm{ant}^\mathrm{free\ space}$	Antenna efficiency of the antenna in free space

η_{bw}	Body-worn efficiency, $\eta_{\text{bw}} = \eta_{\text{rad}}^{\text{body-worn}} / \eta_{\text{rad}}^{\text{free space}}$
η_{rad}	Radiation efficiency
$\eta_{\text{rad}}^{\text{body-worn}}$	Radiation efficiency of the body-worn antenna
$\eta_{\text{rad}}^{\text{free space}}$	Radiation efficiency of the antenna in free space
η_{tissue}	Wave impedance in (lossless) tissue
$\eta_{\text{tissue}}^{\text{lossy}}$	Wave impedance in tissue, with losses
f	Frequency
f_0	Free-space centre frequency
F/B	Front-to-back ratio (of gains), usually in dB; F/B $= 1/\lvert B\rvert^2$
FM	Frequency modulation; refers to the FM broadcast frequency band 87…108 MHz in this thesis
G	Gain, $G = \eta_{\text{rad}} D$
G_{real}	Realised gain, $G_{\text{real}} = MG = M\eta_{\text{rad}} D = \eta_{\text{ant}} D$
Γ	Field reflection coefficient (dimensionless)
GPS	Global positioning system, operating at 1575 MHz (and other frequencies not relevant to this thesis)
$\Im\{\cdot\}$	Imaginary part
IC	Integrated circuit, especially the IC that controls the backscattering in an RFID tag
IEEE	Institute of Electrical and Electronics Engineers
ISM	Industrial–Scientific–Medical frequency bands, e.g. around 2.45 GHz
j	$\sqrt{-1}$
λ	Wavelength (in free space if not otherwise specified)
λ_{tissue}	Wavelength in tissue
LHCP	Left-hand circular polarisation
M	Mismatch factor, ratio of power transmitted through impedance mismatch to power incident at the mismatch ($0 \leq M \leq 1$). $-10\log(M)$ is often called mismatch loss.

$M^{\text{body-worn}}$	Mismatch factor of the body-worn antenna
$M^{\text{free space}}$	Mismatch factor of the antenna in free space
μ	Permeability of medium, in this thesis usually $\mu = \mu_0$
μ_0	Permeability of vacuum, $\mu_0 = 4\pi \cdot 10^{-7}$ H/m
n	0, 1, 2, ...
ω	Angular frequency, $2\pi f$
PCB	Printed circuit board
PEC	Perfect electric conductor
Q	Q value, quality factor
$\Re\{\cdot\}$	Real part
r	Distance from the antenna to the observation point
R	Resistance, $R = \Re\{Z\}$
Return loss	Ratio of power incident an impedance mismatch to power reflected from the mismatch (in dB)
RF	Radio frequency
RFID	Radio frequency identification (at 866 MHz in this thesis)
RHCP	Right-hand circular polarisation
s	Antenna–body-separation distance (in mm or λ)
σ	Conductivity
SAR	Specific absorption rate
$\tan\delta$	Loss tangent, $\tan\delta = \Im\{\varepsilon\}/\Re\{\varepsilon\} = \sigma/(\omega\Re\{\varepsilon\}) \approx \sigma/(\omega\varepsilon)$
UHF	Ultra high frequency, the frequency band between 300 and 3000 MHz
VHF	Very high frequency, the frequency band between 30 and 300 MHz
X	Reactance, $X = \Im\{Z\}$
Z	Impedance, $Z = R + jX$

Chapter 1

Introduction

A wearable antenna is an antenna that is designed to be integrated as a part of a garment and to be worn on the body. Antennas and radios in clothing are less cumbersome to the user than traditional handheld radios and whip antennas. This is advantageous especially in long-term use: wearable antennas will be first adopted in hospital patient clothing or home-nursing, and in the working clothes of such groups as rescue workers.

This thesis discusses the effect of the human body on wearable antennas. Until recently, designers of wearable antennas have separated the antenna and the body by a metallic sheet, thereby completely excluding the human effect. We show that although the body effect on antennas can be strong, it can also be used to improve antenna performance.

To the antenna, the human body is lossy and deteriorates the communication link, especially if the antenna is not designed to be body-worn. We show that the nature and magnitude of this effect depend on the frequency, on the antenna–body-separation distance, on the structure of the antenna, and in certain cases also on body proportions, posture, and antenna placement on the body. This thesis sets out to analyse these effects in order to facilitate the design process of wearable antennas in the future.

Special attention is paid to the feasibility of and body effect on single-layer antennas. By single-layer we mean that all the metal parts of the antenna are coplanar. Multilayer topologies include two or more superimposed metallic layers. One of these layers often acts as a ground plane.

The frequency range discussed in this thesis is from 100 MHz to 2.5 GHz. Example frequencies of 100 MHz, 866 MHz, 1575 MHz, and 2450 MHz have been chosen because of the important applications at those frequencies. From the measurements made at each frequency, the body effect across the entire frequency range is extrapolated and analysed.

The discussion focuses on scenarios in which only one of the communicating nodes is body-worn. It is, therefore, beneficial to transmit power away from the body, rather than to couple into the tissue or to launch surface waves. This choice rules out body-area networks and nodes in medical implants.

1.1 Structure of the Thesis

This thesis consists of nine publications and seven chapters of preceding text summarising and expanding the findings of the publications.

To set the starting point for the research, Chapter 2 of the thesis begins with a review of potential applications and earlier research on wearable antennas. Various traditional antenna properties are introduced, along with new parameters for wearable antennas that have been proposed in the literature. The electromagnetic properties of the human body are reviewed, to gain an understanding of the environment in which wearable antennas operate. Lastly, the research methodology and approach of this thesis are described.

The most important content of the thesis is presented in Chapters 3 and 4, which discuss the effect of the human body on antenna properties. First, Chapter 3 details the body effect on antenna impedance and matching, and separates the low and high frequency ranges. Chapter 4 continues by introducing a model of the reflection from the human body, which is then refined with the help of measurements. The effect of the antenna–body-separation distance on gain and efficiency is studied. The low and high frequency ranges are treated separately in Chapter 4.

Apart from the presence of the human body, there are many additional problems associated specifically with wearable antennas. After a brief summary of the body effect, Chapter 5 introduces the challenges in wearable antenna design. The chapter ends with a discussion of the possible need for new parameters for wearable antennas.

Until now, most wearable antennas have been two-layer designs with a ground plane between the antenna and the user's body. Chapter 6 compares the performance of single- and multilayer antennas, with special attention on the effect of the human body. Contrary to common belief, single-layer antennas are not necessarily inferior to multilayer antennas, and can in some cases provide greater benefits. Each topology has its own advantages, and the designer should always consider both options.

Finally, in Chapter 7, the findings of the thesis are summarised.

1.2 Scientific Contribution

The primary research question of this work is, how does the human body affect the properties of wearable antennas? This can be further divided into subquestions: How is the impedance affected? How is the pattern affected? Is there a difference in the effects at different frequencies? Does body size or posture matter? Where should the antenna be attached? Can we find a general rule for a good antenna–body-separation distance, and how large is this value?

The effect of the human body on wearable single-layer antennas is not systematically investigated in the literature. The publications in this thesis include studies of the human effect on wearable single-layer antennas in both the resonance and the optical (high frequency) regions. The effect of antenna–body-separation distance is investigated in detail.

While many different antennas have been studied in this thesis, the results cannot necessarily be generalised to apply to all antennas. The exact performance of antennas near the body must be verified by measurements, although the guidelines presented in this thesis can be used as a starting point and a preliminary estimate of the antenna performance on-body. This thesis is intended to assist designers of wearable antennas to avoid the many pitfalls inherent in the design process.

Publication [P1] investigates the effect of the human body close to the resonance region (at 100 MHz), where the size of the body is comparable to the wavelength. It is seen that body size and posture have a significant effect on

the impedance and resonant frequency, and that the radiation pattern can be almost omnidirectional because of the absence of the body shadowing effect.

Publications [P2, P3, P9] discuss the body effect on a small dipole above the resonance region, at 866 MHz. Single-layer and multilayer RFID tag designs are compared. The performance of the dipole tag can be kept constant despite the varying detuning caused by the fluctuating antenna–body-separation.

Publication [P4] presents the results of an examination of the human effect on several antennas in the optical region (at 1575 MHz), where the dimensions of the human body are several wavelengths. The effect of the body on the efficiency and pattern is presented, and some guidelines on the antenna shape are given. A body-worn efficiency of approximately 75% is achieved with an antenna–body-separation of $\lambda/(2\pi)$.

Publication [P7] examines the effect of bending on antenna properties. Large wearable antennas must be made flexible, and it is very important to ensure their operation in bent conditions. Circular polarisation is especially sensitive to bending.

Publications [P5,P6] present the results of a case study of using non-uniform ground planes and antenna elements at 2.45 GHz. The antennas are fabricated on a wound-care plaster and designed to be attached directly to the skin. The effect of the human body on the antennas is studied with the help of measurements.

Publication [P8] introduces a practical and inexpensive feeding arrangement for wearable antennas, using commercial snap-on buttons. The performance characteristics are analysed with measurements and simulations, and the structure is found to be feasible up to at least 2.5 GHz.

Chapter 2

Background for the Research

This chapter first presents a short survey of possible applications of wearable antennas and radio systems. The roots of wearable antenna research are investigated to set the starting point for the thesis. Some traditional and wearable antenna parameters are introduced and the electromagnetic properties of the human body in the frequency range of interest are reviewed. Last, the methods used in wearable antenna research are presented.

2.1 Why Wearable Antennas?

Apart from the realms of science fiction, wearable antennas will find their users in the sectors of healthcare, authorities such as police and firefighters, and in recreation. Ubiquitous communications and positioning are almost prerequisites for life in the modern world. People carry numerous antennas in their mobile devices, often without even being aware of them. In some cases, handheld devices may be too cumbersome, and the communications devices have to be integrated into other equipment such as clothing. Applications for wearable antennas are illustrated in Fig. 2.1.

We can distinguish between wearable antennas, which are integrated in the clothing, and body-worn antennas, which can be wearable or worn for example on a bracelet. Wearable antennas are still in the prototyping and testing

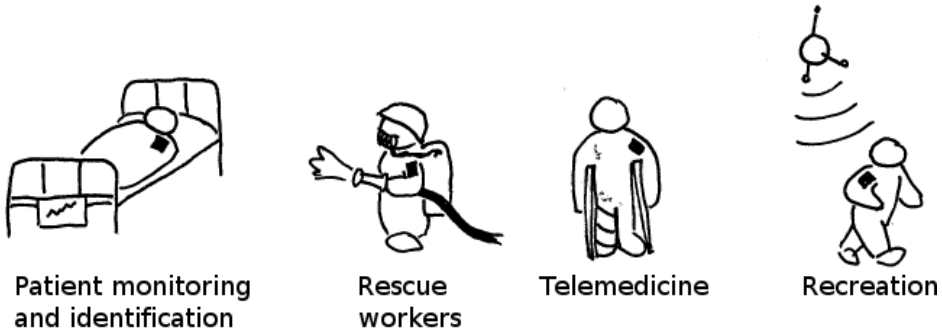

Figure 2.1: Applications for wearable antennas.

phase. Consumer level applications are rare or nonexistent, but body-worn antennas, especially bracelets, are already available on the market.

Healthcare and care of the elderly are among the first user sectors of body-worn antennas. Body-worn RFID tags are used in patient monitoring, positioning, and identification in numerous hospitals [39,55]. The so-called emergency alert bracelet facilitates easy emergency calls via the mobile phone network, and certain models can also send an emergency message if the bracelet is taken beyond limits, e.g. out of a nursing home [28, 47].

In the future, the importance of telemedicine and home-nursing is expected to grow. Telemedicine requires the body status to be monitored by devices that measure heart or brain activity, blood pressure, body temperature, or other body functions. The data can be sent to a physician or an automatic monitoring system. Telemedicine allows patients with chronic diseases to skip frequent controls while also reducing the data collection intervals, thus, increasing patient safety.

Another application for telemedicine is in the recovery of patients after an operation: instead of being hospitalised for recovery monitoring, the patients can be discharged to return home sooner. In addition to reducing the cost of the operation, home-nursing can increase the patient's physical activity, thus also speed up recovery. In the case of the elderly, especially, post-operative recovery from a hip fracture can lead to permanent impairment of the patient's mobility.

Rescue workers such as police officers or firefighters need constant communications as they work. Nowadays the solution is a handheld radio, which is often worn on a belt clip or a designated pocket, with the whip antenna

protruding rather clumsily from the pocket. The distance of the whip antenna from the body varies with the user's movements, which makes antenna performance unstable. Prototypes for wearable antennas integrated in the firefighter's outfit have been made by Vallozzi *et al.* [52,53]. Because firefighters must wear special clothing at work, it is easy to include communications equipment in their garments.

One can only guess at the recreational applications of wearable antennas. These range from built-in positioning equipment in outdoor clothing or sports wear to games based on clothing antennas [24]. Even today, athletes in mass race events are identified using an RFID tag integrated in the number tag [11, 37]. Some scenarios predict a sensor cloud surrounding the body, monitoring the bodily functions such as heart rate, all communicating with a master node, forming a body-area network.

A good wearable antenna must both be comfortable to wear and perform well in the communication link. The structure must be flexible, and thick or rigid padding must be avoided. If the antenna is large, it also has to be breathable. The antenna must withstand washing and wear, and should be resistant to moisture. In order to be truly wearable, the antenna must have a low profile, which means that it should conform to the body and not protude from the clothing. As a part of the communication link, the antenna should be as efficient as possible, and meet the specifications for the impedance and radiation properties. Most importantly, the link must operate reliably, especially in life-saving applications.

Even though wearable antennas can be made lightweight and integrated into the clothing, the radio equipment will pose a problem. The options include a wired connection between the antenna and the radio or an inductive or capacitive link. In the case of body-worn sensors, the sensor nodes may use an energy-scavenging scheme to power up. For example, wearable passive RFID tags are powered by the electromagnetic wave emitted by the reader. An emerging trend in electronics is the printed electronics, which enables thin and flexible devices. Perhaps in the near future the entire radio system including the antenna, the transmitter/receiver, and the battery will form an integral part of clothing.

2.2 Previous Research

The work on antennas near the body began with handheld radios and the human effect on dipoles [21] and whip antennas, investigated with the help of measurements. As early as 1968, after making a series of measurements of the human effect on whip antennas between 35 and 170 MHz, Krupka noted that "the rates of radiation absorption by the body are surprisingly high" [25].

As an alternative to whips, a body-mounted (wearable) antenna was proposed by King in 1975 [20], perhaps the first of its kind. Even the use of the human body itself as a radiator was studied in [3], followed by a study of ways to excite the radiating current to the body [4].

Later, when enough computational capacity became available for simulations, attempts to simulate the human effect on portable antennas were reported in numerous papers, e.g. [50]. The need for this research was amplified by the growing mobile phone industry, and the frequencies were chosen accordingly, mostly 450 and 900 MHz.

Recently, as fully wearable antennas started to emerge, the effect of the body became a major concern. The earliest antennas were mostly microstrip patches on a textile substrate, presented for example in [41] and its references. Wearable antennas were designed mostly for the GPS (1575 MHz) and 2.45 GHz ISM frequency bands, but also for the 900 MHz and 5.8 GHz bands. At the same time, a new trend in wearable antennas arose: the desire for communication between body-worn nodes.

Today in conferences on antennas and propagation, there is at least one special session devoted to body-worn antennas, body-area networks, and on-body propagation. The first textbook on the subject, *"Antennas and propagation for body-centric wireless communications,"* was published in 2006 by Hall and Hao [13]. The book covers not only antennas and antenna design methods, but also body properties, on-body propagation, and medical implant antennas, each topic written by a specialist in the field.

The authors of the textbook [13] seek to establish a standard language for the diverse area of body-worn communications. They divide the area into three domains with each domain requiring a completely different kind of antenna:

- *Off-body* communications, where only one of the communicating nodes is body-worn, or where the nodes are worn by two different people.
- *On-body* communications, in which all the nodes are worn by the same user and form an on-body network.
- *In-body* communications, where at least one of the nodes is implanted into the human body.

This thesis discusses only antennas for off-body communications.

Properties of textile materials have been investigated for example in [29, 56] and [41, Sec. 6.4]. The dielectric constants of textile materials range from 1 to 2, lowest in the fleece fabric with the highest air content. This means that wearable patch antennas are much larger than regular antennas on printed circuit boards. With respect to losses, textile materials are comparable to lossy printed circuit board materials. Conductive textiles that allow the fabrication of textile-only structures have been classified e.g. in [29]. Research on materials and research on antenna structures have, unfortunately, mostly been conducted by separate groups.

2.2.1 Traditional Antenna Parameters

Antennas are traditionally characterised by their impedance and radiation parameters, which are applicable to wearable antennas as well. The impedance parameters describe how the antenna acts as a part of an electric circuit, and include the impedance with its real and imaginary parts (resistance and reactance), return loss, mismatch factor, and Q value.

The radiation parameters describe how the antenna acts from an electromagnetic point of view. Gain and directivity describe the radiation intensity in a given direction. The efficiency of an antenna can be defined in two different ways. The *radiation efficiency* is the ratio between the power radiated to the power accepted by the antenna [17]. Thus it is a measure of how much power is lost in the antenna itself. The *antenna efficiency*, on the other hand, combines the mismatch factor in the antenna feed point and the radiation efficiency: $\eta_{\text{ant}} = \eta_{\text{rad}} M$. In other words, antenna efficiency is the ratio between the power radiated to the power available from the transmission line. We note that

$$0 \leq \eta_{\text{ant}} \leq \eta_{\text{rad}} \leq 1.$$

We cannot usually measure gain, but it is possible to measure the directivity, the impedance mismatch factor, and the *realised gain*. Realised gain is defined by the IEEE as "the gain of an antenna reduced by the losses due to the mismatch of the antenna input impedance to a specified impedance," [17] which we can express as

$$G_{\text{real}} = \eta_{\text{ant}} D = \eta_{\text{rad}} M D = M G \ \leq \ G = \eta_{\text{rad}} D \ \leq \ D.$$

The realised gain can be seen as a combination of impedance and radiation parameters. Realised gain is the most common radiation parameter to be measured.

The radiation parameters are generally only defined in the far-field of an antenna. According to the IEEE, this means that the observation point must be at least $2d^2/\lambda$ away from the antenna, where d is the largest dimension of the antenna [17]. The region $0.62\sqrt{d^3/\lambda}$ away from the antenna or closer is called the reactive near-field. For small antennas, the limit is commonly taken as $\lambda/(2\pi)$. The transition region called the radiating near-field falls between the two.

A more detailed description of the parameters can be found in antenna textbooks such as [7]. The formal definitions of terms for antennas are given in [17].

2.2.2 Parameters for Wearable Antennas

With the advent of body-worn antenna systems, new parameters were needed to classify new antennas. Scanlon and Evans propose two figures of merit: *body-induced gain* and *body-worn efficiency* [44, p. 219 and 222].

Put simply, body-induced gain is the ratio (in decibels) of gains between the body-worn antenna and the antenna in free space. Theoretically, body-induced gain can range from $-\infty$ dB to 6 dB for dipoles or other omnidirectional antennas.

Body-worn efficiency is defined as the ratio of total radiated power when the antenna is body-worn to total radiated power when in free-space isolation, and represents the overall power losses in the user's body. For example, if the radiated power is 2 W in free space and 1 W body-worn, the body-worn efficiency will be 50%.

The definition of body-worn efficiency does not take into account changes in impedance. Therefore it is independent of detuning or other changes in the mismatch factor. In other words, body-worn efficiency is the ratio of radiation efficiencies when the antenna is body-worn and in free space [43]:

$$\eta_{\mathrm{bw}} = \frac{\eta_{\mathrm{rad}}^{\text{body-worn}}}{\eta_{\mathrm{rad}}^{\text{free space}}}.$$

2.3 The Human Body from the Electromagnetic Point of View

Water makes up two thirds of the human body. Because the molecules are polar, the dielectric constant of water is very high. In the presence of an external electric field, water becomes polarised and causes changes in the antenna properties. This phenomenon is known as dielectric loading. If impurities (ions) are present, water should also be modelled as a poor conductor in which ohmic losses are present. Additional RF losses result from the friction between molecules when they rotate at a gigahertz frequency. As a lossy material, impure water absorbs power and hence reduces the efficiency of any antenna nearby.

If we assume the time-harmonic model, thanks to linearity we can characterise the human body with the dielectric constant ε_{r} and loss tangent $\tan\delta$. These properties are different for each tissue, and also frequency-dependent. We can distinguish several classes of tissues:

- Fat tissues: low water content; lowest dielectric constant and low losses
- Bone: low water content; low dielectric constant and low losses
- Lung: properties vary with varying air content
- Soft tissues (muscle, internal organs, skin): high dielectric constant and high losses
- Blood: highest water content; highest dielectric constant and losses.

Figure 2.2 shows the key electromagnetic properties of selected tissues. The data is taken from [10], a resource that allows the computation of the parameters for many tissues in the frequency range 10 Hz to 100 GHz. From

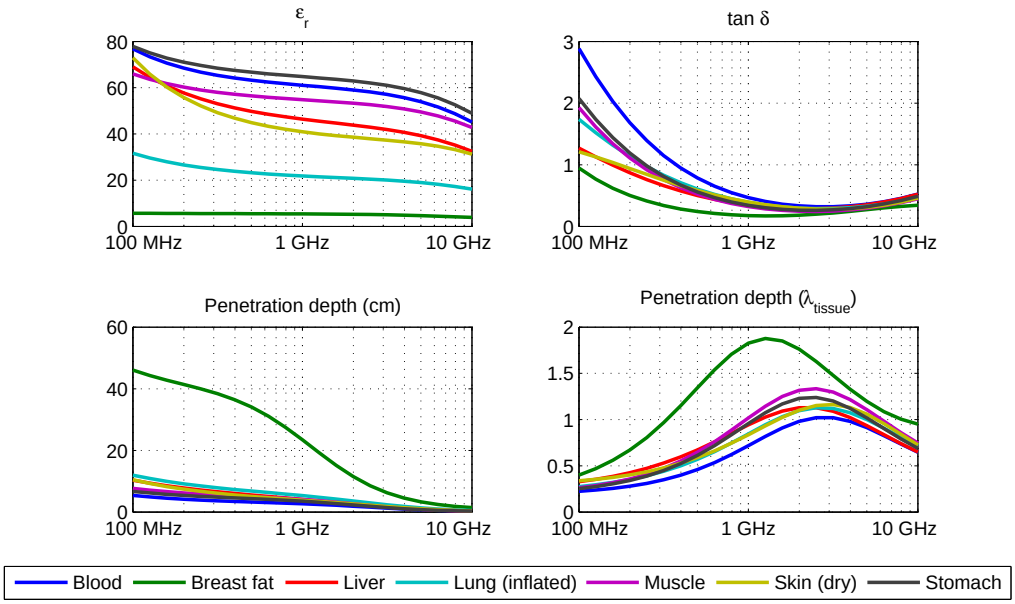

Figure 2.2: Tissue properties vs. frequency, from [10].

Figure 2.2 it is obvious that intricate body models are needed if accurate results are desired. Especially fat is different from other tissues.

The thicknesses of tissue layers (skin, fat, muscle) are of the order of millimetres or centimetres, and blood vessels in organs can be thinner than 1 mm. In the frequency range from 1 GHz to 10 GHz, the wavelength in tissue ranges from 5 mm to 4 cm in muscle, or 15 mm to 13 cm in fat. At 100 MHz, the wavelength is 29 cm in muscle and 1.1 m in fat. Sub-wavelength scale details are averaged, and need not be modelled precisely in simulation models. The required level of detail depends on the application, in addition to the frequency.

Above 1 GHz, the human body is several penetration depths thick. A very small portion of the field that surrounds the antenna reaches the core of the body. Thus the effect of tissues deep inside the body is relatively small, and again, the internal organs can be modelled rather coarsely.

2.4 Research Methodology

The problem of the human body near an antenna has been assessed by means of both simulations and measurements, and to some extent also with analytical tools.

The human body is an intricate composition of different tissues. To model the body, tissue properties must be known as well as the precise geometry. Moreover, the composition of the body varies from person to person, and even changes over time as the person ages. Wearable antennas must be designed to operate regardless of the wearer's personal traits such as body shape and size, and hence the performance should be modelled or measured not only for one standard model but for a range of potential users.

Simulation models use tissue parameters measured from human or animal tissue samples. Such parameters with frequency dependency are available e.g. in [10, 12]. The simulation models can be classified according to their level of detail:

- Homogeneous phantoms of simple geometrical shape (e.g. elliptical cylindrical phantom with $\varepsilon_\mathrm{r} = 53$ and $\tan\delta = 0.24$, which are the parameters of muscle at 2.45 GHz)
- Homogeneous phantoms of the shape of a human being (e.g. data from a computer graphics model, with $\varepsilon_\mathrm{r} = 53$ and $\tan\delta = 0.24$)
- Layered phantoms of simple geometrical shape (e.g. elliptical cylindrical phantom where the outer 2 mm layer is with skin parameters, next 10 mm with muscle parameters, and the core with parameters of internal organs averaged)
- Realistic phantoms based on magnetic resonance imaging data or sliced corpses of dead volunteers (e.g. Visible Human, with 1 mm^3 spatial resolution [36]).

The accuracy of any computational result is limited by the accuracy of the model and the parameters used, as well as by the feasibility of the chosen method. The tissue parameters and their frequency dependency must be well-known. When greater accuracy is desired, the model must be made more detailed, which in turn makes the computation slow. At frequencies above 1 GHz, the wavelength in tissue can be less than 3 cm, leading to a huge computational grid for whole-body models.

Analytical methods model the human body as a simple shape, such as an infinite cylinder. The input impedance of a dipole next to such a cylinder has been calculated in [19]. To take full advantage of the analytical models, only simple antennas are usually analysed, because their equivalent sources are known. While the analytical examinations provide excellent basic information and proofs to be used in other research, the results cannot be directly applied to realistic wearable antenna design.

Measurements are often performed using volunteer subjects. There are two undeniable advantages to this approach: by definition, the tissue parameters and the body proportions are correct. On the other hand, each subject can only represent one possible body shape. Another drawback of using human subjects is the lack of exact repeatability in measurements. It is quite demanding to obtain the same body position twice. Also involuntary movements such as breathing may cause inaccuracy in measurements. It is obviously impossible to measure the field distribution inside the individual.

An alternative to measurements with human subjects is to use standard phantom models filled with tissue-equivalent liquid [14]. The phantoms often correspond to full-size humans, or are limited to torsos, heads, or hands. The mobile phone industry is an important user of the phantom hands and heads. Physical phantoms have a limited frequency range defined by the liquid properties. Also so-called dry phantoms have been manufactured, which consist of ceramics with the desired dielectric properties [23].

Inexpensive prototype phantoms have been used in e.g. [34, 48, 49]. These phantoms are often of simple shape (cube), but filled with similar liquids as commercial phantoms. These physical phantoms are nearly always homogeneous and cannot exactly represent the layers of skin, fat, muscle, and bone, or the internal organs. Different recipes for the liquid are available in the literature, for example in [27, 46] and [14, Tab. 2.3]. Usually the body-simulating liquid is a solution of sugar and salt in water.

Sometimes even pieces of meat have been used as phantoms [31]. While the tissue properties are easily matched in such measurements, the phantom may often be too small. A phantom of a correct size is needed especially for accurate radiation pattern measurements, while a smaller phantom can be used for impedance measurements.

Carefully made measurements and simulations can provide results that agree very well, for example in [52] where the measured and simulated impedances

are within fifteen ohms, the resonant frequencies within few megahertz, and peak gains within two decibels. The only major difference between the measured and simulated results in [52] is the radiation efficiency, with the simulated efficiency 30 percentage units (2 dB) higher.

The major advantage of measurements is that the geometry of the antenna and the antenna material parameters are taken into account. In measurements with human subjects, the body composition is also correct. On the other hand, the measurement setup, such as cables, or reflections may affect the result. The setup is eliminated in simulations, and with simulations it is also possible to examine the effect of one phenomenon at a time. However, accurate simulations require careful modelling.

The studies conducted for this thesis are experimental. The measurements were made using volunteers of different sizes and sexes. The input impedances were measured using a vector network analyser in a regular office. For the radiation patterns we used an anechoic chamber (azimuth patterns only) and an outdoor measurement range at 100 MHz. Some of the free-space patterns were measured using the Satimo Starlab [42]. In [P4], some radiation patterns were measured using a head-and-shoulders phantom using the Satimo Stargate [42]. The Satimo equipment allows the measurement of three-dimensional patterns as well as antenna efficiency.

Dr. W. G. Whittow made the SAR (specific absorption rate) simulations for [P5] using a truncated homogeneous torso model, and for [P6] using a flat and a cylindrical homogeneous phantom. SAR cannot be measured from humans, because it involves moving a probe inside the tissue.

A true statistical analysis of the measurement results cannot be made, because the number of measurements is quite small. Moreover, the measurements were often performed using the same equipment and the same anechoic chamber. To introduce variability in the results, we have fabricated several seemingly identical prototypes, used a number of volunteers, and repeated the measurements on different days. The antenna position on the body has also been varied and the effect of body posture investigated. However, the measurement accuracy can only be estimated for each study. The uncertainty associated with the radiation patterns measured in the anechoic chamber is of the order of ± 1 dB to ± 3 dB in peaks, depending on the frequency, and greater for lower pattern levels. The uncertainty stated for the Satimo equipment is ± 0.8 dB or better in peaks.

Chapter 3

Body Effect on Antenna Impedance

Antenna properties are significantly affected by the human body. Tissues may absorb a substantial part of the power fed into the antenna and further radiated by it. Being a reflective obstacle, the body alters the radiated field as well as the near-field of the antenna. These changes are visible in the measured or modelled antenna parameters.

This chapter describes the effect of the human body on the input impedance of antennas. The effect of the human body on the key impedance parameters–resonant frequency, bandwidth, and the resonant resistance–is described with the help of example antennas at three selected frequencies: the FM band around 100 MHz, the ISM band at 866 MHz, and the GPS band at 1575 MHz. The difference and limits of the low and high frequency domains are discussed in the summary.

3.1 Input Impedance and the Near-Field

Near the resonant frequency, the impedance of small antennas can be modelled as a simple electric network consisting of the radiation resistance R_{rad}, loss resistance R_{loss}, capacitance C, and inductance L. In circuits, resistance represents the phenomenon of power losses in the circuit. In antennas, radi-

ation resistance describes the part of power that is transferred in the form of electromagnetic radiation, which is obviously a desirable property. The power lost as heat in ohmic losses in the antenna or the user's body is taken into account in the loss resistance.

The reactive components, capacitance and inductance, are related to the energy stored in the so-called near-field of the antenna. Similarly to a coil that creates a magnetic field around itself, antennas create a near-field. A predominantly magnetic near-field is visible in the input impedance as inductive reactance; electric near-field makes the input reactance capacitive. At resonance, when the input reactance is zero, the electric and magnetic near-fields carry equal energy.

The reactance part in the antenna input impedance is related to the energy that is stored in the near-field and re-absorbed by the antenna and the transmission line. When the human body is near the antenna, it will both change the field distribution and absorb power from the near-field. This absorbed power cannot re-enter the antenna during the next half-cycle. By altering the reactive near-field of the antenna, the body also affects the input impedance.

The IEEE characterises the reactive near-field as "that portion of the near-field region immediately surrounding the antenna, wherein the reactive field predominates" [17]. The boundary of the reactive near-field is generally taken to be $0.62\sqrt{d^3/\lambda}$ with d the largest dimension of the antenna, or $\lambda/(2\pi)$ for small antennas [7, p. 34], although the definition does not state any condition for the "predominating field." Indeed, the boundary of the reactive near-field of a half-wave dipole can be set to 2λ by choosing a more restricting limit [26].

Not all antennas are alike in terms of the sensitivity of the input impedance to nearby objects or humans. The sensitivity is determined by the strength of the reactive near-field and how fast the field decays when the distance to the antenna is increased. For example, dipole antennas exhibit strong near-fields that decay slowly, as described in [26]. On the other hand, in microstrip or inverted-F antennas the near-field maximum occurs in the gap between the element and the ground plane, and the reactive near-field is negligible anywhere else [P4]. We can say that the reactive near-field region in the case of inverted-F antennas and especially microstrip antennas is much smaller than $\lambda/(2\pi)$ or $0.62\sqrt{d^3/\lambda}$.

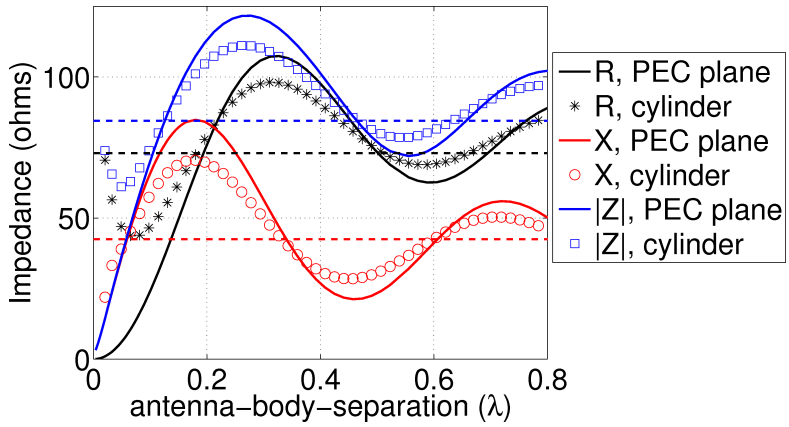

Figure 3.1: Input impedance of a half-wave dipole next to an infinite cylinder with tissue parameters ($\varepsilon_r = 47–j16$) and an infinite perfectly conducting (PEC) plane. The dipole is parallel to the cylinder and the plane. Curves show the resistance, reactance, and the magnitude of the impedance. The free-space values are indicated by the dashed lines ($R = 73\ \Omega$, $X = 42.5\ \Omega$, $|Z| = 84.5\ \Omega$). Data from [19].

3.2 Body Effect on Impedance

An interesting analytical result for the input impedance of a body-worn half-wave dipole is presented in [19]. The human body was modelled as an infinite circular cylinder with tissue parameters at 2.45 GHz ($\lambda = 12$ cm, $\lambda/(2\pi) = 2$ cm, cylinder diameter 28 cm). The dipole was modelled parallel to the cylinder, their axis directions coincident. Fig. 3.1 shows the computed input impedance of the dipole near the cylinder and a perfectly conducting plane. Close to the cylinder, the magnitude of the input impedance of the dipole decreases from the free-space value. [19]

Figure 3.1 shows that both the resistance and the reactance of the dipole are smaller than in free space when the antenna–body-separation distance is very small. Further away, reactance exceeds its free-space value at 0.07λ (0.8 cm), and resistance at 0.20λ (2.5 cm). The magnitude of the input impedance is smaller that in free space until 0.12λ (1.5 cm).

The resistance and reactance can be approximated with by their values next to a conducting plane. Fig. 3.2 shows the error that results from this approximation. When the antenna–body-separation exceeds 0.2λ (2.5 cm), the approximation gives the resistance and impedance magnitude with an error

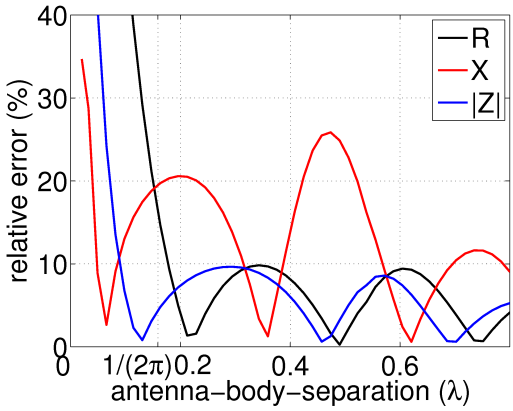

Figure 3.2: Error in approximating the effect of the body using a perfectly conducting plane instead of a lossy cylinder. The impedance data is plotted in Fig. 3.1, originally from [19].

less than 10% (of the order of ten ohms). To some accuracy, it is possible to test the behaviour of the antenna input impedance with a conducting plane instead of a body. This is especially useful in simulations, where conducting boundary conditions are much more convenient than large tissue models.

Image theory can be used to intuitively explain the lowered input impedance. If a dipole is brought close to a conducting plane, the surface currents and charges on the plane will give rise to a 'mirror image' of the dipole. When the antenna–body-separation distance, or the distance of the antenna from the conducting plane, is much smaller than the wavelength, the electric field strength near the antenna decreases and the magnetic field strength increases, and thus, the impedance is lowered. The phenomenon can also be modelled as capacitance between the antenna and the ground, or as coupling between the antenna and its image.

When the perfect conductor is replaced by a lossy tissue, the current in the image is weaker, and thus its effect on the input impedance smaller. In Fig. 3.1 this is visible in that the curves representing the dipole close to tissue appear damped, compared to the dipole next to a perfect conductor.

Usually wearable antennas are worn quite close to the body, which implies that the input impedance will be lower than in free space. Although this has been analytically shown only for dipoles, the same phenomenon was observed in our measured results in [P5, P6], results simulated for [P2], and many other case studies. When designing wearable antennas, the input impedance

in free space should be designed too high to match the system impedance. This makes it possible to avoid excess mismatch loss when the antenna is body-worn. Especially the tag in [P2, P3] was designed this way.

The losses in the human body are visible in the widened bandwidth when the antenna is body-worn. In other words, the body lowers the Q value of antennas. In some extreme cases this effect can be utilised to make the antenna meet the bandwidth specification, but using the body losses in this way is equivalent to connecting a resistor in series with the antenna. Rather, excess lowering of the Q value on the body should serve as a warning signal: this antenna will not radiate well on-body.

3.3 Detuning by the Body

The dielectric constants of body tissues are high, of the order of 20 to 50 in soft tissues. This dielectric loading shifts the resonant frequency of an antenna located nearby. We call this phenomenon *detuning*. The same can be observed when antennas are printed on PCBs of different materials: the resonant frequency of the antenna printed on the high-ε_r material becomes lower. Similarly, the high dielectric constant of the body causes the resonant frequency to move downwards. Again, the amount of detuning depends on the antenna shape and the near-fields, as well as on the antenna–body-separation distance.

In the case of broadband or multiresonant antennas it should be noted that resonances at different frequencies are not necessarily affected in a similar manner. The dielectric constant and penetration depth in the body are frequency-dependent, and obviously the antenna–body-separation distance in wavelengths depends greatly on frequency. Some antennas may even be of different topologies at different frequencies: for example the antenna in [30] is a microstrip patch antenna at 2.45 GHz but a top-loaded monopole at 5.8 GHz. Detuning appears more severe at 5.8 GHz than at 2.45 GHz, again showing that dipole and monopole structures are more sensitive to the body presence than patches.

We have addressed the problem of detuning in several publications: for 100 MHz dipoles in [P1], for 866 MHz dipoles in [P2, P3], and for various 1575 MHz antennas in [P4]. In the publications dealing with plaster anten-

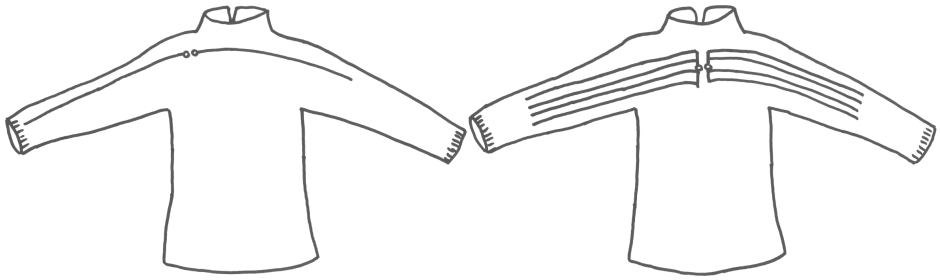

Figure 3.3: Body-worn dipoles for 100 MHz: a thin dipole on the left (1 cm wide), wide dipole on the right (total width 10 cm). In the measurements, the input impedances and radiation patterns of both antennas were measured with the feed point on the shoulder (as on the left) and behind the neck (as on the right).

nas [P5,P6] the change in resonant frequency was measured, but it was minor because of the chosen microstrip antenna topology. In all the publications we measured the input impedances of antennas worn by human subjects.

3.3.1 Detuning of Dipoles near 100 MHz

At 100 MHz the size of the human body is comparable to the wavelength (λ = 3 m). The penetration depth is 10 cm in skin, and 8 cm in muscle, and 18 cm in bone. Thus the skin is practically invisible, and even the muscle layer in the arms is not thick enough to block radiation. Only the torso is comparable to the penetration depth. The research involved four dipole antennas worn on the shoulders, with the antenna–body-separation s only 1 cm (0.3% of wavelength). Two of the antennas are illustrated in Fig. 3.3. We made a series of measurements with users of different sizes [P1]:

- Woman, 170 cm, 70 kg
- Small man, 170 cm, 70 kg
- Medium man, 180 cm, 80 kg
- Tall man, 190 cm, normal weight
- Tall and overweight man, 190 cm.

Variation in the body posture was seen to cause major detuning of the 100-MHz dipoles [P1]. With the user's arms outstretched, the effective (average) dielectric constant near the antenna is smaller than with the user's arms

Table 3.1: Detuning of 100 MHz dipoles in per cent. Resonant frequencies in each case are compared to the free-space resonant frequency 120 MHz: 91 MHz/120 MHz = 0.76, which gives 24% detuning. Antenna–body-separation distance is about 1 cm.

	Wide dipole		Thin dipole	
	arms down	arms up	arms down	arms up
Woman	24	16	20	13
Small man	22	15	19	16
Medium man	17	18	14	14
Tall man	24	18	20	16
Overweight man	30	20	21	14
Average	23	17	19	15
Standard dev.	4	3	3	1

hanging at his sides. The change in the effective dielectric constant is seen in the resonant frequencies, or detuning percentages as shown in Table 3.1. The detuning percentage is simply

$$100\% \cdot \frac{\text{detuning}}{\text{centre frequency}},$$

where the centre frequency can mean the resonant frequency or the frequency where the desired matching is achieved, depending on the application. We see that the detuning percentage is closely related to the traditional definition of fractional bandwidth (bandwidth divided by the centre frequency).

The size of the user's body affects the detuning at 100 MHz, but somewhat less than the posture. In the extreme comparison of the small and the overweight man wearing the wide dipole, we see almost equal detuning (20%) for the small man with his arms at his sides, and the large man with arms outstretched. In the case of a small man, the amount of tissue in the arms and shoulders is considerably less than for the overweight man, and the effective dielectric constant around the antenna smaller, causing less detuning. We note that the body size has the largest effect in the arms-down case, where the dipole is close to the torso.

In use, the resonant frequency itself is not of concern, but what matters is the impedance band around it. Ranging from 87 to 108 MHz, the 100-MHz FM band exhibits a 21% bandwidth. If an antenna with a 21% bandwidth is used on-body, only parts of the FM band will be within the defined bandwidth at any given time because of detuning.

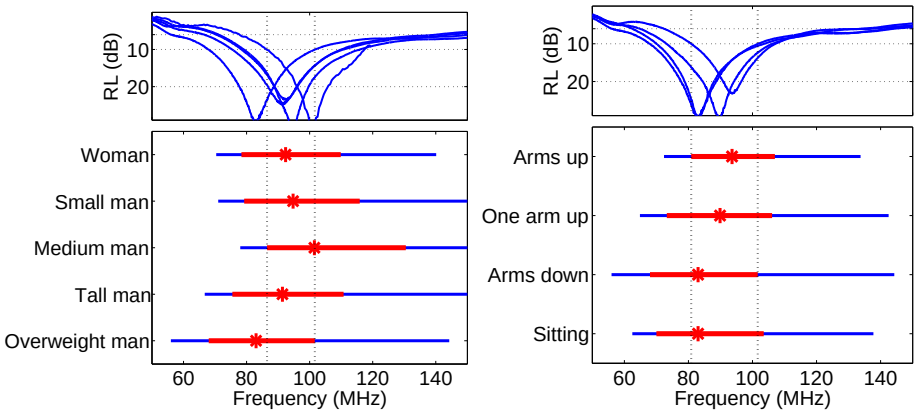

Figure 3.4: Above: Return loss of the wide dipole in different use cases. Below: The 6-dB bands (blue), 10-dB bands (red), and resonant frequencies. Left: worn by different users, arms hanging. Right: worn by overweight man in different body postures. Dashed lines show the usable 10-dB bandwidth where the return loss remains better than 10 dB in all the cases shown in the figure. The frequency axis limits are the same in all the figures.

We define the *usable bandwidth* as *the frequency range that satisfies the (impedance) specification in all use cases.* The use cases must be specified according to the application and can include, for example, different body postures, different user sizes, and different antenna–body-separation distances. The usable bandwidth cannot be measured as such because it would involve an infinite number of measurement cases, but in practice the cases can be restricted to the extremes and worst cases.

To illustrate the concept of usable bandwidth, Figure 3.4 shows the 6-dB and 10-dB return loss bands of the wide dipole, worn by different people with arms hanging down, and worn by the overweight man in different positions. The bandwidths in megahertz in different positions or with different users are all reasonably large. However, detuning causes the bands to move, so that the actual usable bandwidth becomes quite narrow. Usually a broadband antenna is needed for applications where the effect of body posture is significant.

More recently, the FM dipoles were studied further by Hu, Gallo, Bai, *et al.* [16]. The simulation model was very simple, consisting of an elliptical cylinder for the torso, another cylinder for the arms, and a sphere for the head. The phantom was homogeneous, with the properties of blood ($\varepsilon_\mathrm{r} = 77$, $\tan\delta = 2.9$, $\delta_\mathrm{s} = 5$ cm). The phantom was standing upright, with the arms

Table 3.2: Simulated detuning of a 100-MHz dipole as a function of the antenna–body-separation distance s, after [16]. The dipole is placed on the shoulders, with arms stretched out.

s (mm)	1	10	20	30
detuning (%)	18	9	6	4

outstretched. A thin dipole of the same size as in our measurement was placed 1.5 mm from the body, to get the simulation results to match our measured ones with an antenna–body-separation of 1 cm.

The simulations in [16, Fig. 12 and Tab. 4] show how the detuning is affected by the separation distance. A 9% detuning is presented for an antenna–body-separation of 1 cm. The results are repeated in Table 3.2 for convenience. If the antenna is printed on a coat, its distance from the body can vary between 10 mm (thickness of the coat and the clothes underneath) and 30 mm (very thick clothes, or loose coat). Thus the 1-mm case can be omitted from the comparison. The variation in detuning between the cases 10 and 30 mm is of the same order of magnitude as the effect of posture, and thus it should be taken into consideration when the usable bandwidth is determined.

In [16, Fig. 10], the effect of body posture was also investigated. A difference of only 1 MHz (about 1%-unit) is seen between the arms-stretched and arms-hanging cases. This major difference between the simulation and the measurement suggests that this very simple phantom is probably not detailed enough to represent the real situation.

3.3.2 Detuning of Dipole near 866 MHz

While the effect of posture is pronounced at 100 MHz, it becomes less and less important when the frequency is increased. At 866 MHz the body posture does not affect the resonant frequency [P2]. Instead, the antenna–body-separation distance is now the variable that determines the resonant frequency.

Our study at 866 MHz concerned a wearable, dipole-like RFID tag antenna of length 0.2λ [P2, P3], shown in Fig. 3.5. The antenna must be matched to a complex and frequency dependent impedance of the IC ($(16–j150)\ \Omega$ at 866 MHz), and thus the resonant frequency itself is not of concern. The

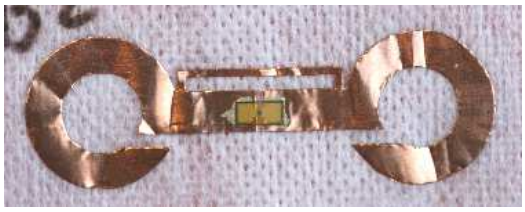

Figure 3.5: An RFID tag designed to operate at 866 MHz, 68 mm in length. An integrated circuit with impedance (16–j150) Ω is connected at the centre.

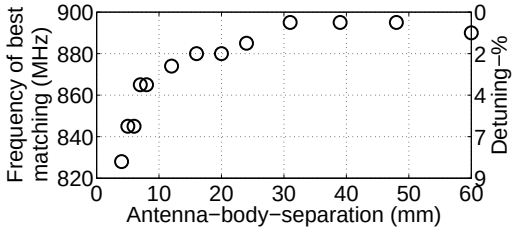

Figure 3.6: Detuning of the tag vs. antenna–body-separation distance.

detuning observed in our results was affected by the change in resonant frequency, the lowering of the antenna impedance, as well as the variation of the impedance of the IC with frequency. It is estimated that the actual detuning of the resonant frequency is greater than the detuning in best matching.

When the IC is connected to the antenna, it is possible to measure the realised gain when the IC sensitivity (the smallest input power to make the IC respond to commands) is known. Additionally, a known tag is needed to calibrate the measurement. The peak in the realised gain indicates the frequency of best matching since gain varies much more slowly with varying frequency than the impedance matching.

Figure 3.6 shows the observed detuning by the body when the antenna–body-separation distance is varied. With the smallest distances (4 to 10 mm, corresponding to 0.01λ and 0.03λ), the frequency of best matching changes more than 15 MHz/mm (2%/mm), but when the distance exceeds 10 mm, the rate slows down to less than 10 MHz/mm (1%/mm or less). There is no detuning for distances greater than 30 mm (0.09λ). This distance is significantly smaller than the 1.75λ reactive near-field distance suggested for quarter-wave dipoles [26].

The thickness and looseness of indoor clothing can be approximated to vary from 3 mm to 30 mm or more. This represents an uncontrolled detuning of

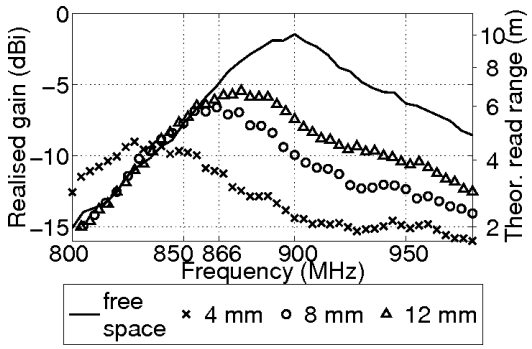

Figure 3.7: Realised gain measured with different antenna–body-separation distances. The goal is to have a constant realised gain at 866 MHz for the antenna–body-separation distances around 1 cm.

9% at the maximum. With the restricted antenna size we could not achieve a broadband design, and thus another approach was adopted. In designing the antenna, the expected distribution of antenna–body-separation distances was estimated, and based on that, the antenna was primarily designed for a distance of 1 cm. When the separation is large, we allow the frequency of best matching to be too high, but for small separations we aimed the best matching at 866 MHz, as shown in Fig. 3.7 (for clarity, only selected measurements are shown in the figure). As a result, the realised gain at 866 MHz is relatively insensitive to the variation in antenna–body-separation distance greater than 5 mm (0.01λ).

3.3.3 Detuning of Various Antennas near 1575 MHz

An investigation of the detuning effect at 1575 MHz was conducted in [P4], including a single-layer slot antenna, a two-layer slot antenna, an inverted-F antenna in one layer, and a printed dipole. The inverted-F antenna is presented in Fig. 3.8. The measurements were conducted using a male subject, 180 cm, 80 kg. The input return losses of the antennas were measured at different antenna–body-separation distances, from 0.6 mm (t-shirt only) to 37 mm (0.19λ), with bubble wrap and styrofoam between the antenna and the user. To find the maximum effect, the antennas were attached to the abdomen.

Figure 3.9 presents the return losses of the inverted-F and the dipole. Of the tested antennas, the dipole was the most sensitive to the presence of the

Figure 3.8: Single-layer inverted-F antenna for 1575 MHz.

human body. The resonant frequency of the inverted-F antenna, on the other hand, was only significantly affected when the user was closer than 3 mm to the antenna. The difference can be explained by examining the near-fields, shown in Fig. 3.10. Near the inverted-F antenna, the strongest electric field is confined to the gap between the F arm and the ground plane, and the field strength decreases very rapidly with increasing distance. The electric field of the dipole spreads wider, and thus, the user can influence the near-field and the impedance from further away.

Although the measurements showed no detuning in the case of the inverted-F antenna with an antenna–body-separation greater than 3 mm, the value of the resonant resistance was different from the free-space value. However, this presented no practical problem, because the impedance bandwidth was stable after the 3-mm distance.

The traditional near-field boundary for small antennas, $\lambda/(2\pi)$, is 30 mm at 1575 MHz. The resonant frequency of the inverted-F antenna was not affected by the user more than 3 mm away from the antenna. The input return losses of the two slot antennas returned to their free-space values at distance $s = 30$ mm $= \lambda/(2\pi)$. For the resonant frequency of the dipole to settle, a $\lambda/3 = 60$ mm distance was required. This is again smaller than the 1.75λ suggested in [26], but considerably larger than the value measured for the antennas with some form of gap where the near-field is the strongest.

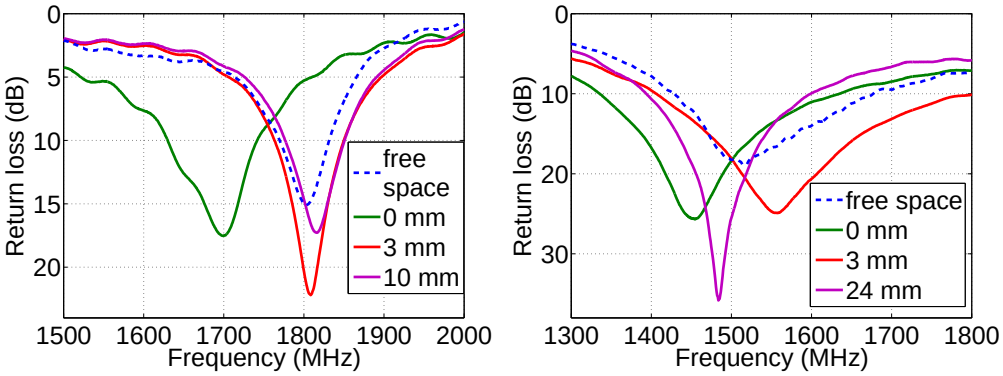

Figure 3.9: Left: The return loss of the inverted-F antenna is relatively stable for antenna–body-separation distances greater than 3 mm. Right: The return loss and resonant frequency of the dipole fluctuate even for quite large antenna–body-separation distances.

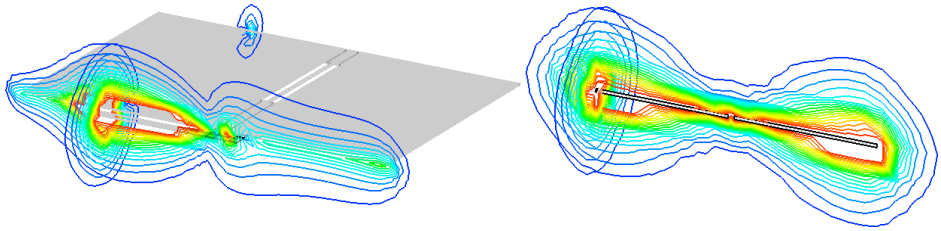

Figure 3.10: Simulated near-fields of the inverted-F antenna and a half-wave dipole. The electric field amplitude is shown. The fields are normalised to yield the same total radiated power.

3.4 Summary: Body Effect on Impedance

The input impedance of an antenna is related to the electromagnetic parameters in the near-field and the far-field. The resistance part describes the power that is removed from the system either as electromagnetic radiation or as heat in ohmic or dielectric losses. The imaginary part of the impedance represents the reactive near-field in the immediate vicinity of the antenna: electric and magnetic fields that oscillate but do not transfer power.

Because the greatest field strengths are found in the reactive near-field very close to the antenna (often taken to end at the distance of $0.62\sqrt{d^3/\lambda}$ or $\lambda/(2\pi)$ for small antennas), only objects or users very close to the antenna can affect the input impedance. Antennas in which the near-field is confined to a gap between the element and the ground plane (e.g. microstrip, inverted-F, or slot antennas) are more immune to surrounding objects than dipole-like antennas with the reactive near-field extending far away from the antenna.

A useful rule of thumb is to keep the user at least $\lambda/(2\pi)$ away from the antenna, if possible. Small antennas are traditionally defined as having the largest dimension smaller than $\lambda/(2\pi)$. Although small, most wearable antennas exceed this, but the general $0.62\sqrt{d^3/\lambda}$ reactive near-field limit is, on the other hand, certainly an overstatement.

If a human body is near the antenna, within the reactive near-field region, the resonant frequency will be detuned downwards. The larger the separation distance between the antenna and the user, the smaller the detuning will be. The impedance band of the antenna will move along with the resonant frequency, and we can determine the usable bandwidth of antennas by measuring their bandwidths in different conditions: varying distance, user size, or posture. The band covered in all the cases will be called usable bandwidth.

The input impedance of an antenna will be lowered by the user too close to the antenna. It is beneficial to design the impedance too high in free space, to allow good matching when body-worn. When losses are increased by the body presence, the Q value is lowered, and hence the bandwidth on-body is usually larger than in free space.

It is estimated that the body posture and proportions cease to affect the input impedance between 200 and 500 MHz, depending on the antenna size and its position on the body. We call this the *transition region* from low to high

frequencies. At 200 MHz, the adult thorax is approximately two penetration depths thick, and can be approximated as an infinitely thick tissue layer. For other body parts, the $2\delta_s$ thickness is achieved at higher frequencies, for the arms only at 1 GHz. With measurements it has been seen that posture plays a major role in impedance parameters of dipoles at 100 MHz, whereas at 866 MHz the impedance of a small dipole is unaffected by the position on the body or the posture. The separation distance (in wavelengths) between the antenna and the user is a key parameter at all frequencies, although at low frequencies the distance is always small.

Chapter 4

Body Effect on Radiation Properties

Being very lossy, the human body blocks nearly all the radiation backwards (through the body). This is commonly called shadowing. If omnidirectional radiation characteristics are desired, the antenna must be placed on the shoulder or on the head, or multiple antennas with a diversity scheme must be used. In multipath environments it is possible to utilise the reflections from the surroundings to communicate backwards.

This chapter describes the body effect on radiation parameters. An analytical model of reflection from a dielectric interface is presented first, and the results derived from this model are used to illustrate a new concept called *crossover distance.* The validity of the model in the context of wearable antennas is discussed, with special attention paid to the effect of losses in tissues. Next, we will first examine the body effect on the shape of the radiation pattern. Gain greatly depends on the antenna–body-separation distance, and we will treat this phenomenon separately from the pattern. Efficiency, a parameter closely related to gain, is also examined as a function of the distance. The chapter ends with a summary of the body effects on the radiation properties of wearable antennas.

4.1 Reflection from Dielectric Interface

When an antenna is placed next to a perfectly conducting plane, its radiation pattern is distorted because of reflection. Similarly, the wave impedance discontinuity at the boundary between air and tissue can be modelled as a reflector. Next, we examine the effect of this reflection on antenna radiation and especially the gain in the forward direction. Many simplifications are made in the model, and their applicability to wearable antennas is discussed. In Section 4.3, the simple model is refined with an efficiency model, and finally compared with measured and simulated gain data in Section 4.4.

4.1.1 Modelling Choices

For convenience, the following simplifications are assumed in the model:

1. The input impedance of the antenna is not affected by the body.
2. The antenna radiates a plane wave even when observed very close to the antenna.
3. The antenna is close to the body so that radiated power is not dispersed into free space.
4. The forward and backward gains of the antenna ($+z$ and $-z$ directions) are equal.
5. The body is locally planar and large, and can be approximated with a half-space of dielectric material.
6. The body is lossless or low-loss.
7. The body is homogeneous.

Impedance matching was already discussed in Chapter 3, where it was concluded that a surprisingly small antenna–body-separation distance is sufficient for simplification 1 to hold. Even if the input impedance changes, we can still assume that the radiation characteristics of the antenna remain the same as in free space, and that only mismatch loss (thus, realised gain) changes because of the body.

Any wavefront can be locally expressed as a linear combination of plane wave fronts, known as the plane wave expansion [7, Sec. 17.2.4A]. When we are only interested in the forward gain of an antenna close to the body, simplification 2, one plane wave only, will give reasonable results. The gain in directions other than perpendicular to the body would involve calculating the response of several plane wave fronts with polarisations parallel and perpendicular to the body surface.

Simplification 3 ensures that the free-space attenuation (dispersion of power on a spherical surface) between the antenna and the body is negligible. This holds true for all practical antenna–body-separation distances when the antenna is integrated into clothing. Simplification 4 is naturally false for most antennas, but its effect can be easily corrected, as will be shown later.

Even at 100 MHz, the thickness of the human torso is more than two penetration depths ($\delta_s = 8$ cm). If the antenna is considerably smaller than the torso, the torso can be regarded as large or even infinite, satisfying simplification 5. As an example limit we can choose that the antenna size must not exceed half the torso width, or $d < 20$ cm. Thus half-wave dipoles at 700 MHz satisfy the condition, as well as antennas smaller than $\lambda/2$ at lower frequencies.

Losses in the tissue, simplification 6, are discussed at the end of this section, and the effect of absorption by tissues is revisited in Section 4.3. Simplification 7 regarding the human as a homogeneous object is perhaps the most challenging one in applying the following results to real-life conditions. At each frequency and for each antenna–body-separation, the body can be represented by one average ε_r, similarly to the effective ε_r of microstrip lines, but how this number should be calculated remains unresolved.

To conclude, the listed simplifications can be regarded valid at least from 100 MHz onwards, depending on the antenna position on the body, and provided that the antenna is sufficiently small, and sufficiently far away from the body to return the input impedance to the free-space value.

4.1.2 Model

A conducting plane would reflect a plane wave with the reflection coefficient –1: the amplitude of the reflected wave is equal to the incident, but the phase

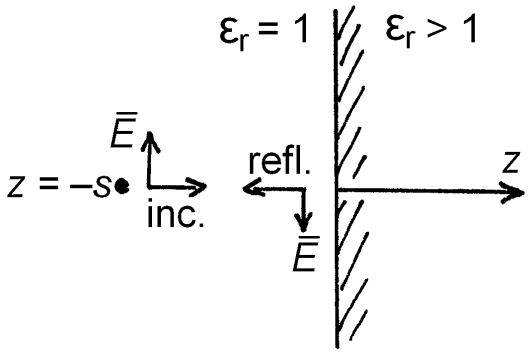

Figure 4.1: Simplified reflection model. The observation point or the antenna is placed at $z = -s$ in air, and the body is modelled as a half-space ($z \geq 0$) of dielectric material. When a plane wave is incident at the boundary, a reflection occurs.

is reversed. On the basis of simplifications 2 and 5, we can treat the human body as a similar reflector. The body is not a good conductor but the wave impedance in tissues is very low compared to the free-space value $\eta_0 = 377\ \Omega$, and this dielectric interface gives rise to a reflection. We can calculate the wave impedance in tissues using ε_r, the dielectric constant of the tissue:

$$\eta_\mathrm{tissue} = \sqrt{\frac{\mu_0}{\varepsilon_\mathrm{r}\varepsilon_0}} = \frac{\eta_0}{\sqrt{\varepsilon_\mathrm{r}}}. \tag{4.1}$$

The reflection coefficient at the dielectric boundary is obtained from

$$\Gamma = \frac{\eta_\mathrm{tissue} - \eta_0}{\eta_\mathrm{tissue} + \eta_0} = \frac{1 - \sqrt{\varepsilon_\mathrm{r}}}{1 + \sqrt{\varepsilon_\mathrm{r}}}. \tag{4.2}$$

Because η_tissue is always smaller than η_0, the reflection coefficient will be negative, i.e. the phase is reversed in reflection. This poses a problem: if the antenna is placed near the body, the direct and reflected fields will be out of phase, and the reflected field will cancel the field radiated by the antenna.

To model the reflection from the human body, we place a wave impedance discontinuity in the $z = 0$ plane and the antenna at $z = -s$, as in Fig 4.1. The half-space with $z < 0$ is air, whereas $z \geq 0$ is filled with dielectric material or perfect conductor. The total field amplitude at $z = -s$ can now be expressed as [9, Eq. 8-144]

$$|E_\mathrm{tot}(z = -s)| = |E_0| \left|1 + \Gamma e^{-j2\beta s}\right|, \tag{4.3}$$

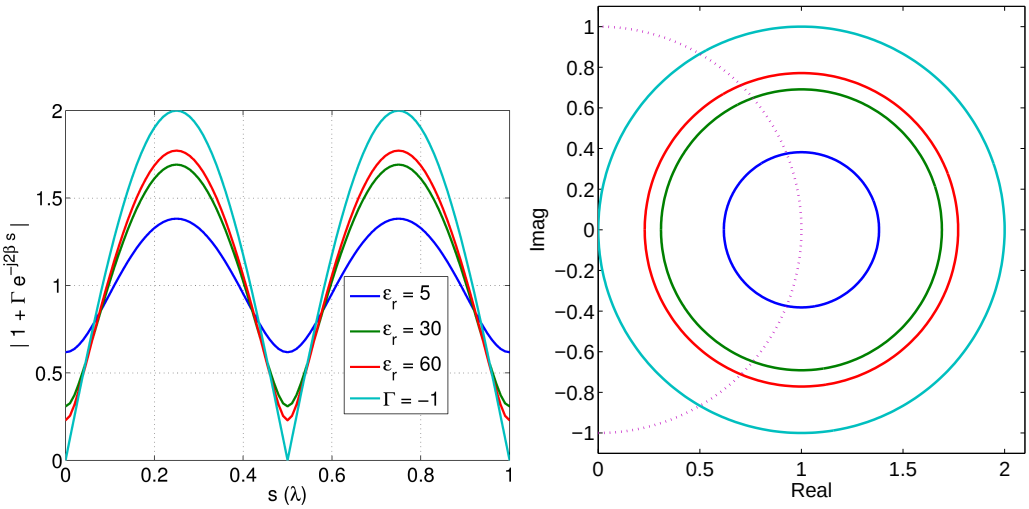

Figure 4.2: The field amplification $1 + \Gamma e^{-j2\beta s}$ as a function of antenna–body-separation distance s. The graph on the left shows the magnitude. The complex plane representation is shown on the right, with the dotted curve indicating the complex numbers whose magnitude is one.

where E_0 is the amplitude of the field radiated by the antenna alone, and β the wavenumber. From the point $z = -s$ onwards, the original and the reflected wave will continue to travel to the left, both gaining phase represented by $e^{+j\beta(z-s)}$. However, the amplitude remains constant:

$$\begin{aligned} |E_{\text{tot}}(z<0)| &= |E_0| \left|1e^{+j\beta(z-s)} + \Gamma e^{-j2\beta s} e^{+j\beta(z-s)}\right| \\ &= \left|E_0 e^{+j\beta(z-s)}\right| \left|1 + \Gamma e^{-j2\beta s}\right| = |E_0| \left|1 + \Gamma e^{-j2\beta s}\right|. \end{aligned} \quad (4.4)$$

The term $1 + \Gamma e^{-j2\beta s}$ in Eq. 4.4 represents the amplification or attenuation in the outward ($-z$ direction) going wave, caused by the reflection. We can plot it in the complex plane or its magnitude as a function of the antenna–body-separation distance s, as in Fig. 4.2. If the reflection is weak (small Γ caused by small ε_{r}), the field variation will be small as well. On the other hand, if the reflection from the wave impedance discontinuity is total ($\Gamma = -1$), there will be no radiation forward if the antenna is placed at $s = n\lambda/2$ ($n = 0, 1, 2, \ldots$) from the body. The square of this amplification, $|1 + \Gamma e^{-j2\beta s}|^2$, is the body-induced gain for omnidirectional antennas.

The most interesting aspect in Eq. 4.4 is not the position of the peaks and the pits. A distance of practical interest is the distance where the reflection neither cancels nor adds in the original wave amplitude. This is found in

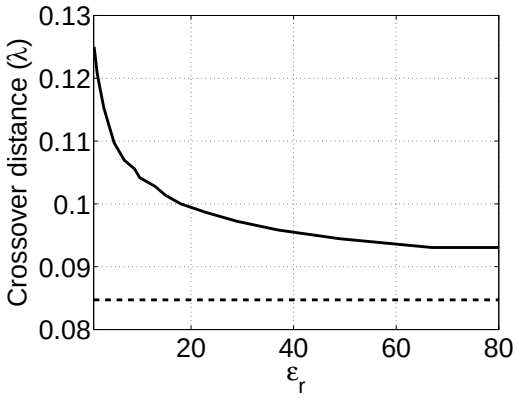

Figure 4.3: Crossover distance: if the antenna is placed at this distance from the body, the reflected wave will neither cancel nor add to the forward wave. The model assumes no absorption by the tissues. The horizontal line at 0.085λ indicates the limit set by the total reflection. Note that the vertical scale is relatively small: in determining the crossover distance in millimetres, the frequency (wavelength) plays a much greater role than the tissue dielectric constant.

Fig. 4.2 at the point where the $\left|1+\Gamma e^{-j2\beta s}\right|$ crosses one. Figure 4.3 shows this *crossover distance* in wavelengths as a function of ε_{r}.

When the field is fully reflected from the discontinuity, the reflection adds to the forward-travelling field in about 66% of all distances. This is seen in Figure 4.2: the magnitude curve is above 1 in 66% of the distances. For weaker reflections ($\varepsilon_{\mathrm{r}} = 5$) the portion is about 57%.

Figure 4.4 shows an example of how the dielectric constant of the tissue affects the body-induced gain. The antenna–body-separation distances are shown in wavelengths and translated to millimetres at 2.45 GHz. At this frequency, 15 millimetres is enough to yield positive body-induced gain. Beyond $\varepsilon_{\mathrm{r}} = 20$, the body-induced gain can be regarded constant with respect to the dielectric constant, except for the extreme cases where the antenna–body-separation distance is close to $n\lambda/2$ ($n = 0, 1, 2, \ldots$).

4.1.3 Modelling Choices Revisited

At the beginning of this section, simplification 4 stated that the antenna should radiate equally in the $+z$ and $-z$ directions. If this is not the case,

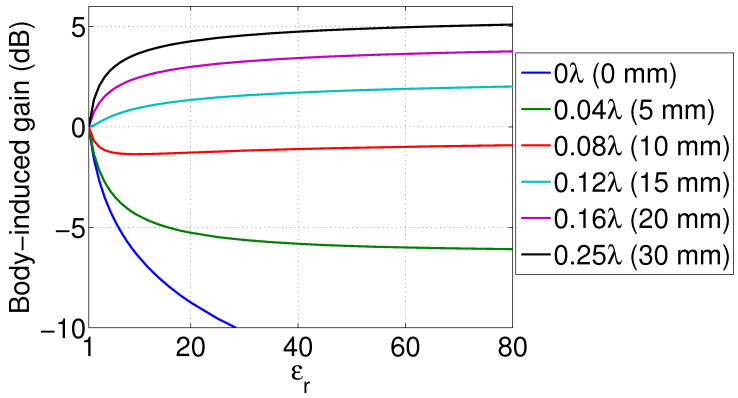

Figure 4.4: Body-induced gain as a function of the dielectric constant of the tissue, calculated from Eq. 4.4. The antenna–body-separation distances are given in millimetres at 2.45 GHz for convenience. The curve for 0.5λ would coincide with the 0λ curve.

we should modify Equation 4.4 to take the free-space radiation pattern into account. For the gains we can write

$$G_{+z} = |B|^2 G_{-z}, \tag{4.5}$$

where G_{-z} and G_{+z} are the gains in the $-z$ and $+z$ directions ($+z$ is towards the user) and $|B|^2$ is the inverse of the front-to-back ratio. The inverse has been chosen to avoid infinity for antennas that do not radiate backwards at all. When the antenna is placed on the body with its main lobe (if any) pointing outwards, we have $|B|^2 \leq 1$. Equation 4.4 can now be written in the form

$$|E_{\text{tot}}(z<0)| = |E_0| \left|1 + B\Gamma e^{-j2\beta s}\right|, \tag{4.6}$$

with B not squared because the equation refers to electric fields. The forward gain according to the model is

$$G(z<0) = G_{-z} \left|1 + B\Gamma e^{-j2\beta s}\right|^2, \tag{4.7}$$

where the term $\left|1 + B\Gamma e^{-j2\beta s}\right|^2$ is the body-induced gain. If we assume total reflection ($\Gamma = -1$) and omnidirectional antenna ($B = 1$), we get the body-induced gain given in [44, Eq. 8.2]. (For coefficient for gain, [44, Eq. 8.2] should be squared.) The maximum gain can be calculated from

$$G_{\max} = G_{-z}(1 + |B\Gamma|)^2. \tag{4.8}$$

This is achieved for $s = \lambda/4$ if B and Γ are real. At most, the reflection can add 6 dB to the gain, assuming that the magnitude of B is not greater than

one. It is evident and also intuitive that the reflection plays a smaller role if there is less radiation backwards.

The coefficient B can be complex, including information of the phase pattern of the antenna. Thus the total phase difference between the original and the reflected field at $z = -s$ would be $(\angle B + \angle\Gamma - \beta s)$, which would cause the magnitude curve in Fig. 4.2 to shift either left or right. For omnidirectional antennas such as dipoles or monopoles, the coefficient B is one, and B can be assumed a real number for most simple small antennas, indicating no extra phase shift.

So far we have discussed lossless dielectrics and a real wave impedance. Depending on the frequency and tissue, this may or may not be a sufficiently accurate model. At sufficiently high frequencies the tissue can be approximated low-loss, when $\tan\delta$ is small enough. The wave impedance in lossy dielectrics is given by [9, Eq. 8-50]

$$\begin{aligned}\eta_{\text{tissue}}^{\text{lossy}} &= \sqrt{\frac{\mu}{\Re\{\varepsilon\}}}\left(1 - j\frac{\Im\{\varepsilon\}}{\Re\{\varepsilon\}}\right)^{-1/2} \\ &= \frac{\eta_0}{\sqrt{\varepsilon_\text{r}}}\left(1 - j\tan\delta\right)^{-1/2} = \eta_{\text{tissue}}\left(1 - j\tan\delta\right)^{-1/2}, \end{aligned} \tag{4.9}$$

where η_{tissue} is given by Eq. 4.1.

To validate the low-loss tissue simplification, Figure 4.5 presents the error in the reflection coefficient calculated with Eq. 4.2 using the lossless model η_{tissue} given by Eq. 4.1. The contours in the figure show the $(\varepsilon_\text{r}, \tan\delta)$ points that would introduce a certain error, as indicated next to each contour curve.

The coloured curves in Fig. 4.5 present the points $(\varepsilon_\text{r}, \tan\delta)$ of different tissues between 100 MHz and 10 GHz. To distinguish between lossy and low-loss tissues, we can set the error limits of for example ±10% (–0.5 dB. . . +0.4 dB) in the reflection coefficient magnitude and ±20° in phase. We see that this condition is only violated by the fat and inflated lung tissues at 100 MHz. Already at 200 MHz, all soft tissues can be considered low-loss according to the condition. Thus the lowest frequency where the model can be considered valid is 200 MHz for small antennas, and 700 MHz for half-wavelength antennas, as set in Section 4.1.1.

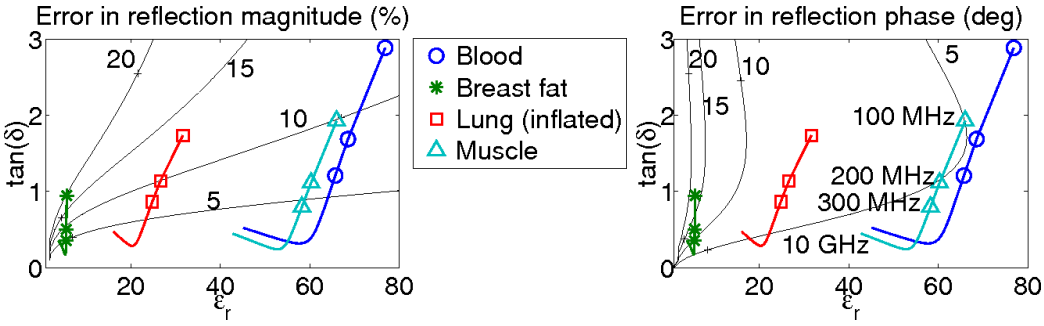

Figure 4.5: Tissues are low-loss above 200 MHz, according to the condition ±10% error in reflection coefficient magnitude, ±20° in phase. Contours show error (in % or degrees) in the "lossless" approximation (using η_{tissue} from Eq. 4.1), compared to the exact value ($\eta_{\text{tissue}}^{\text{lossy}}$ from Eq. 4.9). Error in reflection coefficient magnitude is shown on the left, error in phase on the right. In each set of tissue data, the first three frequencies are marked (100, 200, 300 MHz), and the line continues until 10 GHz. Tissue data is taken from [10]. Values for other soft tissues are close to muscle.

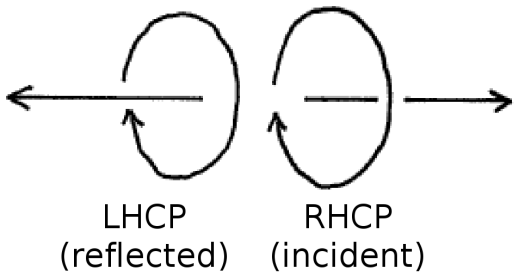

Figure 4.6: Sense of polarisation changes in reflection. The curved arrow shows the rotation of the electric field, and the straight arrow the direction of propagation.

4.1.4 Effect of Reflection on Circular Polarisation

From Equation 4.3 it is evident that reflection does not change the polarisation. However, if circular polarisation is used, the sense will change from left- to right-hand or vice versa. This happens because the propagation direction is reversed: although there is no change in the circle drawn by the electric field as a function of time, the direction of propagation defines the sense of polarisation. Figure 4.6 illustrates this.

If the antenna radiates right-hand circular polarisation (RHCP) equally in all directions, the wave front reflected from the wave impedance discontinuity

will be left-hand circularly polarised (LHCP). When RHCP and LHCP waves of equal amplitude are added together, linear polarisation will result.

In practice wearable antennas would not radiate RHCP in all directions. For example, RHCP microstrip antennas exhibit very little backwards radiation, and thus the reflection would not alter the polarisation in the forward lobe. Another example is the elliptically polarised inverted-F antenna, illustrated in Fig. 3.8 and examined e.g. in [P4]. Being single-layer and implemented on a thin low-permittivity substrate, the inverted-F radiates equally in both directions–but the senses of polarisation are opposite, as in Fig. 4.6. In this case the forward wave front will be in RHCP, the backward in LHCP, and the reflected wave again RHCP. The sense of polarisation of the sum wave front is now not changed by the reflection.

4.2 Shape of the Radiation Pattern of Antenna near the Body

In the context of wearable antennas, the human body is usually large compared to both the antenna size and the wavelength. Radiation does not penetrate the large and lossy body, and, as a result, a pronounced null appears in the radiation pattern of any antenna.

At low frequencies, where the body size is comparable to the wavelength and thin compared to the penetration depth, the shadowing effect is weaker. In the context of scattering, this frequency range is called the resonance region [45, Sec. 3.4.2]. Note that this refers to the fact that the human is of a resonant size, not the antenna. In some cases the human can actually act as a lens, enhancing backwards radiation. This was shown in [4] for 80-MHz dipoles held 10 cm from the body. However, the resonance region has little practical importance, and the main focus in this thesis is on the human effect on antennas at higher frequencies.

Creeping waves, or travelling waves that propagate along the human body on the shadow side, can provide some backwards radiation [2]. Travelling waves are only created under specific conditions: the electric field of the wave front must have both a normal and a parallel component to the body surface [22, p. 242]. In the context of wearable antennas, the condition means

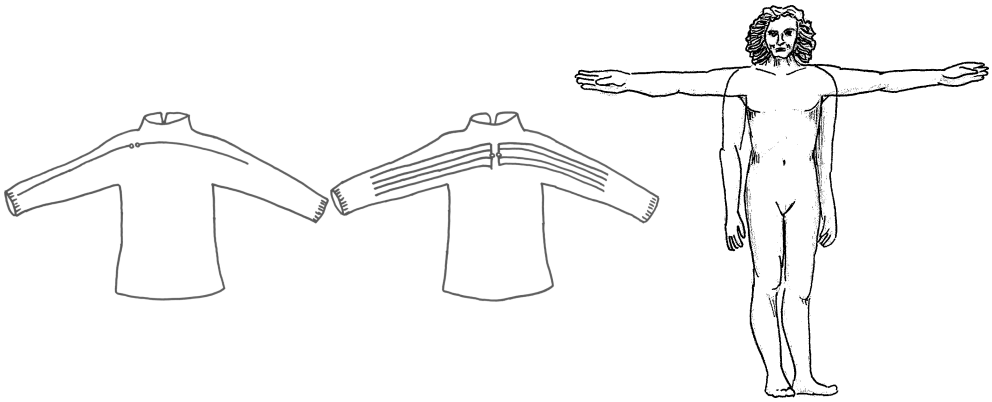

Figure 4.7: The 100 MHz dipoles under test, and the positions of the test subject. The dipoles are worn on the back.

that travelling waves can be created using monopole-like structures with the electric field normal to the body.

Propagating on the body surface, creeping waves exhibit a major attenuation of the order of 0.7 dB/cm at 1 GHz, less at lower frequencies [2]. Because of this attenuation, the magnitude of creeping waves is smaller than backwards radiation caused by multipath propagation [54]. We conclude that while creeping waves may be useful in on-body communications, it is usually not feasible to use them to provide backwards radiation in off-body systems.

4.2.1 Patterns of Dipoles near 100 MHz

The radiation patterns of body-worn half-wave dipoles placed on arms were measured in [P1] with a coarse 90-degree resolution. Figure 4.7 shows the dipoles, their alignment on the body, and the user postures: arms outstretched or hanging. Later, other research groups have shown interest in the results and conducted some further studies: The radiation patterns were simulated in [16], and Roh *et al.* experimented with embroidered dipoles and measured their radiation patterns [40].

In [P1], we measured the coarse radiation patterns of the body-worn half-wave dipoles on a rooftop measurement site, utilising a local FM broadcast station as the transmitter. The received power was recorded in four directions: the user facing the broadcast site, with the right or left side towards the site, and with the back towards the site. Note that the "forward" direc-

tion means that the user's back is towards the site and there is a line of sight from the antenna to the site.

At this frequency, the body is less than one penetration depth thick, and the shadowing effect is thus weak, if existent. Moreover, the position of the antennas on the shoulders was chosen to minimise the amount of tissue between the antenna and the horizon, i.e. the antennas were mounted on the upperside of the arms. The measured radiation patterns were relatively omnidirectional, with only a 4 dB variation in the wide dipole pattern, and 8 dB in the thin dipole. The lowest pattern levels were recorded when the wearer's side was towards the transmitter, regardless of whether the arms were raised or lowered.

No clear relation was observed between the size of the user and the gain, pattern, or front-to-back ratio. Although the shape of the radiation pattern was not affected by the body posture, the gain decreased by 4 to 8 dB when the arms were lowered, indicating greatly reduced efficiency. The measured maximum gains were approximately –17 to –13 dBi with arms stretched, and –20 to –17 dBi with arms hanging. Table 4.1 lists the front-to-back ratios and gains.

The low gains seen in Table 4.1 are an indication of power coupling into the body. The good matching shows that power is coupled effectively into tissue, but being lossy, the body radiates very ineffectively. The radiation efficiency of the system is thus low.

Roh *et al.* measured the horizontal patterns of an embroidered multiresonant folded dipole antenna. The antenna structure consisted of five folded dipoles of slightly different sizes, placed within each other. In free space the radiation pattern of a folded dipole resembles that of a simple half-wave dipole. The antenna was worn by a medium-sized male subject. In the cases where the user stretches his arms to the sides or forwards, the dipole is behind the arms and the shoulders. When he lets his arms hang down on the sides, the dipole rests on the sides of the arms. The measured realised gains are about –9 dBi with arms stretched at the sides, and –16 dBi with arms lowered. [40]

Hu, Gallo, Bai, *et al.* simulated the radiation patterns of a thin body-worn half-wave dipole. The simulation setup involved a simple phantom with properties of blood. The simulated front-to-back ratio is about 3 dB regardless of the antenna–body-separation distance (1 mm. . . 30 mm, only

Table 4.1: Front-to-back ratios and maximum gains of 100 MHz dipoles worn on the shoulders. "Front" means line-of-sight link between transmitter and receiver, "back" communication through the body. A positive F/B implies that the line-of-sight gain is larger than the gain in the shadow side.

	F/B		Max. gain	
	arms up	arms down	arms up	arms down
Thin dipole, measured [P1]	–1 dB	0 dB	–14 dBi	–17 dBi
Wide dipole, measured [P1]	+1 dB	+3 dB	–13 dBi	–20 dBi
Folded dipole, measured [40]	+2 dB	+6 dB	–9 dBi	–16 dBi
Thin dipole, simulated [16] (10 mm from the body)	+3 dB	–	–8 dBi	–

$0.0003\lambda \ldots 0.01\lambda$). The shape of the radiation pattern does not change with the separation distance. [16]

The simulation model in in [16] differs from the measured case in being homogeneous and of a simple shape. In addition, the antenna is placed exactly behind the arms when the user is seen face forward. In the measurements, the dipoles were worn above the arms and over the shoulders. This may be the reason for the slightly larger front-to-back ratio than the measured ones in [40, P1].

As seen in Table 4.1, the front-to-back ratios of body-worn dipoles at 100 MHz are close to 0 dB. A stronger shadowing effect can be seen at 300 MHz, where the measured front-to-back ratios of a body-worn dipole and a spiral antenna are reported at 15 dB [35]. A part of the increased F/B is due to the vertical antenna placement along the side of the body, which means that there is more tissue on the line-of-sight path behind the user. In any case, severe shadowing is seen already at 300 MHz. This is a further indication of the transition region from low to high frequencies between 200 and 500 MHz, discussed at the end of Section 3.4.

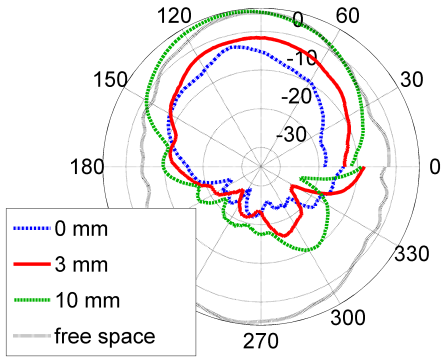

Figure 4.8: An example radiation pattern, in dBi, measured in free space and body-worn with different antenna–body-separations. The antenna under test is a single-layer slot antenna at 1575 MHz [P4]. The discontinuity at 0° is due to the measurement setup: uncertainty in the turntable angle as well as the posture of the wearer. The figure shows the horizontal plane cut, vertical polarisation.

4.2.2 Patterns of Antennas at 866 MHz and Above

Several radiation pattern measurements have been made in the high frequency range above the transition region (200 to 500 MHz). Above the transition region, the human body can be regarded as large compared to the wavelength, the penetration depth, and the antenna size. The body acts as a reflector, as described in Section 4.1, and shadowing is strong.

In our studies of a dipole at 866 MHz [P2, P3] and various single-layer antennas at 1575 MHz [P4] we have measured the radiation patterns of the antennas mounted on the body with different antenna–body-separation distances. The pattern of any antenna at these frequencies will be directional, with the main lobe pointing in the line-of-sight direction. Front-to-back ratios can be 20 or 30 dB. The polarisation in the main lobe was not affected by the reflection. As expected, no rise in the cross-polarisation level was detected.

Many other studies, for example [1,20,21,30,34,35,38,44] show a similar body effect to the radiation pattern: no radiation through the body. Figure 4.8 shows an example of the radiation pattern of an antenna in free space and body-worn.

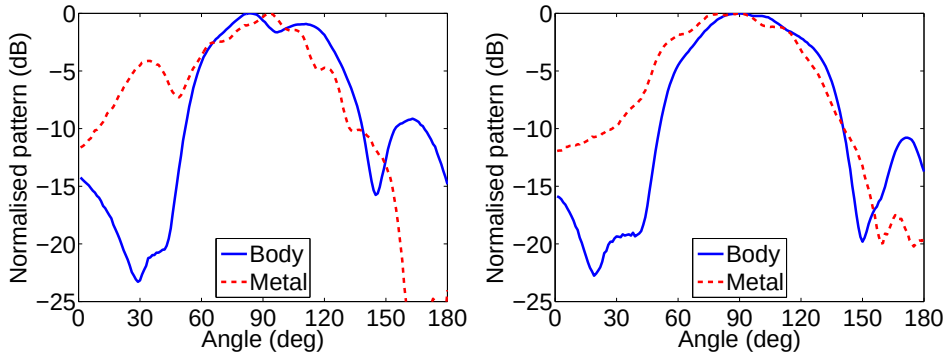

Figure 4.9: Normalised radiation patterns of the inverted-F antenna at 1575 MHz, measured body-worn and attached to a metallic plate of 38 cm by 38 cm. Left: 10 mm antenna–body-separation, right: 24 mm. The figures show the vertical plane cuts, vertical polarisation.

The effects of the human body and metal were compared in [P4]. The radiation pattern of the inverted-F antenna (Fig. 3.8) at 1575 MHz was measured with the antenna mounted on the body and on a metallic plate of 38 cm by 38 cm (2λ by 2λ). In terms of Equation 4.4, we changed the value of the reflection coefficient Γ from –0.7 (body) to –1 (metal). The measured forward patterns were seen to agree to some extent when the antenna–body-separation distance was 24 mm or more. Figure 4.9 illustrates the normalised patterns. The peak gains for the metal- and human-mounted antennas were different, as predicted by Eq. 4.7 and seen in Figure 4.2.

4.3 Efficiency vs. Antenna–Body-Separation

The efficiency of an antenna is often greatly reduced because of absorption when the antenna is placed near a human body. To describe this change, the quantity called *body-worn efficiency* has been proposed, defined as "the ratio of total radiated power when the antenna is body-worn to total radiated power when in free-space isolation" [44, p. 222]. The definition assumes no change in the impedance matching between the free-space and the body-worn cases, and hence body-worn efficiency can also be expressed as the ratio of radiation efficiencies with the antenna body-worn and in free space [43].

In practical applications where detuning is inevitable, such as body-worn dipoles at 100 MHz, a more reasonable figure of merit is the "body-worn

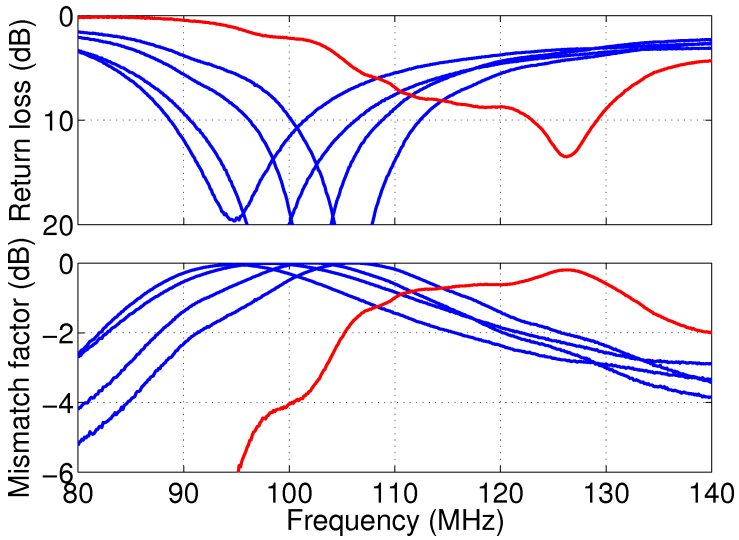

Figure 4.10: Return loss and mismatch factor of a wearable dipole. The red curve is measured in free space; the blue curves represent various body-worn cases. At the target frequency, 100 MHz, we have $\eta_{\mathrm{bw}}^{\mathrm{mismatch}} = \eta_{\mathrm{bw}} M^{\text{body-worn}} / M^{\text{free space}} = 2.5\eta_{\mathrm{bw}}$.

efficiency, including mismatch," $\eta_{\mathrm{bw}}^{\mathrm{mismatch}}$. It can also be written as the ratio of antenna efficiencies with the antenna body-worn and in free space, or

$$\eta_{\mathrm{bw}}^{\mathrm{mismatch}} = \frac{\eta_{\mathrm{ant}}^{\text{body-worn}}}{\eta_{\mathrm{ant}}^{\text{free space}}} = \frac{\eta_{\mathrm{rad}}^{\text{body-worn}} M^{\text{body-worn}}}{\eta_{\mathrm{rad}}^{\text{free space}} M^{\text{free space}}} = \eta_{\mathrm{bw}} \frac{M^{\text{body-worn}}}{M^{\text{free space}}}, \tag{4.10}$$

where the superscripts "body-worn" and "free space" refer to the set-ups where the quantity is measured, and M is the impedance mismatch factor ($0 \leq M \leq 1$).

In the case of well-designed detuning, the mismatch factor of the antenna worn on the body can be greater than in free space (indicating better power transmission into the antenna when it is body-worn). This is illustrated in Fig. 4.10, where detuning causes the "body-worn efficiency, including mismatch" to exceed body-worn efficiency more than twofold at the target frequency. In extreme cases of detuning, "body-worn efficiency, including mismatch" could even exceed 100%, which would indicate that the total radiated power from the system is greater in the body-worn case than in free space.

Representing the power losses in the human body, the body-worn efficiency is a useful figure of merit in wearable antenna design. It allows concept tests with poor materials, since the losses in the antenna itself are not visible in

body-worn efficiency. It is especially suitable for comparing the body effects on various antenna structures. On the other hand, antenna efficiency is a very useful figure of merit as it gives a number comparable to the overall power losses that reduce gain and are proportional to the power consumption of the wearable system.

The problem of efficiency dependency on the antenna–body-separation distance has been addressed with measurements. In the study of a dipole-like RFID tag antenna at 866 MHz in [P3] we measured the efficiency of the tag with the antenna–body-separation distances 8 and 20 mm (0.02λ and 0.06λ). The antenna was worn by a human subject. At 1575 MHz in [P4], we used a head-and-shoulders torso to measure the efficiencies of a dipole, an inverted-F, and a single-layer slot antenna. The antenna–body-separation distance was varied from 0 to 75 mm (0.4λ).

Simulations have been made by other researchers, for example, for multiple one- and one-and-half-layer antennas with the antenna–body-separation distance up to 8 mm (0.07λ at 2.44 GHz) [1]. These one-and-half-layer antennas include a ground plane but not under the radiating element such as the arm in an inverted-F antenna.

Figure 4.11 presents the simulated and measured body-worn efficiencies taken from the publications [1, P3], and from the measurements made for [P4]. If the body is $\lambda/(2\pi)$ away from the body, the body-worn efficiency for the investigated antennas is 60 to 80%. Beyond this antenna–body-separation distance the efficiency increases much less rapidly.

The data in Figure 4.11 can be estimated using a simple piecewise polynomial:

$$\eta_{\mathrm{bw}} = \begin{cases} -1460s^2 + 603s + 17 & , \quad s < 0.2\lambda \\ 3.3s + 78 & , \quad s \geq 0.2\lambda \end{cases} \tag{4.11}$$

which gives the body-worn efficiency in per cent when s is given in wavelengths. The equation is not applicable to antenna–body-separation distances of several wavelenghts. It is evident from Fig. 4.11 that the exact efficiency value depends on the antenna in question, especially with $s < 0.1\lambda$. However, this equation can be used as a starting point in estimating efficiencies or a reasonable antenna–body-separation for a certain application.

A sinusoidal behaviour is seen in the measured efficiencies in Fig. 4.11 between the antenna–body-separation distances 0.3λ and 0.7λ, indicating that the efficiency might be reduced when the antenna–body-separation distance

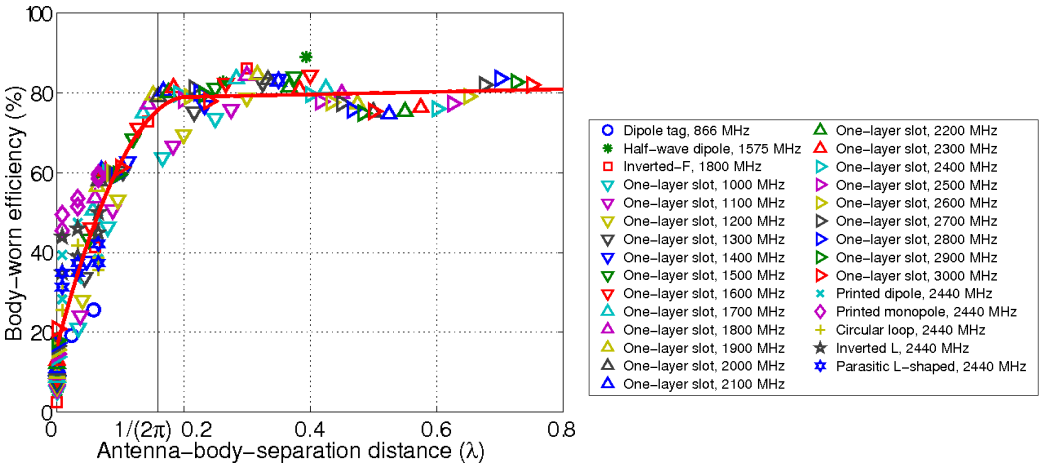

Figure 4.11: Body-worn efficiency as a function of antenna–body-separation, with the plot of Equation 4.11. Measured 866 MHz data from [P3], simulated 2440 MHz data from [1], and the rest of the data from the measurements made for [P4]. When the antenna–body-separation distance is increased to several wavelengths, the radiated power from the system will approach the free-space case, giving a 100% body-worn efficiency. The upper limit of the horizontal axis, 0.8λ, corresponds to 24 cm at 1 GHz and 8 cm at 3 GHz.

is increased. These data points have only been measured for one antenna (the single-layer slot [P4, Fig. 1a)]) and in one measurement setup, and hence no conclusions should yet be drawn.

4.4 Gain vs. Antenna–Body-Separation

The peak forward gain of body-worn antennas was treated analytically in Section 4.1. In this section the presented model is compared to experimental and simulational results.

Again, low and high frequencies should be addressed separately. For example, at 100 MHz the body is not large compared to a half-wave dipole, the human affects the impedance and near-field, and thus the simplifications in Section 4.1 are not valid. Moreover, the antenna–body-separation is very small compared to the wavelength in any reasonable use case. A transition region is found between 200 and 500 MHz, as discussed in Sec. 3.4. We will now consider only the frequency range above the transition region.

The measured and simulated results include data points with antenna–body-separation distances from 0 to 0.4λ, measured at 866 MHz and 1575 MHz, and simulated at 2.44 GHz. In our study in the neighbourhood of 866 MHz [P2, P3] we measured the realised gain of an RFID tag antenna placed at distances from 4 mm to 60 mm (0.01λ to 0.2λ) from the body. In a similar study at 1575 MHz [P4] the range was extended to 80 mm (0.4λ). The antenna under test was the inverted-F antenna in Fig. 3.8.

Alomainy *et al.* [1] simulated antennas at 2.44 GHz using a multi-tissue phantom [36], but the distances only ranged up to 8 mm (0.07λ). While some of the antennas were two-layer structures to allow microstrip feeding, there was no metal between the radiating element and the body (one-and-half-layer antennas), and the patterns were omnidirectional in free space.

Before comparing the measured and simulated data to the model, we must make sure that the model is valid for the case studies. Choice 1 given in Section 4.1.1 (impedance does not change because of the body) does not hold true for the tag at 866 MHz [P2, P3] and the 2.44 GHz antennas [1]. However, near 866 MHz we will observe the peak realised gain in the measured frequency range, and the mismatch loss can be estimated to vary from 0 to 3 dB. As for the 2.44 GHz antennas, the simulated far-field frequency 2.44 GHz falls in the –10-dB impedance band of the antennas in all the cases. This gives a mismatch loss smaller than 0.5 dB in all the cases, and we can simplify this as a constant mismatch loss. The rest of the choices are valid for all the measurements and simulations in [1, P2–P4]. In particular we note that all the antennas under test were omni- or bidirectional in free space, with equal gains towards and away from the body.

Figure 4.12 shows the measured and simulated results of the (realised) body-induced gain plotted against antenna–body-separation distance. The analytical solutions from Sec. 4.1 are also shown. While the overall trend in the measurements follows the model, the exact values do not match. The most striking difference is that the largest body-induced gain (in the region $0.15\lambda < s < 0.35\lambda$) is relatively low in any of the measurements.

One major difference between the analytical model and the data points in Fig. 4.12 is the absorption and the reduced efficiency: the model assumes no change in the radiation efficiency. If we include the simple efficiency model derived in Eq. 4.11, the peak gain predicted by the model decreases, as seen in Fig. 4.13. However, the model with efficiency now underestimates the body-induced gain for very small antenna–body-separation distances.

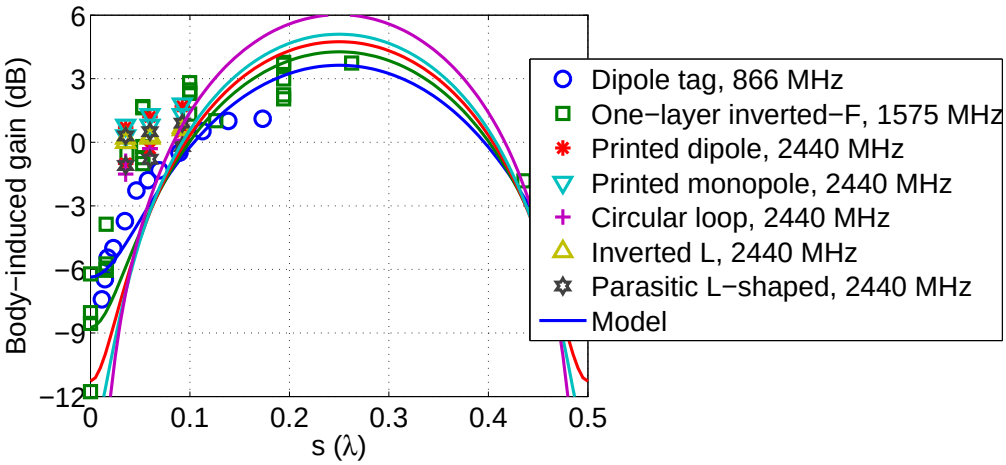

Figure 4.12: Measured or simulated body-induced gains of various antennas at different frequencies. Body-induced gain is the (realised) gain normalised to the free-space gain. Curves representing the model from Equation 4.7 and Fig. 4.2 ($\varepsilon_r = 10$, 20, 40, 80, and $\Gamma = -1$) are also shown. 866 MHz experimental data from [P3], 1575 MHz measurements from [P4], 2440 MHz simulation results from [1].

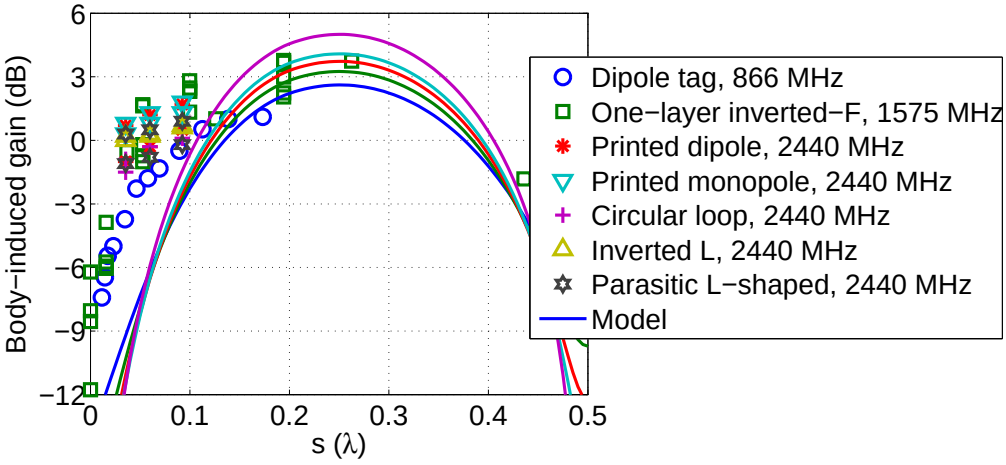

Figure 4.13: Measured or simulated body-induced gains of various antennas at different frequencies. Curves representing the model from Equation 4.7 ($\varepsilon_r = 10$, 20, 40, 80, and $\Gamma = -1$) multiplied by the simple efficiency model of Fig. 4.11 and Eq. 4.11 are also shown.

Next, we discuss the possible sources of difference between the model and the data points. First of all, the data points are few and concentrated in the region with small antenna–body-separation distances. The measurement uncertainty in both the gain and the antenna–body-separation must be taken into account. The mismatch factor was assumed constant in the model, but this is not the case in the measurements. The body cannot be taken as exactly homogeneous, large, and planar, especially with varying antenna position on the body. Finally, we note that the simulations in [1] seem to give a larger body-induced gain and efficiency than the measurements.

As seen from Figures 4.12 and 4.13, only two antennas have been measured with antenna–body-separations greater than 0.1λ. Although there are numerous different antenna–body-separation distances, and measurements have been repeated, more measurements would be needed in order to draw more general conclusions.

The uncertainty associated with the antenna–body-separation values in the measurements is of the order of 10%. The simulated antennas in [1] are modelled on a PCB substrate with $\varepsilon_\mathrm{r} = 4$ and thickness 1.6 mm. This extra thickness is taken into account in Figures 4.12 and 4.13 by increasing the distance by the thickness. The uncertainty of each individual gain measurement can be ± 1 dB or ± 2 dB. This also applies to the free-space gain which is used to normalise the body-worn gain values.

Possible changes in the mismatch loss (modelling choice 1) may alter the measured realised gain. The changes are small for other antennas, but for the 866-MHz tag antenna the mismatch loss can vary from 0 to 3 dB, being greatest for the largest antenna–body-separations. To make the data points that represent the tag follow the curve traced by the inverted-F antenna, we can add 2 dB to the realised gain of the tag for $s = 0.17\lambda$ and 1 dB to the data with $s = 0.11\lambda$ and $s = 0.14\lambda$. These corrections are in accordance with the estimated change in mismatch loss from 1 dB for small s to 3 dB for the free space.

Because the body is not homogeneous (modelling choice 7), any interface between different tissues can be seen as a wave impedance discontinuity. Multiple reflections occur between the antenna and the body, and this clutter can cause the measured body-induced gains to differ from the analytical result. This effect can, however, be approximated as quite small, since the multiple reflections are strongly attenuated by the losses in the tissues.

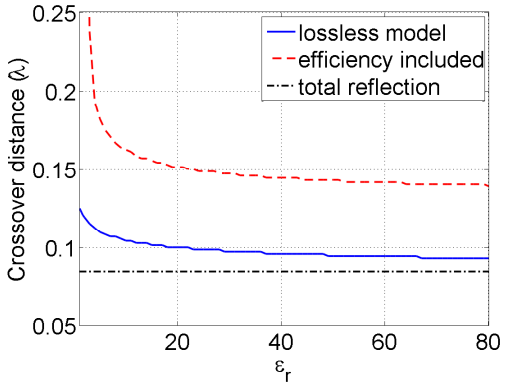

Figure 4.14: Crossover distance as a function of ε_r: with and without efficiency from Eq. 4.11. Crossover distance for total reflection ($\Gamma = 1$) is 0.085λ. Compare to Figure 4.3.

The 866-MHz tag was measured mounted on the arm and the inverted-F mounted on the chest. Plane (modelling choice 5) is a bad approximation of the shape of the arm at 866 MHz ($\lambda = 35$ cm), and the true magnitude of the reflection may be smaller than from a plane. On the other hand, the chest can be approximated planar at 1575 MHz ($\lambda = 19$ cm).

According to the simulations in [1], the position of the antenna on the body (chest, ear, waist, or thigh) causes the gain to vary ±2 dB at most from the mean value over all positions. Best gains were obtained when the antenna was placed on the waist and on the chest. Similarly, a ±1 dB variation in realised gain was seen when the tag antenna at 866 MHz was measured on the collar, back, upper arm, and wrist [P2]. The upper arm was found the best location in terms of gain, probably because of reduced absorption.

Reduced efficiency plays a major part in the body-induced gain. Figures 4.12 and 4.13 show that the simple efficiency model presented in Equation 4.11 overstates the efficiency reduction compared to the measured results for small antenna–body-separation distances. As seen in Figure 4.12, the crossover distance, where the forward gains in free space and on-body are equal, is well predicted by the simple model of body-induced gain. If the efficiency is included in the model, the crossover distance will be greater than in the lossless case, as illustrated in Figure 4.14. This means that a larger antenna–body-separation distance is needed for a 0-dB body-induced gain. However, the difference is approximately 0.05λ, which translates to a few millimetres between 1 and 3 GHz.

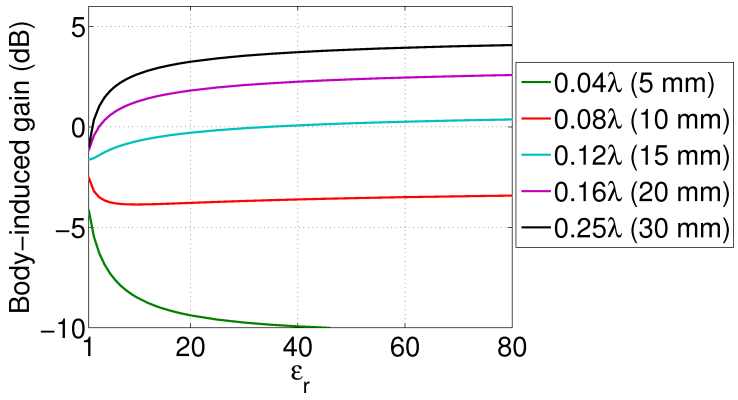

Figure 4.15: Body-induced gain calculated from Eq. 4.7, including the efficiency model of Eq. 4.11. An omnidirectional antenna ($B = 1$) is assumed. For convenience, antenna–body-separation distances are given in millimetres at 2.45 GHz. Compare to Figure 4.4.

Figure 4.15 shows the dependency of the body-induced gain on the tissue dielectric constant, calculated from Eq. 4.7 using the efficiency model Eq. 4.11. With reduced efficiency, positive body-induced gain is reached with an antenna–body-separation distance of 0.15λ.

In conclusion, the model developed in Section 4.1 and refined with efficiency in Section 4.3 does not completely succeed in predicting the peak forward gain. In particular, the efficiency model overstates the loss for small antenna–body-separations distances. However, the model can be used as a first step in designing wearable antenna systems or link budgets.

4.5 Summary: Body Effect on Radiation Parameters

The effect of the human body on antenna radiation properties is two-fold: When the antenna–body-separation distance is very small, absorption dominates, and reduction of efficiency is the major effect. If the distance is increased, the body can be modelled as a reflector that blocks radiation backwards but increases the forward gain.

Body-worn efficiency is the ratio of radiation efficiencies when the antenna is body-worn and in free space. According to measurements, the antenna–

body-separation of $\lambda/(2\pi)$ results in a body-worn efficiency of 60 to 80%. Below this limit, the body-worn efficiency decreases rapidly, but increasing the separation further results in only a small increase. A simple model of the effect of antenna–body-separation on body-worn efficiency was given in Eq. 4.11.

To model the human as a reflector, certain conditions have to be met: the body must be large compared to both the antenna and the wavelength, and the antenna–body-separation distance must be large enough to exclude detuning but small enough so that the antenna and the body can be reasonably treated as one electromagnetic system. A simplified reflection model was presented in Section 4.1 and improved by adding the efficiency in Sections 4.3 and 4.4. The model can be used as a starting point in designing wearable communication systems, but because the body-worn efficiency of different wearable antennas varies considerably, especially with small antenna–body-separation values, it is wise to check the results with measurements. The model is usable above 200 MHz for small antennas, and above 700 MHz for half-wave antennas.

The concept of crossover distance arises from the model of the human as a reflector. When the antenna–body-separation distance equals the crossover distance, the forward gain equals the gain in free space. The crossover distance can be used to indicate a reasonable minimum antenna–body-separation for wearable antennas, and perhaps used to compare different wearable antennas. Suggested by the model as well as measurements, the crossover distance is approximately 0.1λ to 0.15λ, depending on the antenna. This is equivalent to 1 to 2 cm at 2.5 GHz, or 3 to 4 cm at 1 GHz.

Although the forward gain can be increased with the reflection from the body, the radiation backwards is almost completely blocked above the transition region (200 to 500 MHz). Omnidirectional patterns can only be achieved by using multiple antennas or by placing the antenna, for example, on a hat or helmet.

Chapter 5

Specific Problems Associated with Wearable Antennas

The effect of the human body on antennas has been detailed in the previous two chapters. This chapter summarises the findings, and expands the problem field by introducing other aspects specific to wearable antennas: bending and other deformation, feeding, and materials. Finally, a list of new parameters for wearable antennas is presented. For clarity, most of the cross-references to the previous two chapters have been omitted.

Because most of the applications for wearable antennas are in the high frequency region, the discussion in this chapter is limited to wearable antennas that operate above the transition region (200–500 MHz).

5.1 Effect of the Human Body on Antennas

The human body makes wearable antennas less efficient radiators and may also interfere with the impedance matching between the transmission line and the antenna. Depending on the geometry of the human and antenna and the dimensions in wavelengths, the human can be approximately modelled either as a dielectric load and absorber, or as a reflector.

The strongest electric field intensities will be found near the antenna, in the so-called reactive near-field. For example, the field of the half-wave dipole can be presented with terms that are proportional to $1/r$, $1/r^2$, and $1/r^3$, where r is the distance of the observation point from the antenna. Only the terms with $1/r$ dependency are visible in the far-field. The higher-order terms mainly contribute to the near-field, and thus also the input impedance.

If the human body enters the reactive near-field of the antenna, it will both alter the field distribution and absorb power. Because power loss is comparable to the square of the electric field, absorption is especially strong in the near-field. The altered field distribution is seen as a change in the input impedance, whereas absorption affects both the impedance and the radiation efficiency.

Traditionally, the boundary of the reactive near-field is set at a distance of $\lambda/(2\pi)$ from a small antenna. This also gives a rule of thumb for wearable antenna designers: if the antenna–body-separation distance exceeds $\lambda/(2\pi)$, the impedance will be unaffected in most cases. With measurements it has also been shown that the body-worn efficiency of wearable antennas placed at $\lambda/(2\pi)$ from the body will be between 60 and 80%. Beyond this distance, the efficiency increases slowly. This indicates that absorption indeed is strongest in the reactive near-field. It is important to note that even if the impedance ceases to change at some antenna–body-separation smaller than $\lambda/(2\pi)$, this does not guarantee a good body-worn efficiency.

The input impedance of an antenna is usually lowered by the body. The change in impedance may also be seen as detuning of the resonant frequency towards lower frequencies. Because the amount of detuning mostly depends on the antenna–body-separation, it is important to measure the bandwidth of the antenna in many use conditions, to make sure that the required impedance band remains covered.

Apart from the reduction in efficiency, other radiation properties are affected by the body as well. The radiation through the body is blocked almost completely, and multiple antennas are needed for omnidirectional patterns. On the other hand, the forward gain can be increased by the reflection from the body. According to the simple model, the body-induced gain crosses 0 dB approximately at the antenna–body-separation of 0.1λ to 0.15λ, which we call the crossover distance. The 0.15λ limit coincides with the traditional near-field boundary $\lambda/(2\pi) \approx 0.16\lambda$. Measurements show even smaller crossover distances for some antennas. Crossover distance is unique for each antenna,

and the smaller the better. A smaller crossover distance often indicates greater body-worn efficiency.

The antenna position on the body, the size of the body, or the body posture do not affect the input impedance above the transition region (200 to 500 MHz), if the antenna–body-separation distance remains constant and the antenna is not covered e.g. by a hand. The shape of the radiation pattern and the forward gain are subject to change, but the variation in gain is only of the order of ±1 dB. The arm is commonly taken the best place for wearable antennas because it provides a stable shape, is usually elevated from the ground, and there is a line of sight to a broad angle.

Finally we note that low frequency antennas, such as antennas at 100 MHz, may exhibit small front-to-back ratios even when body-worn. Because the body size is comparable to the wavelength, penetration depth, and often also the antenna size, the impedance and detuning are affected by the body size and posture.

5.2 Other Problems that Arise from Wearability

In addition to the dielectric and lossy human body, wearable antennas are affected by bending, crumpling, folding, and stretching, as well as hostile environmental conditions in machine laundering. The performance should be guaranteed regardless of the weather and especially the ambient humidity, and the antennas should be as durable as the clothes they are integrated into.

The effect of bending GPS antennas was studied with measurements in [P7]. Bending and crumpling of coplanar and microstrip patch antennas has also been studied extensively by Bai, e.g., in [5, 6]. Bending changes the antenna impedance and may detune the resonant frequency, whereas the gain pattern is more robust. Circular polarisation is difficult to maintain in bent antennas.

Wearable antennas are used as a part of a body-worn radio system or connected to a handheld device. The user of such a system must be able to make all the necessary connections unaided. As a possible solution to the problem in connecting clothing antennas to transmitters, we proposed a snap-on button arrangement [P8], inspired by [8]. Commercial off-the-shelf buttons

were used to connect a thin coaxial cable to a microstrip line on a textile substrate. According to the measurements, buttons of diameter 7 mm proved feasible at least up to the 2.45 GHz ISM band. A larger frequency range is expected if smaller buttons are used because the transition is approximately two button diameters long.

Antenna materials–both conductive and substrate materials–pose a problem that has to be solved before any consumer applications can emerge. Conductive textiles are commercially available and have been used in many designs, for example in [29, 40, 51]. Antennas can also be inkjet printed using conductive ink, screen printed, or even sprayed using conductive paint.

Although antennas are traditionally made of solid copper or other metal sheets, it is possible to use web-like and meshed materials. In some cases the effect of the meshed material can be similar to the behaviour of a frequency-selective surface or an electromagnetic band-gap, and, for example, unwanted stop-bands can appear on a microstrip line. This phenomenon only occurs at high frequencies (near 10 GHz when one mesh cell was 0.3 mm or 0.01λ) and will not pose a problem if fine textile meshes are used. The antenna element or the microstrip line can also be made of the meshed material, not just the ground plane. [33]

Wearable antennas can be made of water-repellent materials. Synthetic fibres dry quickly. With meshed conducting materials, the whole structure can be made breathable. In washing, water may be trapped between insulating and conductive layers, possibly causing severe detuning and losses. Wet antennas will be very lossy, but according to [56], moist antennas can perform very well.

5.3 New Parameters for Wearable Antennas

Traditionally, antennas are rigid and their environment is not lossy. Their characteristics remain constant once they have been erected in their intended positions. Wearable antennas, on the other hand, are used near a lossy body and made flexible. Both bending and the presence of the body affect the antenna properties, and to describe the performance of wearable antennas, new parameters are often useful. Body-worn efficiency and body-induced gain have been used for wearable antennas in the literature, while the usable

bandwidth, detuning percentage, and crossover distance have been suggested in this thesis.

Body-worn efficiency and body-induced gain were introduced to the wearable antennas community some years ago [44]. Because body-worn efficiency is independent of impedance matching, the "body-worn efficiency, including mismatch" is sometimes a more useful figure of merit. It is defined in Eq. 4.10 as the product of body-worn efficiency and the ratio of mismatch factors, or as the ratio of antenna efficiencies.

The bandwidth of an antenna is traditionally defined as "the range of frequencies within which the performance of the antenna, with respect to some characteristic, conforms to a specified standard" [17]. Often the –10-dB return loss bandwidth is used. Because bending and body presence may detune wearable antennas, it is not sufficient to give only the –10-dB bandwidth of the flat antenna in free space, or of a bent antenna placed at one distance from the body. Rather, the bandwidth of the antenna should be measured in many use cases and the *usable bandwidth* given as a result. We define the usable bandwidth as "the range of frequencies within which the performance of the antenna, with respect to some characteristic, conforms to a specified standard *in any use case.*" Figure 3.4 illustrated the usable bandwidth. Strictly speaking, usable bandwidth cannot be measured, but it can be estimated from measurements of extreme cases.

At low frequencies the usable bandwidth of a single wearable antenna can be very narrow because of major differences in detuning by bodies of different size. This was seen in [P1]. The phenomenon must be considered when designing wearable low-frequency antennas: because dielectric loading by larger people introduces more detuning to lower frequencies, an easy solution is to make physically smaller antennas for larger wearers. This is easy to take into account when making clothes of different sizes, but it requires extra design work.

Detuning can also be expressed in per cent of the free-space centre frequency f_0: $100\% \cdot \text{detuning}/f_0$ gives the detuning towards lower frequencies. If the *detuning percentage* is given for a range of antenna–body-separation distances, it is possible to evaluate the sensitivity of the antenna impedance to the body presence, and hence estimate its applicability to body-worn systems. Detuning percentage is closely related to expressing the bandwidth in per cent. If detuning percentages for different body-worn cases vary greatly, this indicates a narrow usable bandwidth.

A new concept called *crossover distance* has been introduced. When a wearable antenna is placed at this distance from the body, its forward gain equals the free space value. Closer, the gain is smaller, and increases if the antenna–body-separation distance is further increased. Crossover distance can be used to indicate the required antenna–body-separation distance for a certain wearable antenna. According to a simple model and measurements, the crossover distance is approximately 0.1λ to 0.15λ (2 to 3 cm at 1500 MHz, or 1 to 2 cm at 2450 MHz), but it is unique for each antenna.

With the definition of body-induced gain, a purely sinusoidal approximation was given [44, p. 220] for a short dipole:

$$\text{body-induced gain} \sim \left(2\sin\left(\frac{2\pi s}{\lambda}\right)\right)^2,$$

where s is the antenna–body-separation distance. This approximation assumes a total reflection from the body surface, and the gain goes to zero ($-\infty$ dB) with $s = \lambda/2$. A more realistic model for the body-induced gain was given in Equation 4.7, where the magnitude of the reflection is taken into account.

Chapter 6

Single-Layer and Multilayer Antennas

Until now, most wearable antennas have been microstrip patches or inverted-F antennas with a ground plane between the antenna element and the user. The usual argument against single-layer antennas is that the body effect on single-layer antennas is stronger. Indeed the body effect on microstrip antennas can be negligible, whereas single-layer antennas are often greatly affected. However, there are many advantages to single-layer antennas that should not be overlooked.

This chapter compares the benefits and drawbacks of single- and multilayer antennas. First, examples of single- and multilayer antennas are presented. Once the benefits and drawbacks of each topology have been discussed, we will see that there are certain applications for both approaches, but also that single-layer antennas are often more practical than designers have been inclined to think.

6.1 Single-Layer Antennas

Single-layer antennas are the only reasonable choice in the VHF band, where the antennas must be physically large. At 100 MHz, the wavelength is 3 m. Options are more or less limited to dipoles, dipole-like monopoles with a

wired counterpoise, loops, and meandered variants of these. Any multilayer structures would be electrically very thin, less than one per cent of the wavelength, and therefore inefficient.

Examples of single-layer wearable VHF/UHF antennas include the 100 MHz dipoles in [P1], the dipole-like "asymmetrical meandered flare antenna" at 300 MHz in [38], and the wideband spiral antenna operating between 100 and 1000 MHz in [35]. In all these cases the antenna design aimed at a low profile for easy integration into clothing. The input matching was tuned for good matching when body-worn.

In designing the wearable RFID tag at 866 MHz (Fig. 3.5), the size was restricted to 10 cm by 3 cm, and there was no space for a ground plane of a reasonable size. Therefore a dipole-like single-layer structure was chosen. The antenna dimensions were tuned to ensure a stable performance at 866 MHz although the detuning by the body depends on the antenna–body-separation distance. At 866 MHz the wavelength is only 35 cm, and it is possible to make convenient antennas for example 0.03λ (1 cm) thick in clothing, if the area covered by the antenna is not restricted. [P2, P3]

The GPS antennas at 1575 MHz were designed to be single-layer for ease of fabrication. The wavelength is 19 cm, allowing two-layer structures and even $\lambda \times \lambda$ ground planes. In terms of fabrication and body effect on impedance, the inverted-F antenna (Fig. 3.8) was found to be a good design. The antenna includes a ground plane of $0.6\lambda \times 0.4\lambda$, but in the same layer with the F element. The strongest near-field is confined to the gap between the element and the ground plane. [P4]

Alomainy *et al.* experimented with single-layer wearable antennas at 2.45 GHz, in attempting to find the optimum design for operation close to the body. Their conclusion was the same as above: antennas with a narrow gap between the radiating element and the ground plane have the best performance. [1]

6.2 Two- and Multilayer Antennas

When low-profile antennas need to be very close to the body, the only option is to use multilayer antennas with a ground plane between the antenna and the user. Such was the case with the plaster antennas that are attached

directly to the user's skin [P5, P6]. The overall antenna height from the skin to the top of the antenna was 1.4 mm (0.01λ), and the body-worn efficiency of a single-layer antenna placed that close to the body would be about 10%, as approximated from Fig. 4.11.

Salonen and Rahmat-Samii present many conventional wearable antennas in [41]. All the antennas are microstrip patches designed on a fleece or felt fabric substrate with ε_r approximately 1.1. The circularly polarised GPS antenna (1575 MHz) is a square patch on a 4 mm thick substrate, with a $0.7\lambda \times 0.7\lambda$ ground plane. It is noted that the ground plane size affects the antenna resonant frequency even when the antenna is in free space. The ground plane of the dual-band U-slot patch operating at 1.9 GHz and 2.45 GHz is 110 mm $\times$ 130 mm in size, corresponding to $0.7\lambda \times 0.8\lambda$ at the lower resonant frequency. The substrate is 3.5 mm thick. Finally, a three-layer EBG patch structure is presented with a total height of 8 mm and a total size of $1.4\lambda \times 1.4\lambda$ at 2.45 GHz.

The effect of the body on a 2.45 GHz patch is studied with simulations by Salonen in [41]. This rectangular patch uses a substrate thickness of 3 mm and a ground plane of $0.6\lambda \times 0.6\lambda$. Detuning is shown to be minor, but the bandwidth is seen to widen considerably, which can be a sign of losses in the body. In addition, the resonant impedance changes, though it is not stated whether there is an increase or decrease. There is no significant difference in the radiation patterns simulated body-worn and in free space.

Vallozzi *et al.* have integrated a dual-polarised 2.45 GHz microstrip patch antenna in the protective garments of a firefighter. The structure is fabricated using textile materials only. The square patch rests on a 4 mm textile substrate and a ground plane of $0.8\lambda \times 0.8\lambda$. An antenna–body-separation distance of 2 mm is used in the measurements and simulations. Again, detuning by the body is minor, and the bandwidth is not significantly affected. The gain and radiation efficiency in free space and on-body are almost equal. [52]

A textile GPS antenna is proposed by Vallozzi *et al.* in [53]. This antenna is also designed for integration into the protective garments of firefighters. The textile substrate is 6 mm thick, and the ground plane made of conductive textile measures $0.9\lambda \times 0.9\lambda$. Some detuning is caused by the textile layers on top of the antenna, but the body effect on matching is quite small. However, the axial ratio band is shifted towards lower frequencies both by the superstrate and the body. The measured gain on-body is 1 dB smaller than in free space.

In [15], Hertleer *et al.* propose a circularly polarised textile patch antenna for 2.45 GHz. The ground plane dimensions are $0.8\lambda \times 0.8\lambda$, making the side length of the ground plane twice the patch side length. The authors suggest that the ground plane size should be at least 1.5 times the patch size for high and stable radiation efficiency. The design with ground length twice the patch length exhibits a radiation efficiency of 62% in free space.

The 1575 MHz circularly polarised textile patch presented by Kaivanto *et al.* [18] uses a ground plane $0.6\lambda \times 0.6\lambda$ in size. The substrate is 3 mm thick. The publication presents no results of the antenna worn on the human body, and hence gives no insight into whether the ground plane is of adequate size.

6.3 Benefits and Drawbacks of Single- and Multilayer Antennas

With the effects of the human body on antennas and other problems specific to wearable antennas detailed in previous chapters, we can now provide guidelines for choosing the antenna topology between the single- and multilayer options.

6.3.1 Benefits of Single-Layer Antennas over Multilayer

Perhaps the greatest benefit of single-layer antennas lies in their size. At low frequencies, the dielectric loading by the body helps to miniaturise the antenna. Dipole-like antennas without a ground plane can be made small to fit small features in the clothing. The antennas can be made thin, although some insulation must be ensured between the antenna and the user. This results in flexible and breathable structures that do not feel clumsy or uncomfortable.

Two-layer antennas tend to be large and thick and therefore unsuitable for certain garments. If a well-shielding ground plane is needed, it has to be of the order of $0.7\lambda \times 0.7\lambda$ in size or larger. This exceeds 20 cm × 20 cm at 1 GHz. Smaller ground planes can be used, but only at the cost of letting the body affect the antenna properties.

Single-layer antennas are easy to manufacture. Manufacturing multilayer antennas requires careful alignment of the layers. Possible vias between the two layers must be made especially sturdy. In use, the vias will be subjected to stress and are the first part of the antenna to break. In humid environments, dendritic growth of metal "whiskers" between metallisation layers may eventually short-circuit the antenna. On the other hand, dendritic growth is a problem in narrow slots in single-layer antennas as well. Because of their relative simplicity compared to multilayer antennas, single-layer antennas are expected to be more durable in use. No comprehensive studies exist of the durability of wearable antennas.

Compression does not affect the properties of single-layer antennas, and no constant thickness is needed. However, there is a minimum allowable antenna–body-separation distance for each single-layer antenna. In order to make the bandwidth of a microstrip patch antenna wide enough, it must be made thick enough, for example 0.07λ for a 10% bandwidth [7, Fig. 14.27]. In use, pressure or stretching may change the thickness of a multilayer antenna, which leads to detuning.

Deformation such as bending can significantly change the performance of microstrip patch antennas [6, P7]. Because thin patch antennas are usually quite narrowband, the impedance band may move completely off the desired frequency of use. To prevent changes in thickness, the substrate can be made rigid, but that renders the antenna inconvenient to use. Studies of the deformation of single-layer antennas have not been conducted, and it cannot be said which antenna topology would be more robust with regard to bending.

Single-layer antennas make wideband designs possible. The antennas can be made frequency-independent, like the spiral antenna in [35]. Even regular dipoles are relatively wideband compared to thin microstrip patches.

The human body can in some cases be used as a reflector. If more than 0.1λ to 0.15λ of antenna–body-separation distance can be allowed, the reflection will increase the forward gain (see Sec. 4.1). This phenomenon is sometimes applicable down to 1 GHz ($0.1\lambda = 3$ cm), and it is certainly useful at 2.45 GHz ($0.1\lambda = 1$ cm).

6.3.2 Benefits of Multilayer Antennas over Single-Layer

The greatest benefit in multilayer antennas is the shielding effect of the ground plane: the body effect on the antenna properties can be reduced to nil. The properties are stable regardless of the antenna–body-separation distance. On the other hand, lengthy testing and re-designing is required to design single-layer antennas that perform well in all conditions.

A very low absorption by the body guarantees a low SAR, allowing high transmitter power if needed in the application. Body-worn communication systems are often quite low power, and especially in receiving antennas and RFID systems the SAR is not of concern. However, for example, the portable radios used by firefighters or radio amateurs can use a transmitting power of five watts, and in order to conform with standards, low absorption must be guaranteed. Usually this requires the use of multiple layers in the antenna structure.

Microstrip patch antennas can be made of relatively poorly conducting materials without significantly affecting the radiation efficiency. In contrast, in narrow dipole-like single-layer wire antennas the conductivity is essential because the ohmic losses dominate. [32]

Although multilayer antennas, especially microstrip patches, are relatively narrowband, their impedance band is stable because detuning by the body is absent. The usable bandwidths of single- and multilayer antennas are often of the same order of magnitude.

Sometimes an EBG (electromagnetic band-gap) structure is suggested between the antenna and the user, and it is claimed that the EBG greatly reduces SAR and the human effect on the antenna properties. In most of these publications the EBG layer is both thick and large in area, and using a regular ground plane as large while making the antenna as thick would probably have resulted in the same improvement, if not better. The EBG structure usually even includes a ground plane, which provides a natural explanation to the lowered body effect. Carefully designed EBG structures can, however, be used to reduce the body effect. An EBG layer without a ground plane may be more convenient to wear than a solid ground plane.

6.3.3 Summary: How to Choose the Topology

Single-layer antennas should be used in wearable applications at low frequencies where it is not possible to use two-layer antennas. When the application requires a small antenna, single-layer antennas should be considered. The design should be measured carefully in all the expected use cases, especially for detuning. At high frequencies (at 2.45 GHz and above), the reflectivity of the body should be utilised in increasing the forward gain.

The best single-layer designs include a ground plane and a radiating element close to it. This configuration minimises the impedance changes and detuning. However, the body will still absorb radiated power.

Two-layer antennas are sometimes needed when the antenna is very close to the body or the absorption of power by the body must be lowered for health reasons. Generally, two-layer antennas require more space than single-layer antennas and are less comfortable to wear, but because the effect of the body can be considerably reduced, their properties are stable and they are easy to design and to test.

Most two-layer antenna designs are narrowband. Because of the minor body effect on the antenna impedance, the band is stable. However, deformations such as bending may detune the antenna.

The benefits and drawbacks of single- and multilayer antennas are summarised in Table 6.1.

A hybrid between single- and multilayer antennas would be a single-layer antenna (e.g. dipole) printed on the outer layer of a thick coat, and a thin, sparse conducting mesh sewn on the inner layer, close to the skin. When the coat is uncompressed, the dipole impedance would be unaffected by the body and the conducting mesh. Ideally, the mesh would improve the reflection properties of the body. With compression applied on the structure and the thickness reduced, the mesh could act as a ground, reducing radiation into the body. However, the mesh would also affect the impedance when the antenna is compressed, and this should be taken into account in the design process.

During the research conducted for the 866 MHz RFID tag, it was found that the presence of metal detunes the dipole less than the body but that the loss

Table 6.1: Summary of benefits (+) and drawbacks (–) of single- and multilayer antennas. The asterisk (∗) indicates no benefit nor drawback, and the question mark (?) means that no information is available.

	Single-layer	Multilayer
Detuning	–	+
Antenna–body-separation distance	–	+
Body reflection	+/–	∗
Deformation	?	–
Size	++	–
Thickness	+	–
Manufacturing	+	–
Quality of conducting materials	∗	+
Efficiency	–	–
Realised gain	∗	∗
Impedance bandwidth	+	–
Usable bandwidth	∗	∗
SAR	–	+

of forward realised gain is greater [P9, Fig. 2]. The results are also presented in Figure 6.1. This shows that the operation of a single-layer antenna with a conductive mesh backing must be carefully characterised, and it is not wise simply to add a conductive mesh to any single-layer design. It is also unwise to assume that any antenna designed to be used close to metal would operate close to the body.

Nonsolid ground planes were tested to some extent in [P5,P6], and a meshed ground plane in [33]. This is a subject worth further research. There are many open questions such as how sparse a mesh would act as a reasonable ground plane, and which is the more important parameter, the size of the mesh cell or the fraction of the area covered in metal.

To conclude the comparison between single- and multilayer antennas, we will finally compare their performance parameters, especially the gain. The comparison is based on many examples in the literature as well as the results of the research conducted for this thesis. We will also examine which structural properties determine the gain.

It is not surprising that the antenna gain depends on the size. What is not always evident is that this also applies to wearable antennas. Table 6.2 presents a summary of the antennas listed in Sections 6.1 and 6.2. Excerpts from the

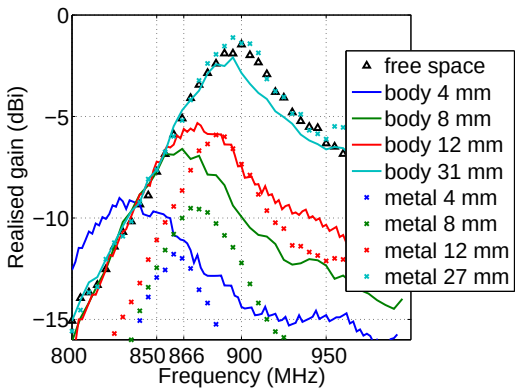

Figure 6.1: Detuning of a single-layer dipole by the body and by a metallic plate. The detuning effect of the body is much stronger.

same data are plotted in Figure 6.2, showing how the gain increases with antenna size but is not similarly affected by the total height of the antenna (thickness plus antenna–body-separation distance). Figure 6.3 presents the same trend for body-worn RFID tag antennas at 866 MHz: size matters much more than the number of layers.

With the gain of wearable antennas mostly determined by the size, not the number of layers or presence of a ground plane, we conclude that single-layer antennas are a choice worth considering when wearable antennas are designed. Especially at 2.45 GHz and above, the body should be used as a reflector, and designed as a part of the antenna.

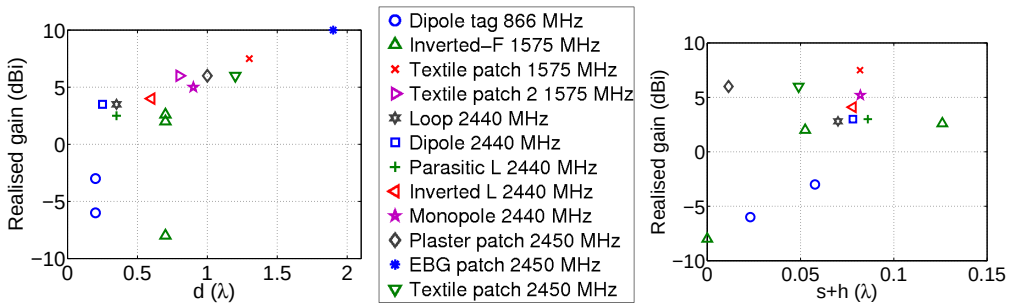

Figure 6.2: Gain depends on the antenna size (d, left), but the correlation between the gain and the total height of the antenna ($s + h$) is small. Measured 866 MHz tag from [P2], measured 1575 MHz inverted-F from [P4], measured 1575 MHz textile patch from [53], measured 1575 MHz textile patch 2 from [18], simulated 2440 MHz data from [1], measured 2450 MHz plaster patch from [P6], and simulated 2450 MHz EBG patch from [41]. The tag and the inverted-F antenna have been measured at multiple antenna–body-separation distances, represented by multiple symbols in the plots.

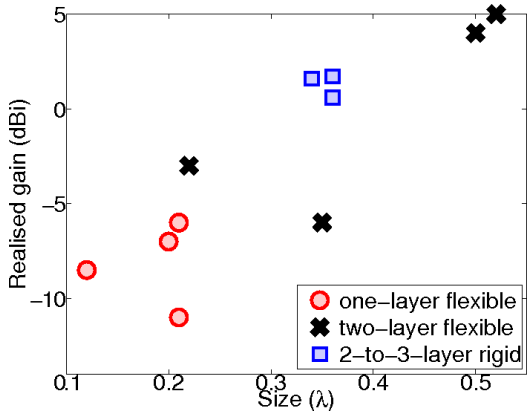

Figure 6.3: Realised gain of single- and multilayer RFID antennas worn on the body, measured or simulated in the 866 MHz band. The data is taken from [P9, Tab. I].

Table 6.2: Summary of the antennas listed in Sections 6.1 and 6.2. Antennas marked "1.5" layers are 2-layer antennas with no ground plane between the antenna element and the user. On-body gain is given if available; s = "–" indicates that the antenna has not been tested on the body. Asterisk (*) in bandwidth marks dual-resonant circularly polarised antennas. Measured results are marked with 'm' and simulated results with 's.' Antennas below 500 MHz are listed first, then the rest ordered by size. d denotes the largest dimension of the antenna, h the thickness, s the antenna–body-separation distance, BW the (impedance) bandwidth, G the gain (on the body if available), ant. eff. the antenna efficiency on the body, and b-w. eff. the body-worn efficiency.

Antenna	layers	d (λ)	h (mm)	s (mm)	10-dB BW	6-dB BW	G (dBi)	ant. eff.	b-w. eff.
AMF "dipole," m 300 MHz [38]	1	0.3	–	10	17%	30%	–13	–	–
FM dipole, m 100 MHz [P1]	1	0.4	–	10	30%	66%	–13	–	–
Wideband spiral, m 300 MHz [35]	1	0.6	–	?	>90%	>90%	–5	–	–
Dipole tag, m 866 MHz [P3]	1	0.2	–	8	–	–	–6	12%	19%
				20	–	–	–3	16%	25%
Loop, s 2.44 GHz [1]	1	0.3	1.6	8	–	–	3	37%	37%
Dipole, s 2.44 GHz [1]	1	0.3	1.6	8	11.8%	20.1%	3	43%	43%
Parasitic L, s 2.44 GHz [1]	1.5	0.3	1.6	8	5.7%	10.5%	3	37%	43%
Inverted L, s 2.44 GHz [1]	1.5	0.6	1.6	8	–	–	4	43%	43%
Inverted-F, m 1575 MHz [P4]	1	0.7	–	10	4.1%	7.6%	2	31%	41%
				24	4.8%	8.5%	2.6	65%	73%
Textile patch, m 1575 MHz [18]	2	0.8	3	–	5.1%*	7.2%*	6	–	–
Monopole, s 2.44 GHz [1]	1.5	0.9	1.6	8	23.6%	37.7%	5	59%	59%
Plaster patch, m 2.45 GHz [P6]	2	1	1.4	0	3.3%	6.4%	6	–	–
Textile patch, m 2.45 GHz [52]	2	1.2	4	2	3.4%	6.7%	6	–	–
Textile patch, m 1575 MHz [53]	2	1.3	5.6	10	9.4%*	13.0%*	7.5	–	–
EBG patch, s 2.45 GHz [41]	3	1.9	8	–	8.1%	18.4%	10	–	–

Chapter 7

Conclusion

Antenna operation near the body has been researched for over half a century. From whip antennas to integrated antennas in handheld mobile devices, the trend is now towards a seamless integration of communications devices and body-worn equipment. Healthcare and rescue services will be among the first domains to adopt body-worn antennas, closely followed by leisure and recreational applications.

The effect of the user's body on the antenna has been a major concern in designing wearable antennas, as well as the effect of the antenna on the user. Therefore it has been a widely accepted design rule to include a large conducting sheet, a ground plane, between the antenna element and the user. Most wearable antennas have been microstrip patches or inverted-F antennas.

Because of the large ground plane, microstrip patches require a large flat space in the garment, sometimes difficult to allocate. Single-layer antennas can generally be fitted into a smaller space, which is the major benefit of this topology. In the absence of a ground plane between the antenna and the user, the effect of the body on single-layer antennas will naturally be significant.

This thesis has set out to investigate and compile the effect of the human body on antennas, in order to provide a starting point for future wearable antenna designers. The emphasis has been on the frequency range from 100 MHz to 2.5 GHz, and on antennas with the metallisation in one layer only. Several

example antennas have been designed and measured at frequencies of interest within the range.

The effect of the human body on antennas is two-fold: If the body is very close to the antenna, in the reactive near-field, it acts mostly as an absorber, changing the impedance and greatly reducing the radiation efficiency. On the other hand, if the antenna is sufficiently far from the body ($\lambda/(2\pi)$), it can be modelled as a reflector with the reflection coefficient derived from the tissue dielectric constant alone.

When the human body enters the reactive near-field of the antenna, it alters the field distribution and absorbs power from the field. This is visible as a change in the input impedance. The input impedance value is usually lowered by the body, and the resonant frequency is tuned downwards. The magnitude of the effect depends on the antenna–body-separation distance as well as the frequency of interest. The effects can be compensated in the initial design by making the structure slightly too small and of a slightly too high impedance.

Dipole-like antennas are the most sensitive to the body presence because their reactive near-field strength decays slowly. This also applies to monopoles, loops, and other structures with slowly decaying fields. Structures with a gap between the element and the ground plane should be preferred since the strongest near-field will be quite local in the gap and rapidly decaying outside. The ground plane can be placed in the same metallisation layer as the element, and not necessarily between the element and the user.

A transition region is found between 200 and 500 MHz. Below this region, the size of the human body is comparable to the wavelength and penetration depth. The input impedance, resonant frequency, and bandwidth are determined by the body size and posture. Patterns of body-worn antennas can be omnidirectional, because the body is not large enough to block radiation.

Above the transition region, where many of the applications for wearable antennas are, the posture of the user or the antenna placement on the body are not significant in terms of impedance. For an on-body impedance equal to the free space value, some antennas need an antenna–body-separation of $\lambda/(2\pi)$, while the limit can be much smaller for some structures.

Because the body is electrically large above the transition region, the radiation pattern of any antenna near the body will be directional, with a deep

null in the direction seen through the body. The forward gain depends on the antenna–body-separation distance in a sinusoidal manner, giving rise to the concept of body-induced gain as proposed in [44, p. 219].

To characterise the losses in the body, we can use the quantity called body-worn efficiency, the ratio of the radiation efficiencies of the antenna body-worn and in free space [44, p. 222]. In measurements it has been seen that the body-worn efficiency of a single-layer antenna worn with the antenna–body-separation distance of $\lambda/(2\pi)$ is about 60% to 80%.

Because detuning depends heavily on the antenna–body-separation distance (and below the transition region, also on posture and body size), the limits of the impedance band vary in use. A new parameter called *usable bandwidth* has been proposed, defined as the bandwidth which satisfies the impedance condition in all expected use cases: all antenna–body-separation distances, all postures, all users. Additionally, detuning can be characterised by *detuning percentage* that indicates the per cent value of detuning and can be given as a function of the antenna–body-separation distance.

A new concept called the *crossover distance* is suggested in this thesis and defined as the antenna–body-separation distance where the presence of the body neither amplifies nor attenuates the forward gain, compared to the free-space case. Under certain conditions well applicable to wearable antennas, the crossover distance was shown to be approximately 0.1λ to 0.15λ. The 0.15λ limit coincides with the traditional reactive near-field boundary $\lambda/(2\pi) \approx 0.16\lambda$. Crossover distance indicates the minimum reasonable antenna–body-separation distance for a certain wearable antenna topology, and it can be used to compare antennas.

When the human effect on antenna impedance and radiation parameters is known, it is possible to design wearable single-layer antennas whose properties are affected by the body but that are nevertheless applicable. With many examples it was shown that the gain of wearable antennas depends mainly on the antenna size, and much less on the number of layers or total height of the antenna including the antenna–body-separation distance.

Both single-layer and multilayer antennas have their benefits, and both options should be considered when a wearable antenna topology is selected for a certain application. Especially, it is possible to design good single-layer wearable antennas if the effect of the body is taken into account in the design process.

A topic for future research is the dependency of body-worn efficiency on the antenna–body-separation distance. Interesting preliminary results have shown that the body-worn efficiency may not monotonically increase with increasing antenna–body-separation distance. This effect should be investigated with various antennas as well as various frequencies. Other open questions that need to be addressed before wearable antennas can emerge in consumer applications include material and manufacturing problems, durability, and the effect of the body on printed transmission lines.

Bibliography

[1] A. Alomainy, Y. Hao, and D. M. Davenport. Parametric study of wearable antennas with varying distances from the body and different on-body positions. In *IET Seminar on Antennas and Propagation for Body-Centric Wireless Communications*, pages 84–89. IET, 2007.

[2] T. Alves, B. Poussot, J.-M. Laheurte, H. Terchoune, M.-F. Wong, and V. Fouad Hanna. Analytical propagation modelling of BAN channels based on the creeping wave theory. In *Proceedings of the European Conference on Antennas and Propagation (EuCAP)*, Barcelona, Spain, April 2010.

[3] J. B. Andersen and P. Balling. Admittance and radiation efficiency of the human body in the resonance region. *Proceedings of the IEEE*, 60(7):900–901, July 1972.

[4] J. B. Andersen and F. Hansen. Antennas for VHF/UHF personal radio: A theoretical and experimental study of characteristics and performance. *IEEE Transactions on Vehicular Technology*, 26(4):349–357, November 1977.

[5] Q. Bai and R. Langley. Crumpled textile antennas. *Electronics Letters*, 45(9):436–438, April 2009.

[6] Q. Bai and R. Langley. Textile antenna bending and crumpling. In *Proceedings of the European Conference on Antennas and Propagation (EuCAP)*. IEEE, 2010.

[7] C. A. Balanis. *Antenna Theory, Analysis & design*. John Wiley & Sons, Reading, MA, third edition, 2005.

[8] I. Belov, M. Chedid, and P. Leisner. Investigation of snap-on feeding arrangements for a wearable UHF textile patch antenna. In *Proceedings*

of the Ambience 08, Smart Textiles–Technology and Design, pages 84–88, Borås, Sweden, June 2008.

[9] D. K. Cheng. *Field and Wave Electromagnetics*. Addison-Wesley Publishing Company, second edition, 1992.

[10] *Dielectric properties of body tissues*. Online, `http://niremf.ifac.cnr.it/tissprop/`; referred May 2, 2011, updated 1997–2007.

[11] *Finlandia-hiihto 2011*. Online, `http://finlandiahiihto.fi/info/`; referred May 2, 2011; updated February, 2011. In Finnish.

[12] C. Gabriel and S. Gabriel. *Compilation of the Dielectric Properties of Body Tissues at RF and Microwave Frequencies*. Online, `http://niremf.ifac.cnr.it/docs/DIELECTRIC/home.html`; referred May 2, 2011; updated November 6, 1997.

[13] P. S. Hall and Y. Hao, editors. *Antennas and Propagation for Body-centric Wireless Communications*. Artech House, 2006.

[14] P. S. Hall, Y. Hao, H. Kawai, and K. Ito. Electromagnetic properties and modeling of the human body. In P. S. Hall and Y. Hao, editors, *Antennas and Propagation for Body-centric Wireless Communications*, chapter 2, pages 11–38. Artech House, 2006.

[15] C. Hertleer, H. Rogier, L. Vallozzi, and L. Van Langenhove. A textile antenna for off-body communication integrated into protective clothing for firefighters. *IEEE Transactions on Antennas and Propagation*, 57(4):919 –925, April 2009.

[16] Z. H. Hu, M. Gallo, Q. Bai, Y. I. Nechayev, P. S. Hall, and M. Bozzetti. Measurements and simulations for on-body antenna design and propagation studies. In *Proceedings of the European Conference on Antennas and Propagation (EuCAP)*, Edinburgh, UK, November 2007.

[17] IEEE. *IEEE Standard Definitions of Terms for Antennas*, 1993. IEEE Std. 145-1993.

[18] E. Kaivanto, J. Lilja, M. Berg, E. Salonen, and P. Salonen. Circularly polarized textile antenna for personal satellite communication. In *Proceedings of the European Conference on Antennas and Propagation (EuCAP)*, Barcelona, Spain, 2010. IEEE.

[19] F. Keshmiri and C. Craeye. A Green's function approach for analysis of body-area-network antennas. In *Proceedings of the Loughborough Antennas & Propagation Conference (LAPC)*, pages 769–772, Loughborough, UK, 2009. IEEE.

[20] H. King. Characteristics of body-mounted antennas for personal radio sets. *IEEE Transactions on Antennas and Propagation*, 23(2):242–244, March 1975.

[21] H. King and J. Wong. Effects of a human body on a dipole antenna at 450 and 900 MHz. *IEEE Transactions on Antennas and Propagation*, 25(3):376–379, May 1977.

[22] E. F. Knott. Phenomenological examples of radar cross section. In E. F. Knott, J. F. Shaeffer, and M. T. Tuley, editors, *Radar Cross Section*, chapter 6, pages 225–268. Artech House, Inc., Norwood, MA, second edition, 1993.

[23] T. Kobayashi, T. Nojima, K. Yamada, and S. Uebayashi. Dry phantom composed of ceramics and its application to SAR estimation. *IEEE Transactions on Microwave Theory and Techniques*, 41(1):136–140, 2002.

[24] M. Konkel, V. Leung, B. Ullmer, and C. Hu. Tagaboo: a collaborative children's game based upon wearable RFID technology. *Personal and Ubiquitous Computing*, 8:382–384, September 2004.

[25] Z. Krupka. The effect of the human body on radiation properties of small-sized communication systems. *IEEE Transactions on Antennas and Propagation*, 16(2):154–163, March 1968.

[26] S. Laybros and P. F. Combes. On radiating-zone boundaries of short, $\lambda/2$, and λ dipoles. *IEEE Antennas and Propagation Magazine*, 46(5):53–64, 2005.

[27] M. Lazebnik, E. L. Madsen, G. R. Frank, and S. C. Hagness. Tissue-mimicking phantom materials for narrowband and ultrawideband microwave applications. *Physics in Medicine & Biology*, 50:4245–4258, 2005.

[28] *Life Alert 911 cell phone.* Online, `http://www.lifealert.com/911phone.html`; referred May 2, 2011.

[29] I. Locher, M. Klemm, T. Kirstein, and G. Tröster. Design and characterization of purely textile patch antennas. *IEEE Transactions on Advanced Packaging*, 29(4):777–788, November 2006.

[30] D. Ma and W. X. Zhang. A dual-band dual-polarized antenna for body area network. In *Proceedings of the European Conference on Antennas and Propagation (EuCAP)*, Barcelona, Spain, April 2010.

[31] L. Ma, R. M. Edwards, S. Bashir, and M. I. Khattak. A wearable flexible multi-band antenna based on a square slotted printed monopole. In *Proceedings of the Loughborough Antennas & Propagation Conference (LAPC)*, pages 345–348, Loughborough, UK, 2008. IEEE.

[32] R. Mäkinen. Personal communication, 2011.

[33] T. Maleszka, M. Preisner, and P. Kabacik. Meshed ground plane structures for textile antennas. In *Proceedings of the European Conference on Antennas and Propagation (EuCAP)*, pages 713–717, March 2009.

[34] G. Marrocco. RFID antennas for the UHF remote monitoring of human subjects. *IEEE Transactions on Antennas and Propagation*, 55:1862–1870, June 2007.

[35] J. C. G. Matthews, B. P. Pirollo, A. J. Tyler, and G. Pettitt. Wideband body wearable antennas. In *IET Seminar on Wideband, Multiband Arrays for Defence or Civil Applications*, March 2008.

[36] *The National Library of Medicine's Visible Human Project*. `http://www.nlm.nih.gov/research/visible/visible_human.html`; referred April 20, 2011; updated 1986–.

[37] *Pirkan hölkkä 2011*. Online, `http://www.pirkankierros.fi/indexho1.html`; referred May 2, 2011; updated Jan 27, 2011. In Finnish.

[38] D. Psychoudakis and J. L. Volakis. Conformal asymmetric meandered flare (AMF) antenna for body-worn applications. *IEEE Antennas and Wireless Propagation Letters*, 8:931–934, 2009.

[39] H. Raunio. Tulevaisuuden sairaala hyödyntää teollisuuden oppeja. *Tekniikka & Talous*. June 14, 2007. Available online, `http://www.tekniikkatalous.fi/kemia/article27019.ece`; referred May 2, 2011. In Finnish.

[40] J. S. Roh, Y. S. Chi, J. H. Lee, Y. Tak, S. Nam, and T. J. Kang. Embroidered wearable multiresonant folded dipole antenna for FM reception. *IEEE Antennas and Wireless Propagation Letters*, 9:803–806, 2010.

[41] P. Salonen and Y. Rahmat-Samii. Wearable antennas: Advances in design, characterization, and application. In P. S. Hall and Y. Hao, editors, *Antennas and Propagation for Body-centric Wireless Communications*, chapter 6, pages 151–188. Artech House, 2006.

[42] Satimo. A Microwave Vision company. Online, `http://www.satimo.com/`; referred May 17, 2011.

[43] W. Scanlon. Personal communication, 2011.

[44] W. Scanlon and N. Evans. Antennas and propagation for telemedicine and telecare: on-body systems. In P. S. Hall and Y. Hao, editors, *Antennas and Propagation for Body-centric Wireless Communications*, chapter 8, pages 211–239. Artech House, 2006.

[45] J. F. Shaeffer. Physics and overview of electromagnetic scattering. In E. F. Knott, J. F. Shaeffer, and M. T. Tuley, editors, *Radar Cross Section*, chapter 3, pages 63–114. Artech House, Inc., Norwood, MA, second edition, 1993.

[46] D. Simunic and D. Saik. Preparation of head tissue equivalent simulating liquid at mobile communications frequencies. In *IEEE International Symposium on Electromagnetic Compatibility (EMC)*, volume 2, pages 1237–1240, May 2003.

[47] *Smartcare turvaranneke*. Online, `http://www.smartcare.fi/web/guest/turvaranneke`; referred May 2, 2011. In Finnish.

[48] M. Švanda and M. Polívka. Extremely low profile UHF RFID tag antennas for identification of people. In *Proceedings of the European Conference on Antennas and Propagation (EuCAP)*, Barcelona, Spain, April 2010.

[49] M. Švanda and M. Polívka. Two novel extremely low-profile slot-coupled two-element patch antennas for UHF RFID of people. *Microwave and Optical Technology Letters*, 52:249–252, February 2010.

[50] J. Toftgård, S. N. Hornsleth, and J. B. Andersen. Effects on portable antennas of the presence of a person. *IEEE Transactions on Antennas and Propagation*, 41(6):739–746, June 1993.

[51] A. Tronquo, H. Rogier, C. Hertleer, and L. Van Langenhove. Robust planar textile antenna for wireless body LANs operating in 2.45 GHz ISM band. *Electronics Letters*, 42(3):142–143, 2006.

[52] L. Vallozzi, H. Rogier, and C. Hertleer. Dual polarized textile patch antenna for integration into protective garments. *IEEE Antennas and Wireless Propagation Letters*, 7:440 –443, 2008.

[53] L. Vallozzi, W. Vandendriessche, H. Rogier, C. Hertleer, and M. L. Scarpello. Wearable textile GPS antenna for integration in protective garments. In *Proceedings of the European Conference on Antennas and Propagation (EuCAP)*, April 2010.

[54] P. Van Torre, L. Vallozzi, C. Hertleer, H. Rogier, M. Moeneclaey, and J. Verhaevert. Indoor off-body wireless MIMO communication with dual polarized textile antennas. *IEEE Transactions on Antennas and Propagation*, 59(2):631–642, February 2011.

[55] S.-W. Wang, W.-H. Chen, C.-S. Ong, L. Liu, and Y.-W. Chuang. RFID application in hospitals: A case study on a demonstration RFID project in a Taiwan hospital. In *Proceedings of the 39th Hawai'i International Conference on System Sciences, vol. 8*, 2006.

[56] S. Zhu and R. Langley. Dual-band wearable textile antenna on an EBG substrate. *IEEE Transactions on Antennas and Propagation*, 57(4):926–935, 2009.

Publication [P1]

T. Kellomaki, J. Heikkinen, and M. Kivikoski.

Wearable antennas for FM reception.

In *Proc. European Conference on Antennas and Propagation (EuCAP)*,

Nice, France, November 2006.

Erratum

Table 1.

Last column reads: max. worn

Should read: min. worn

WEARABLE ANTENNAS FOR FM RECEPTION

T. Kellomaki, J. Heikkinen, M. Kivikoski

Tampere University of Technology, Institute of Electronics, P.O.Box 692, FI-33101 Tampere, Finland,
E-mail: Tiiti.Kellomaki@tut.fi, Jouko.Heikkinen@tut.fi, Markku.Kivikoski@tut.fi

ABSTRACT

The effect of human body on wearable 100 MHz antennas is studied by measurements. At that frequency, the body is very thin compared to the wavelength, but about half a wavelength tall. Antenna performance is most affected by the posture of the antenna wearer, second matter being antenna position on body. Physical traits of the wearer have only a slight effect on the antenna performance. A –13 dBi gain was achieved by the constructed dipole-like antennas, and letting one's arms hang down reduces this by 5 to 15 dB. Most of the power delivered to the antennas is absorbed by the human body, but some is radiated not only by the antenna but also by the body. Wearable antennas need to be shortened by 15 to 25 % from the free-space length to achieve the desired resonance frequency.

Key words: Antenna proximity factors, Antennas, Dipole antennas, Helical antennas, Receiving antennas, VHF antennas, Wire antennas.

1. INTRODUCTION

The antennas commonly used for 100 MHz FM reception by portable radios include monopoles, ferrite antennas, and even hands-free-set cables. Being small and often poorly aligned or wrapped, they degrade reception quality.

At 100 MHz broadcast band, a half-wave antenna is 150 cm long and thus inconvenient to carry. One solution is to integrate the antenna into clothing. If the antenna can be made flexible, its large size will not be of inconvenience to the wearer. However, with the antenna so close to the body, effects of the vicinity of the wet and dielectric human must be taken into consideration. At gigahertz frequencies, the human body can be shielded out with the help of a ground plane, but at 100 MHz, the body being much smaller than a wavelength, that is not possible.

Here, four antennas are examined, all dipole-like. The antennas are described in section 2. Return losses and crude radiation patterns are measured. The effect of the human body on both is studied. Section 3 describes the measurements, and results are listed in section 4.

2. THE ANTENNAS UNDER INVESTIGATION

Four antennas were constructed and measured. They include a thin and a wide half-wave dipole, a meandered dipole, and a normal-mode helix. A loop antenna was also considered, but being so big and clumsy, rejected. The antennas were designed to be resonant near 100 MHz when worn by a human. The 100 MHz broadcast band ranges from 87 to 107 MHz, corresponding to a bandwidth of 21 %, which means that the size of the antennas cannot be reduced much from half a wavelength [1].

All of the four antennas were constructed on a thick fleece fabric. 1-cm-wide copper foil tape was used as the conducting material. A coaxial cable was soldered at the feed point. The dielectric constant of the fleece fabric is approximated to be about 1.1. The antennas were designed to be printed on the inside of a coat, so the fleece fabric was chosen to be as thick as 8 mm to resemble clothing worn under the coat, between the antenna and the skin.

The two straight dipole antennas were both 116 cm long. The thin dipole (Fig. 1) is 1 cm wide, and the wide dipole was constructed of four parallel 1-cm-wide copper foil tapes forming a 10-cm-wide structure (Fig. 2). The meandered dipole (Fig. 3) consists of a zigzag pattern where the wire is bent every 16 to 25 cm. The antenna is 80 cm long and 23 cm wide at most, and a total of 160 cm wire is used. The exact shape of the antenna is not crucial, as shown e.g. in [2].

The helical antenna was constructed in the form of a sleeve, and the wire coils around the arm one and a half times. Between each section, there is a 10-cm space. The helix is about 25 cm long, using a total of 70 cm of wire, and there is a 58-cm-long linear counterpoise. The antenna is depicted in Fig. 4.

It should be noted that all of these antennas are of a relatively low impedance (near 50 ohms). The antennas were made resonant to avoid matching circuits which would be nearly impossible to construct on a real garment.

3. MEASUREMENTS

The return losses of the antennas were measured using a HP8722D network analyzer. For the radiation pattern

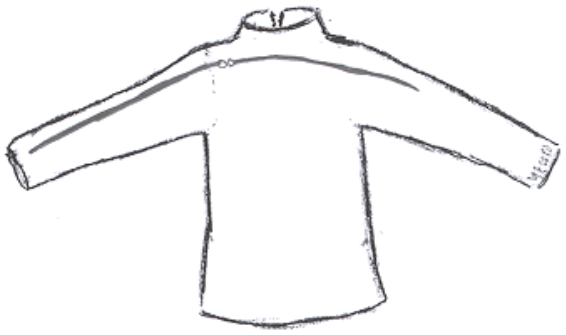

Figure 1. The thin dipole worn asymmetrically.

Figure 2. The wide dipole is made of four parallel wires.

Figure 3. The meandered dipole.

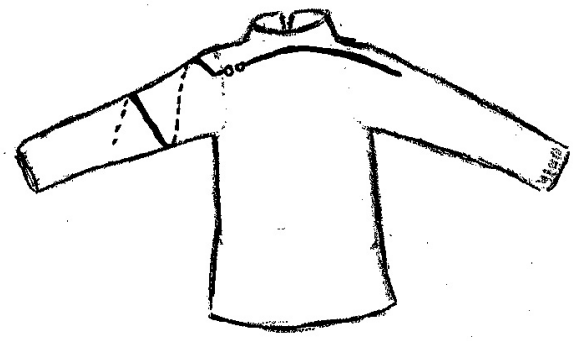

Figure 4. The helical antenna coils around the user's arm.

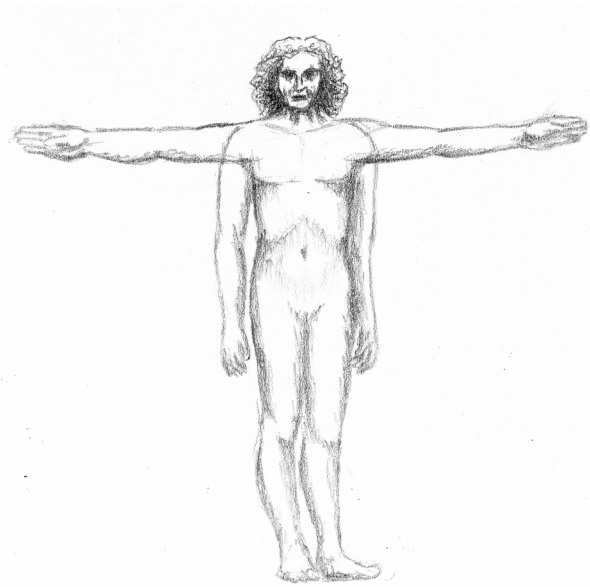

Figure 5. Postures in the measurements.

measurement, an Agilent E4407B spectrum analyzer and an EMCO 93110B antenna were used.

To examine the effect of sex, body height, and weight, five testees were chosen: one female, one tall and overweight male, and three men whose height ranged between the two aforementioned.

In the return loss measurement, the test person wearing the antenna would stand in the middle of a room with his arms hanging down or stretched out (Fig. 5), or sit with the arms on the armrests. The antenna was placed on the arms either symmetrically with the feed point behind the neck (see the antenna position in Fig. 2), or asymmetrically, with most of the wire on one arm (as in Fig. 1).

To avoid measuring the radiation patterns in the near-field, we would have had to build a 20-m free-space measurement range. Instead, we chose to use a local broadcast station as the transmitter. The roof of the university building was chosen as the receiving spot, and thus a 20-km free-space range was created. No turntable was available on the roof, so the antenna gain was measured in few directions only. The radiation patterns were measured with the testees standing with their arms both hanging down and stretched out. The measurement was limited to horisontal polarisation only.

To simulate real listening conditions, the testees walked, crouched, and waved their arms while turning around. Meanwhile, the maximum and minimum gains were recorded.

The helical antenna was not measured worn by the largest man because the sleeve had accidentally been made too tight for him.

The only reasonable antenna positions on the body are resting on arms, from the armpit to feet along the torso, and half along the torso, half on the arm. When the antenna is positioned in one of the two latter ways, its impedance is not much affected by the moving of the arms because the antenna is always near the large dielectric torso.

If the antenna is positioned on torso alone, it radiates in vertical polarisation only but without nulls in horisontal pattern. By placing the antenna on arms a reasonable amount of both polarisations is ensured at least when the wearer lets his arms hang down. However, this position brings about nulls in pattern.

To minimise absorption by the user's body, the only position considered here is the antenna resting on the user's arms.

Error sources in the measurements include the testees posing differently, reflections from surrounding objects and polarisation impurity of the received signal in the radiation pattern measurement, and damaging of the antennas during the measurements.

4. RESULTS

Besides the return loss and radiation patterns, variation due to posture and personal traits was studied. The resonance frequencies of the antennas were lowered by 15 to 25 % when the antenna was brought near the body, and at the same time the resonances were deepened and sharpened. The radiation patterns of the antennas are obviously dipole-like but with only weak nulls. Variation in the wearer's posture affects the antenna performance the most, the second matter being the wearer's personal traits.

4.1. Impedance and resonance

The resonance frequencies of all the antennas were lowered by 15 to 25 %, depending on the position of the wearer's arms, when the antenna was brought near the body. For comparison, the human head lowers the resonance frequency of a monopole at 900 MHz about 10 % [3], [4]. At 1.9 GHz, the effect is 7 % for a monopole antenna [4] and 15 % for a meandered planar antenna [5].

The return loss curves of all the antennas but the wide dipole consist of one resonance only, and are not much affected by the vicinity of the human body, except that

Table 1. Antenna bandwidths (in per cent) in free space and worn. Typical and minimum values are given for the latter. The wide dipole has two 10-dB bands in free space.

	free space	typ. worn	max. worn
thin dipole	5	12…14	11
wide dipole	10 + 5	30…37	27
helix	11	11…12	11
meandered dipole	8	7	4

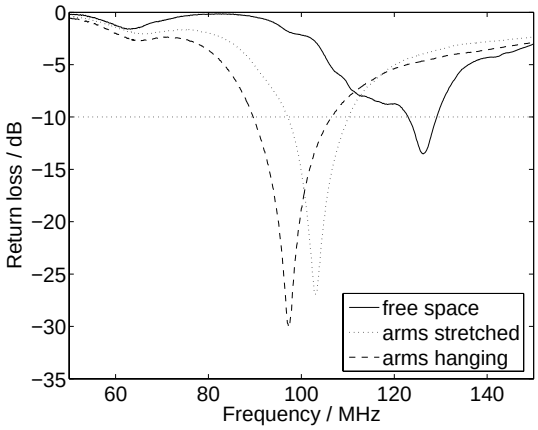

Figure 6. The return loss of the thin dipole. The maximum return loss grows by over 10 dB when the antenna is worn. The wearer is a small man.

the peak moves downward in frequency. The maximum $|S_{11}|$ value of the helix remains the same, that of the meandered dipole grows slightly, and that of the thin dipole grows by over 10 dB, when the antenna is brought near the body. In turn, the bandwidth of the meandered dipole is reduced a bit, while that of the helix is unchanged. The 10-dB bandwidth of the thin dipole doubles in most of the test cases. However, the 6-dB bandwidth remains the same, as seen in Fig. 6. Tab. 1 lists the bandwidths in free space and worn.

As the wide dipole consists of four thin dipoles whose lengths differ a little, its return loss curve consists of multiple resonances, giving the antenna a wide impedance bandwidth. When the antenna is brought near a human body, the maximum $|S_{11}|$ value grows from 14 to over 30 dB. In free space the resonances are separate and the 10-dB bandwidth breaks in the middle, but near the body the separate bands merge, as seen in Fig. 7. Thus the antenna is really useful only near the body, judging by the impedance bandwidth.

Table 2. Antenna gains and typical variation. The fourth line gives the typical loss of gain when the wearer lets his arms hang down instead of stretching them out.

	thin dipole	wide dipole	helix	meandered dipole
absolute maximum (dBi)	–14	–13	–15	–15
range of maxima (dBi)	–15…–17	–13…–15	–15…–18	–15…–21
maximum with arms hanging (dBi)	–17	–20	–22	N/A
typical effect of hanging arms (dB)	6…8	4…5	6	N/A
person-to-person variation (dB):				
arms stretched	1…2	1…2	1…3	1…6
arms hanging	1…3	1…4	1…6	N/A

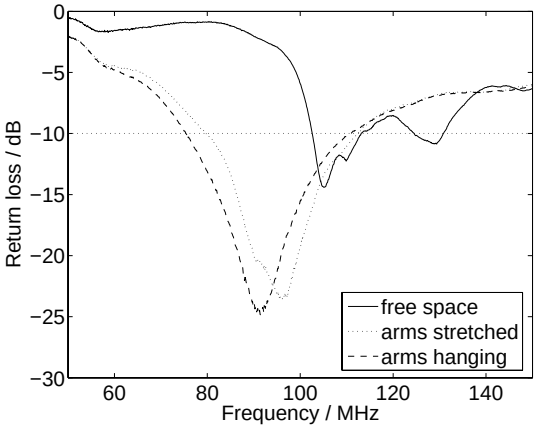

Figure 7. The return loss of the wide dipole. In free space the resonances are separate but merge when the antenna is worn. The wearer is a tall but thin man.

The improvement in return loss of the antennas is partly caused by the losses in the body. A good return loss does not necessarily indicate that the antenna radiates efficiently. Anyhow, the radiation measurements show that all of the antennas do radiate, and body losses are not alone responsible for the good return losses.

4.2. Radiation patterns

The maximum gains of the antennas are in the range of –13 to –15 dBi, taking the maximum of the maxima measured when the antenna was worn by every testee. The worst measured maximum gains were about –20 dBi. The antenna gains are listed in Tab. 2. A reference antenna of the same size exhibits a –10 dBi gain, and judging by the antennas' dipole nature, their free-space gain ought not to be very much below 0 dBi.

We can estimate that most of the radiated power is absorbed by the body, causing a 3 to 6 dB reduction in gain. The human head is estimated to absorb 25 to 50 % [6], 45 % [4], and even 68 % [3] of the radiated power at 900 MHz. If a 150 MHz short monopole antenna is held in hand near the body, about 60 % of the power is absorbed by the body [7].

Naturally, the maximum gains occur when the testee is standing with his arms streched out. When the arms hang down, the maximum reachable gains drop by 5 to 15 dB. The gain of a short monopole at 150 MHz is reported to drop by 7 to 14 dB when the handheld antenna is put into a shirt pocket or on a belt clip [4]. Minimum gains of –30 to –40 dBi are recorded when the testee has his arms coiled about the body.

As expected, the maximum gains of the dipoles occur when the antenna is broadside to the transmitting antenna. An interesting thing to note is that the body does not shadow radiation, but instead the maxima were often found in the direction where the shoulders and neck were in the radiation path, most often in the case of the wide dipole. This ”lens effect” where the body directs radiated power in the backward direction is derived in [4]. However, the same reference states that body may also shadow radiation efficiently, depending on the distance between the antenna and body.

In a dipole free-space radiation pattern, the nulls are very strong. With the wearer's arms stretched out so that the wearable dipole can be considered a straight half-wave antenna, the meandered dipole pattern is omnidirectional with less than 3 dB variation (taken from the maxima in every direction), in the wide dipole pattern the minima are 4 dB lower than maxima, and the two other patterns exhibit a –5 to –10 dB variation. The patterns are quite alike to that of a simple dipole.

With the testees' arms hanging down, the wide dipole and helix are omnidirectional. The minima of the thin dipole are 10 dB lower than the maxima. The meandered dipole was measured only with outstretched arms. The shapes of the radiation patterns resemble that of a dipole.

Table 3. Typical and maximum differences in antenna parameters between the situations where the wearer stands with arms stretched out and hanging down.

	typ.	max.
shortening	1 % unit	9 % units
resonance frequency	2…9 MHz	13 MHz
antenna gain	5…7 dB	15 dB

The filling of the nulls can be taken as evidence of power coupling into the human body and radiation from the outstretched fingers. The finger–free-space boundary is an impedance discontinuity that causes the surface waves to radiate into free space, just as in the case of printed antennas on a substrate with a high dielectric constant.

4.3. Variation in antenna performance

Variation in the wearer's position affects the antenna performance the most. Other factors include the antenna position on body, the wearer's physical traits, and clothing worn under the antenna, in decreasing order.

When the wearer stands with his arms stretched out, the antenna resting on his arms sees a smaller effective dielectric constant than when the hands are hanging down. This means that the resonance frequency is lower in the former case. The difference can be as much as 12 MHz (wide dipole) and is typically 4 to 8 MHz. The resonance frequencies in other postures fall between the two aforementioned. Antenna bandwidth is nearly unaffected by the variation in posture. Tab. 3 lists some differences in antenna parameters introduced by varying wearer position.

As mentioned before, by stretching one's arms out one can add 5 to 15 dB to the antenna gain. This is partially due to reduced body absorption and partially due to straightening of the antenna.

The variation in antenna return loss could be avoided by placing the antenna on torso instead of arms. That way, however, an additional 5 to 10 decibels of antenna gain would be lost because of body absorption. The antenna may be positioned on the arms either symmetrically, with the feed behind the neck, or asymmetrically, with most of the wire on one arm. When the arm is stretched out, the background dielectric constant near the antenna feed point is lower in the asymmetric case than in the symmetric, resulting in a higher resonance frequency in the asymmetric case. The effect on radiation is however small, less than two decibels.

Person-to-person variation in antenna performance is weaker than variation due to the movements of the wearer. The gender of the wearer has no effect on either return loss or radiation.

Tall and heavy people cause the resonance frequency of the antenna to lower. The effect is strongest when the wearer lets his arms hang down, thus increasing the effective dielectric constant seen by the antenna. The size of the wearer also affects the antenna bandwidth so that a small wearer indicates a wider bandwidth, the difference being only one or two percentage units.

The antenna gains differ at most 10 dB when the wearer is changed. Typically the effect is 1 to 6 dB for the meandered dipole, and only 1 to 4 dB for the other antennas. When the arms are stretched out, the effect is 1 to 2 dB weaker than in the other posture.

When the wearer stands with his arms hanging down, the antenna is folded into a small volume. Tall people tend to have wider shoulders than short people, and the antenna volume is reduced less when worn by them. Thus tall wearers imply a slightly greater antenna gain than small ones when the testees stand with their arms hanging down. On the other hand, antennas worn by small people radiate more efficiently than those worn by tall, when the arms are stretched out. This is due to the greater absorption by the larger people.

It can further be assumed that variations in one's physical traits, e.g. a heavy lunch or sweating, can cause the antenna performance to vary more than replacing the wearer by someone else.

5. CONCLUSION

Four antennas were constructed, all dipole-like: a thin and a wide straight dipole, a meandered dipole, and a normal mode helix, i.e., a helically wound dipole. Thick fleece fabric was chosen as the substrate for the antennas and copper foil tape as the conducting element. Return losses of the antennas were measured in free space and worn by people posing in different manners. Crude radiation patterns were measured only worn. The effect of posture and the personal traits of the wearer on antenna parameters were studied.

The presence of a human body affects antennas in two ways: by acting as a substrate with a high dielectric constant, and by absorbing radiated power. Furthermore, the body movements affect the antenna performance greatly.

As the human is thin compared to the wavelength, the wavelength on the body is not shortened as much as it would be at higher frequencies. A shortening phenomenon of about 15 to 25 % is introduced by the

presence of the human body at 100 MHz. Large bodies imply greater shortening. At higher frequencies the body becomes larger compared to the wavelength, and thus the body effect is hypothesised to become more notable, meaning even greater shortening of the antennas. Further studies will show whether or not this is the case.

The movements of the antenna wearer need to be taken into consideration as their effect on return loss is notable. If the antenna is designed so that it is resonant at a certain frequency when the wearer lets his arms hang down, the impedance band might move off the desired frequency when the wearer stretches his arms out. Wearable antennas need to be designed relatively broadband.
The absorption of radiated power by the body is severe. It is estimated that the presence of the body introduces a 3 to 6 decibel loss in gain when the antenna wearer stands with his arms stretched out. With arms hanging down, the loss can be more than 10 dB. Antenna gains of –13 to –15 dBi were achieved by the examined dipole antennas.

Some of the power delivered to the antenna is coupled into the human body and radiated from impedance discontinuities such as fingertips. Thus the antenna radiation patterns do not exhibit strong nulls.

The wide dipole, being the most broadband of the examined antennas, is the most insensitive one to the movements of the wearer with respect to return loss. It also exhibited the greatest maximum gain, –13 dBi, and the change in gain is typically less than 5 dB when the wearer lets his arms hang down. Thus we conclude that the wide dipole performed the best in the measurements. However, as the measured antennas differ quite little in shape, the other antennas do not perform very much worse than the wide dipole.

ACKNOWLEDGEMENT

The authors wish to thank Mr. Harri Raittinen, Janne Kiilunen, Juha Lilja, and Taavi Saviauk for acting as test subjects.
This work was funded by the Finnish Funding Agency for Technology and Innovation under contract no. 40014/06, and by the Graduate School in Electronics, Telecommunications and Automation (GETA).

REFERENCES

1. Hansen R. C., “Fundamental limitations in antennas”, *Proc. IEEE*, vol. 69, no. 2, pp. 170–182, February 1981.
2. Best S. R., “On the performance properties of the Koch fractal and other bent wire monopoles”, *IEEE Trans. Antennas Propag.*, vol. 51, no. 6, pp. 1292–1300, June 2003.
3. Jensen M. A. and Rahmat-Samii Y., “EM interaction of handset antennas and a human in personal communications”, *Proc. IEEE*, vol. 83, no. 1, pp. 7–17, January 1995.
4. Toftgard J., Hornsleth S. N., and Andersen J. B., “Effects on portable antennas of the presence of a person”, *IEEE Trans. Antennas Propag.*, vol. 41, no. 6, pp. 739–746, June 1993.
5. Dong-Uk Sim and Seong-Ook Park, “A triple-band internal antenna: design and performance in presence of the handset case, battery, and human head”, *IEEE Trans. Electromagn. Compat.*, vol. 47, no. 3, pp. 658–666, August 2005.
6. Okoniewski M. and Stuchly M. A., “A study of the handset antenna and human body interaction”, *IEEE Trans. Microw. Theory Tech.*, vol. 44, no. 10, pp. 1855–1864, October 1996.
7. Andersen J. B. and Hansen F., “Antennas for VHF/UHF personal radio: A theoretical and experimental study of characteristics and performance”, *IEEE Trans. Veh. Technol.*, vol. 26, no. 4, pp. 349–357, Nov. 1977.

Publication [P2]

T. Kellomäki, T. Björninen, L. Ukkonen, and L. Sydänheimo.
Shirt collar tag for wearable UHF RFID systems.
In *Proc. European Conference on Antennas and Propagation (EuCAP)*,
Barcelona, Spain, April 2010.

Erratum

Table I.

Reads: $L_t = 12$ mm

Should read: $L_t = 22$ mm.

Shirt Collar Tag for Wearable UHF RFID Systems

Tiiti Kellomäki*, Toni Björninen†, Leena Ukkonen†, Lauri Sydänheimo†
*Tampere University of Technology, Department of Electronics, P.O.Box 692, 33101 Tampere, Finland
tiiti.kellomaki@tut.fi
†Tampere University of Technology, Rauma Research Unit, Kalliokatu 2, 26100 Rauma, Finland

***Abstract*—This paper presents a wearable RFID tag antenna for the European UHF RFID band. The antenna is a one-layer dipole structure optimised to operate very near the human body. At the centre frequency (866 MHz), the tag is readable from a 5-to-6-metre distance if it is worn at 1 cm or more from the body. With the antenna worn on the body, the radiation pattern covers one hemisphere. The changes in the frequency response of the tag are examined when the antenna is worn at different separations from the body, and at different locations on the body. The proposed tag antenna can be integrated on any clothing and used e.g. in passage control applications. The small size, 7 cm by 2 cm, makes it fit easily on the collar, cuff, or even button catch of a dress shirt.**

I. Introduction

Many applications call for person monitoring: Passage control key cards are commonplace. Patient location is vital in both hospitals and elderly care. In construction sites or dangerous working areas, it is important to know the position of the workers.

RFID (radio frequency identification) tags integrated into clothing make it possible to monitor people without their conscious effort. This is especially useful in dementia care, but also convenient in for example workplaces. Normally, hospital patients are given a barcode or an RFID wristband [1]–[3], but it is also possible to integrate the tag into clothing in an unobtrusive way, and made flexible. Moreover, the tags can be made so small that there is no need to bend them.

This paper presents an RFID tag designed for integration into clothing. The proposed antenna is a one-layer design. Because of its small size, 6.8 cm by 2.2 cm, the antenna can easily be integrated on the collar of a dress shirt. The tag is passive, that is, it contains no internal power source.

The structure of the tag antenna is introduced in Sec. II. Sec. III begins with a short introduction to some common RFID figures of merit and a description of the measurement set-up. Different factors affecting the tag in use are then discussed. Section IV concludes the work and suggests topics for future work.

II. Proposed Tag Antenna

The proposed antenna dimensions are presented in Fig. 1 and Table I. The basic structure is a meandered dipole antenna. The one-layer design can easily be integrated into clothing. Because there is no ground plane, the antenna has to be separated from the body by at least 5 mm—a separation easily realised in clothing. Normal fabric (dielectric constant 1 to 1.5) can be used as the substrate. Fig. 2 presents a tag antenna made of copper tape.

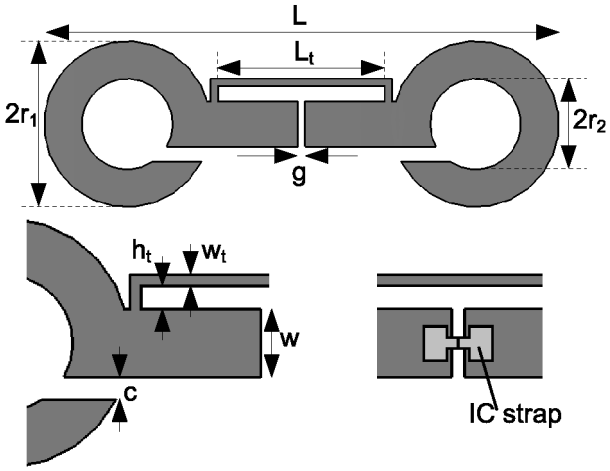

Fig. 1. The proposed tag antenna dimensions and two close-up views. The structure is completely in one layer, and rests on any fabric substrate available. The IC is located at the centre of the strap.

TABLE I
Dimensions of the Tag Antenna (in Millimetres).

L	68	Antenna length
r_1	11	Ring outer radius (half the antenna width)
r_2	6	Ring inner radius
w	6	Width of straight part
L_t	12	Length of T-match
h_t	2	Height of T-match
w_t	1	Width of T-match metal strips
c	2	Width of ring cut-off
g	1	Gap in feed
	60 µm	Gap between the IC strap pads

Instead of 50 ohms, RFID tag antennas must be conjugate matched to a complex impedance. The proposed tag antenna is designed for the Alien H3 strap [4]. The IC impedance is plotted in Fig. 3. At the centre frequency of the European UHF RFID band (866 MHz), the input impedance is $(16–j150)\ \Omega$. More precisely, the IC impedance also changes with received power level, but this effect was excluded from the study. To achieve an inductive antenna impedance for conjugate matching, a T-match [5] is used.

The operating frequency is mainly set by the total length of the antenna, including the length of the ring sections. The T-match (the parallel thin line) controls the inductance: the

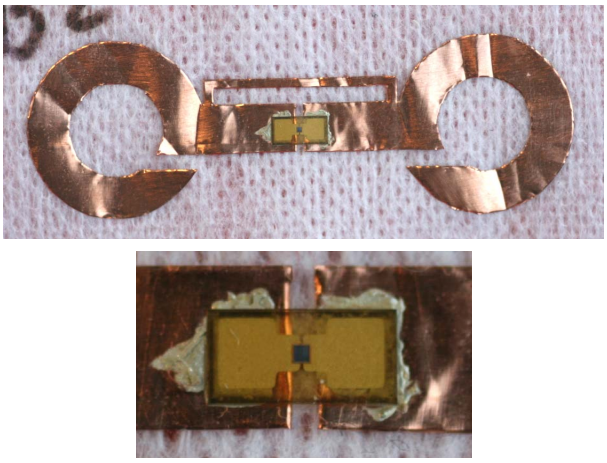

Fig. 2. Photo of the fabricated tag antenna with the IC attached. The antenna is made of copper tape. Lower photo shows a close-up of the strap (yellow) glued with conductive epoxy. The IC is seen in the middle of the strap.

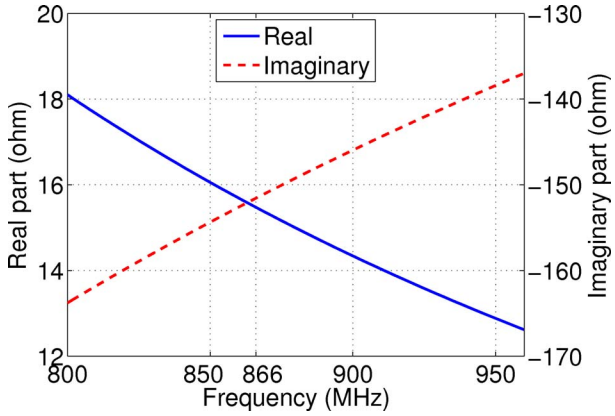

Fig. 3. The input impedance of the Alien H3 IC at a –14 dBm input power.

longer the T-match, the larger the inductance. Wider metal strips make the tag more broadband.

The antenna is designed to be worn on the body, and hence it has been made shorter than a similar antenna would be in free space. Also the impedance has been optimised for on-body use, because the body lowers the input impedance.

III. Tag in Use

RFID tags are often characterised using a quantity called the *threshold power*. It is the smallest power density required to reliably read the tag at a certain frequency. Threshold power can be expressed as the power which an isotropic antenna would receive from that power density. This notation is used in this paper and called *power on tag*. Another common practice is to give the transmitted power, transmitter antenna gain, and the distance between the tag and the reader. Threshold power also translates to *theoretical read range* for a given transmitter power.

A low threshold power means that the antenna impedance is well matched to the IC impedance and that the tag antenna gain is sufficient. Threshold power curves show the frequency of best operation. Because antenna impedance varies much more rapidly than directivity, the shape of the threshold power curve actually shows the impedance match.

There is no easy way to measure the IEEE defined gain of a tag antenna, but the *realised gain* (gain in dBi minus mismatch loss in dB [6]) can be calculated from the threshold power. The sensitivity of the IC is –18 dBm [4], and the realised gain is calculated by subtracting threshold power from it. For example, when the tag is worn at a 1-cm distance from the body, the realised gain is (–18–(–12)) dBi = –6 dBi.

Note that some sources define the word threshold power as the IC sensitivity, and treat the gain and mismatch separately. However, the definition used in this paper combines the IC sensitivity, gain, and impedance mismatch loss into a single number called the threshold power.

The human body affects an antenna in two ways: dielectric loading increases the electrical length of the antenna, and absorption lowers the radiation efficiency. Both can be seen on the threshold curve and to some extent examined separately. Roughly speaking, dielectric loading moves the curve towards lower frequencies, whereas absorption increases the overall threshold power level.

Threshold powers were measured in an anechoic chamber at a measurement distance of 1.6 metres, using the Tagformance™ Lite measurement system [7]. For the purpose of this measurement, Tagformance can be seen as an RFID reader capable of sweeping both frequency and transmitter power. For every frequency, it finds the lowest transmitter power to read the tag, and by comparing this result with the calibration tag, it determines the power on tag or theoretical read range. The overall measurement accuracy including reflections in the chamber is about ±1 dB.

Threshold powers were recorded for different antenna–body-separations as well as different antenna placements. The test subject was a 170-cm, 70-kg female. Vertical polarisation was used in all the measurements. Unless otherwise noted, the tag was placed on the upper arm. Fleece fabric was used to fill the gap between the antenna and the body. The dielectric constant of the fabric was estimated to be about 1.1.

A. Effect of Antenna–Body-Separation

The proposed tag antenna is designed to operate at a 1-cm distance from the body. However, when the antenna is attached to loose clothing, the separation may vary from 0.5 to 5 cm, or even more. Such a variation can completely detune some antenna designs. The behaviour of the tag antenna was measured at 4 to 60 mm from the body, as well as in free space. It is worth noting that the smallest separation is only 1 percent of the free-space wavelength.

When the antenna is close to the body, both its resonant frequency and impedance decrease. The decrease in the resonant frequency obviously decreases the operating frequency of the tag. On the other hand, the decrease in impedance acts in the opposite way: the frequency of the best impedance matching increases. This is due to the fact that the antenna is matched to

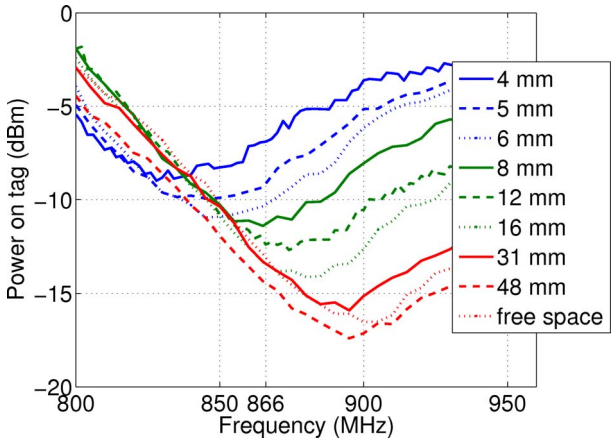

Fig. 4. Threshold power of the tag at different distances from the body. When the antenna is moved away from the body, the operating frequency increases and the minimum required power to read the tag decreases. –16 dBm corresponds to a 10-m read range, –13 dBm to 7 m, –11 dBm to 6 m, and –7 dBm to 3.5 m. Note for monochrome prints: the curves are in the same order as in the legend, except the two lowest.

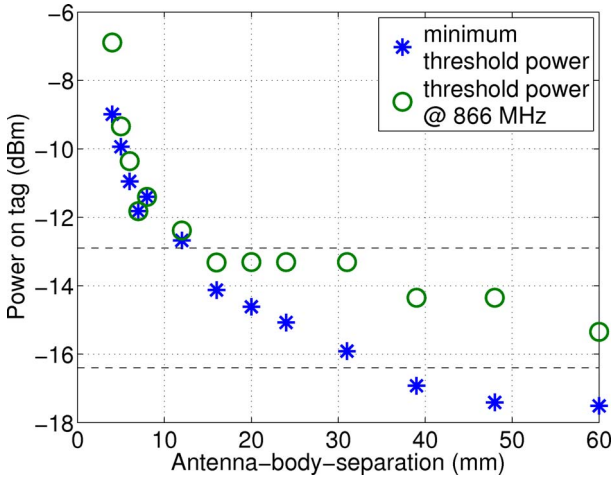

Fig. 5. Minimum threshold power approaches and goes below the free-space value when the antenna–body-separation is increased. The values will continue to oscillate around the free-space value and eventually settle to it. The lower plotted power is the minimum over the measured frequency range for each separation. Dashed lines show threshold powers in free space: minimum and at 866 MHz.

a complex and non-constant impedance. The two combined, the operating frequency of the tag decreases only slightly.

From Fig. 4 it can be deduced that the antenna impedance reaches its free-space value at about a 3-cm separation. At 3 cm, the operating frequency and the general shape of the threshold power curve resemble the free-space case. When the distance is further increased, the wave reflected from the human body starts to add in phase, and the forward gain increases. This is seen in the lowered threshold power in Fig. 5.

The antenna is seen to work well at distances greater than 1 cm from the body, and sufficiently even closer to the body. Figure 6 shows the theoretical read ranges when the tag is placed at various distances from the body. At a 1-cm separation

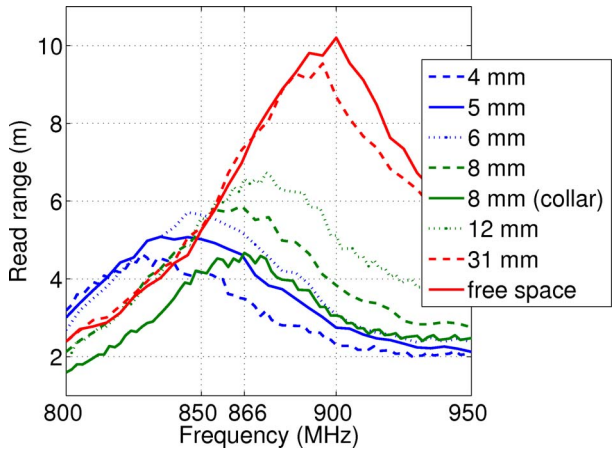

Fig. 6. Theoretical read ranges of the tag placed at various distances from the body. In a multipath environment, blind spots appear before the theoretical limit, but the tag may also be read from further away. Note for monochrome prints: The peaks from left to right correspond to the legend entries from up to down.

from the body and at 866 MHz, the tag can be read from a distance of five to seven metres, using the maximum 2 W ERP allowed. Even when the antenna is at 4 mm from the body, the read range is more than three metres. There is no need to thicken the clothes for the antenna to work properly.

B. On-Body Radiation Pattern

The H-plane (horizontal plane) radiation pattern of the tag was measured in two cases: in free space and worn on the upper arm, at an 8-mm distance from the body. The test subject was sitting on a wooden chair. Only one set of measurements was made, because the measurement took 15 minutes, during which the user was not allowed to move. The radiation pattern is estimated to be similar for all reasonable antenna–body-separations.

Figure 7 presents the normalised radiation pattern of the tag worn on the body. The 3-dB beamwidth covers the full forward hemisphere, but the tag is not readable from behind the body. This behaviour can be used to detect the direction of the user (walking towards the reader or away). If it is desirable to detect the user from all directions, only two tags are needed on the body. In free space, the H-plane pattern is omnidirectional.

If the tag is placed on the wrist with the arm held out, as illustrated in Fig. 8, the radiation pattern will have only one deep null in the direction shadowed by the body. According to measurements, the tag can be read through the wrist, with additional 6 dB loss to the link budget.

C. Effect of Antenna Placement on the Body

To examine the effect of the antenna placement on the body, the tag was mounted on the collar, wrist, back, and upper arm, as shown in Fig. 8. The same antenna–body-separation (8 mm) was used in all the cases. The radiation patterns were not measured because in these standing postures it is impossible to keep steady during the 15-minute measurement.

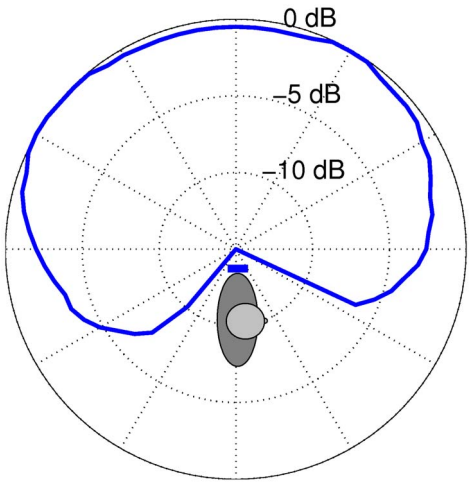

Fig. 7. Measured normalised H-plane radiation pattern of the tag antenna worn on the upper arm. In the figure, the wearer faces right and the antenna is on the upwards pointing arm. Null in the pattern means the tag could not be read: the required power to read the tag from the direction of the null is at least 18 dB higher than at the pattern maximum.

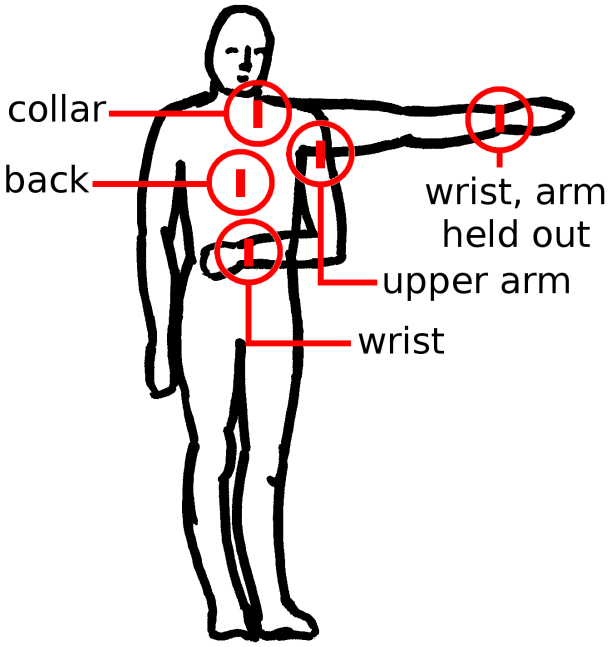

Fig. 8. Antenna placement on the body. Vertical polarisation was used in all the cases.

Measured threshold powers of the tag placed at various locations on the body are presented in Fig. 9. The tag placement on the body has no effect on the frequency of best matching, that is, on the antenna impedance. The minimum threshold power level is seen to vary ±2 dB, caused by the variation of the realised gain.

When the tag is placed on the torso, the threshold power level is independent of the exact position (collar, back, or wrist in front of the torso). If the tag is placed on the upper arm instead of the front of the torso, the realised gain of the antenna

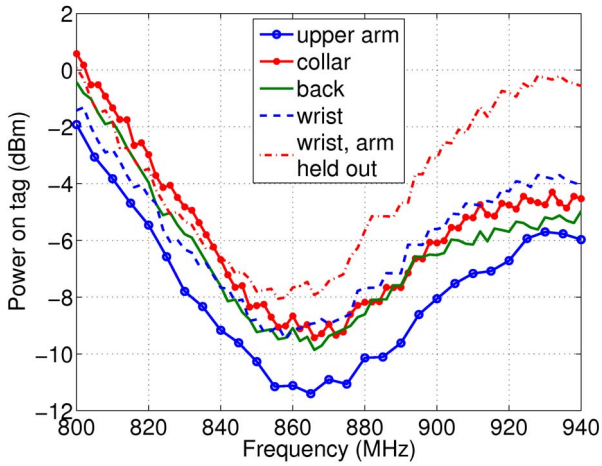

Fig. 9. Threshold power curves of the tag placed at different locations. The separation between the antenna and the body is 8 mm. –11 dBm corresponds to a 5.5-m read range, –9 dBm to 4.5 m, and –8 dBm to 4 m.

increases by 1 to 1.5 dB, due to reduced absorption by the body.

If the antenna is placed on the wrist and the arm is held out, the threshold power is seen to increase by 1.5 decibels compared to the wrist in front of the torso. This means a decrease in the realised gain, linked to the decrease in directivity: as the backwards radiation is not blocked by the body, the pattern becomes more omnidirectional.

To achieve the largest read ranges, the upper arm was found to be the best location for the antenna. If omnidirectionality is desired, the antenna should be mounted on the wrist instead. However, additional polarisation mismatch loss should be expected, because an antenna on the wrist is subject to a free rotation of 180 degrees during normal user movement. Attaching the antenna to the collar minimises the expected polarisation mismatch loss.

D. Use Case: Tagged Clothes after Laundering

In addition to user recognition, the wearable RFID tag can be used to identify clothes after washing. This is useful in for example industrial laundry. Using an RFID reader, it is possible to count the number of shirts in a basket, or to find misplaced size-S clothes among size-L clothes.

As seen from Fig. 6, the tag can be read from seven metres in the free space. Other measurements show that close metallic objects detune the antenna and decrease the read range. However, the tag can be read from a 4-metre distance at 866 MHz if it is on a metallic table, separated by one centimetre. The read range reaches the free-space value if the distance from the metal is 3 cm. It was seen that the frequency shift introduced by metal is smaller than by the body, but the minimum threshold power degrades more severely.

Plastic boxes or wooden tables can be approximated to have no effect on the antenna performance because of their low permittivity and loss.

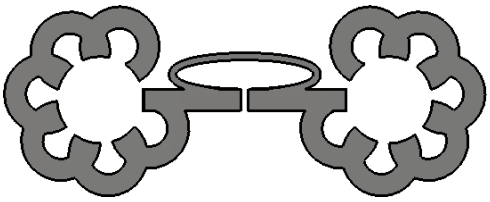

Fig. 10. Flower shape—a variation of the ring-ended dipole. The antenna is 6.4 cm long and 2.5 cm wide.

IV. Conclusion and Future Work

A tag antenna for the European UHF RFID band (866 MHz) has been proposed. When the tag is worn at 1 cm from the body, it can be read from a maximum distance of five to seven metres, depending on its location on the body. The tag is not very sensitive to the separation from the user, and performs well at all the measured antenna–body-separations: 4 to 60 mm. Therefore no thickening is needed between the tag and the user. The tag is also usable in free space. The small design (6.8 cm by 2.2 cm) fits shirt collars and cuffs, or even the button catch between the buttonholes.

Another antenna structure considered in designing the tag was a flower shape presented in Fig. 10. It can be seen as a variation of the ring-ended dipole: the meandered dipole structure comprises of the petals, and the leaf acts as a T-match. The ring-ended dipole can be easily adapted to many pretty designs. When the antenna becomes part of the clothing, it can act as a decorative element.

The proposed tag antenna design is a part of a project aiming to integrate RF electronics and clothing into a washable garment. The antenna will be further developed so that it can be easily attached to the textile in a normal sewing process. Washing temperature and moisture limit the lifetime of the tag, but proper polymer coating will protect the antenna without affecting the electrical properties.

Future work on the antenna design will also include modelling its behaviour close to the body. Especially the bodyworn efficiency of the antenna is of interest.

Acknowledgment

Warm thanks to M.Sc. Juha Virtanen for all the help in measurements and practical problems. Thanks also to M.Sc. Timo Kellomäki and Mr. Joel Salmi for helping with the measurements.

Tiiti Kellomäki's work was funded by the Graduate School in Electronics, Telecommunication and Automation (GETA).

References

[1] B. Chowdhury and R. Khosla, "RFID-based hospital real-time patient management system," in *6th IEEE/ACIS International Conference on Computer and Information Science (ICIS 2007)*, July 2007, pp. 363–368.

[2] J. E. Bardram, "Applications of context-aware computing hospital work: Examples and design principles," in *SAC'04: Proceedings of the 2004 ACM symposium on applied computing*, New York, NY, USA, 2004, pp. 1574–1579.

[3] A. Aguilar, W. van der Putten, and G. Maguire, "Positive patient identification using RFID and wireless networks," in *HISI 11th Annual Conference and Scientific Symposium*, Nov. 2006.

[4] Alien Technology. (2009, Dec.) Higgs-3 product overview. [Online]. Available: http://www.alientechnology.com/docs/products/DS_H3.pdf

[5] G. Marrocco, "The art of UHF RFID antenna design: Impedance-matching and size-reduction techniques," *IEEE Antennas Propagat. Mag.*, vol. 50, pp. 66–79, Feb. 2008.

[6] *IEEE Standard Definitions of Terms for Antennas*, IEEE Std. 145-1993, 1993.

[7] Voyantic Ltd. (2009, Dec.) Tagformance^{TM} Lite. [Online]. Available: http://www.voyantic.com

Publication [P3]

T. Kellomäki.

On-body performance of a wearable single-layer RFID tag.

IEEE Antennas and Wireless Propagation Letters (AWPL).

Vol. 11, 2012.

Pages 73–76.

On-Body Performance of a Wearable Single-Layer RFID Tag

Tiiti Kellomäki

***Abstract*—The effects of the human body on a wearable radio frequency identification (RFID) tag at 866 MHz are presented. We concentrate on the effect of the varying antenna–body separation distance on the antenna properties. The results of the three-dimensional radiation pattern measurements are presented. A 6-m read range, −6 dBi realized gain, and 12% antenna efficiency are achieved when this antenna is worn on the body.**

***Index Terms*—Antennas, identification of persons.**

I. Introduction

In MANY healthcare applications, such as dementia care, it is beneficial to allow patients to move as freely as possible, but at the same time the staff should always be aware of their whereabouts. Radio frequency identification (RFID) provides a reliable and inexpensive means of locating people. Transponders (tags) can be worn as keycards or wristbands, or they can be integrated as part of clothing. Wearable tag designs have been presented in [1] and its references. Most of the published tags are of a microstrip type, but for example, [2] discusses single-layer structures such as dipoles and loops.

In this letter, we examine the effect of the human body on a small wearable single-layer dipole tag antenna. Special attention is drawn to the effect of the antenna–body separation distance on the antenna properties. This distance is the main factor to affect the matching of the tag.

Preliminary results have been presented earlier in [3]. Now, the results of new three-dimensional radiation pattern measurements are presented along with measured antenna efficiencies. Both free-space and on-body patterns and efficiencies will be shown. The method used in the three-dimensional radiation pattern measurement is described in detail. We also examine the effect of the body on detuning and realized gain.

Section II of this letter introduces the tag and the design choices. The measurement setup is described in Section III. Results including radiation parameters are presented in Section IV. Section V concludes the letter.

II. Tag Antenna Under Test

The examined tag antenna is a meandered dipole with a T-match. Its dimensions are presented in Fig. 1 and Table I. Any normal textile material (dielectric constant 1–1.5) can be used as the substrate. The metallized parts can be printed or sewn of conductive textile.

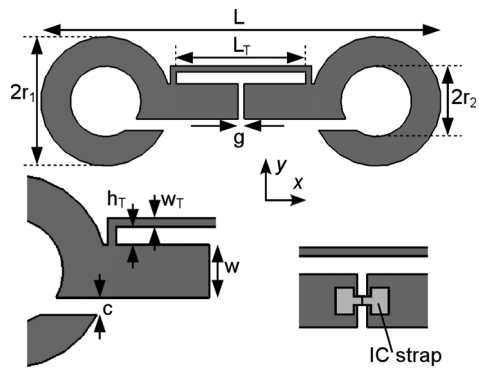

Fig. 1. Dimensions of the tag antenna under test and two close-up views. The structure is completely in one layer and rests on any fabric substrate available. The IC is located at the center of the strap.

TABLE I
Dimensions of the Tag Antenna (in Millimeters)

L	68	Antenna length, 0.2 wavelengths
r_1	11	Ring outer radius (half the antenna width)
r_2	6	Ring inner radius
w	6	Width of straight part
L_T	22	Length of T-match
h_T	2	Height of T-match
w_T	1	Width of T-match metal strips
c	2	Width of ring cut-off
g	1	Gap in feed
	60 μm	Gap between the IC strap pads

In Section IV, it will be shown that the antenna has to be separated from the user's body by at least 5 mm, which is often the case with loosely fitting or thick clothes or, for example, the collar. As long as the distance is greater than approximately 5 mm, it has little effect on the realized gain.

A commercial Alien H3 IC strap [4] is connected at the center of the antenna. The sensitivity of the IC, meaning the lowest accepted power at the IC to allow operation, is −18 dBm. The IC impedance is $(16 - j150)\ \Omega$ at the center frequency, 866 MHz. To achieve an inductive antenna impedance for conjugate matching, a T-match [5] is used.

Table II summarizes the effects of geometry changes on key performance parameters. Larger L_T and h_T and smaller w_T add inductance, which is needed to match the capacitive small dipole to the capacitive IC. To make the antenna physically robust, w_T was chosen to be 1 mm, although a narrower T-match would have increased the inductance further. It is difficult to produce narrow lines with exact dimensions in printed or sewn textile antennas (1 mm corresponds to five threads in some conductive

Manuscript received November 30, 2011; accepted January 02, 2012. Date of publication January 06, 2012; date of current version March 19, 2012. This work was supported by the Nokia Foundation and the HPY Research Foundation.

The author is with the Department of Electronics, Tampere University of Technology, 33101 Tampere, Finland (e-mail: tiiti.kellomaki@tut.fi).

Digital Object Identifier 10.1109/LAWP.2012.2183112

TABLE II
EFFECT OF GEOMETRY CHANGES ON RESONANT FREQUENCY, OPERATING FREQUENCY (WITH BEST MATCHING), INDUCTANCE, AND BANDWIDTH

	f_{res}	f_{oper}	inductance	bandwidth
$L \uparrow$	$\downarrow$	($\downarrow$)		
L_{T}, $h_{\text{T}} \uparrow$		$\downarrow$	$\uparrow$	
$w_{\text{T}} \uparrow$		$\uparrow\uparrow$	$\downarrow\downarrow$	
$w \uparrow$				$\uparrow$
$r_1 - r_2 \uparrow$				$\uparrow$
$r_2 \uparrow$			$\downarrow$	$\downarrow$
dist. from body $\uparrow$	$\downarrow$	$\downarrow$		

textiles). Moreover, thin lines can easily break in use. The antenna size in this application was limited to allow placement on the collar.

The antenna is designed to be worn on the body, and hence it has been made shorter than a similar antenna would be in free space. Also, the impedance has been optimized for on-body use because the body lowers the input impedance.

III. MEASUREMENT SETUP

The *realized gain* and *antenna efficiency* of the tag were measured. The IEEE defines the realized gain as "the gain of an antenna reduced by the losses due to the mismatch of the antenna input impedance to a specified impedance" [6, Definition 2.321], here to the IC impedance $(16 - j150)\ \Omega$. We can write $G_{\text{real}} = GM_2 = D\eta_{\text{rad}}M_2 = D\eta_{\text{ant}}$, with G_{real} the realized gain, G the gain, M_2 the impedance mismatch factor, D the directivity, η_{rad} the radiation efficiency, and η_{ant} commonly termed the antenna efficiency. The inherent losses and the mismatch are combined in antenna efficiency.

The three-dimensional radiation patterns of the antenna were measured in the anechoic RAMS facility [7], using a Tagformance Lite RFID measurement unit (reader) [8]. A constant transmitter power was obtained from the reader, and the tag response was recorded with receiving antennas placed evenly on a sphere surrounding the tag, at a 1-m distance. This fully contactless setup allowed us to measure the realized gain. The measurement was calibrated using a known tag in free space. Fig. 2 illustrates the setup.

The transmitting antenna used vertical polarization, as did the tag antenna under test. The receiving antennas were in $\hat{\theta}$ and $\hat{\phi}$ (vertical and horizontal) polarizations, 32 in each. Measuring both polarization components allowed us to calculate the total radiated power. The antenna efficiency was calculated by integrating the realized gain over the spherical surface.

In this measurement setup, the transmitter feeds a constant power to the IC (about -13 dBm, 5 dB over the IC sensitivity). Because the IC receives a constant power, it also scatters at a constant power. Especially, the radiation pattern does not depend on the location of the transmitting antenna.

Realized gains were measured in free space and with the antenna on the body, separated by 8 or 20 mm of fleece textile. The distances were chosen to represent clothes fitting loosely or thick clothes. Normally, the collar of a dress shirt is at least 1 cm away from the collarbone, and 3 cm is not uncommon.

The test subject was a 170-cm, 70-kg female. The tag was placed on the upper arm. This location is stable enough for long

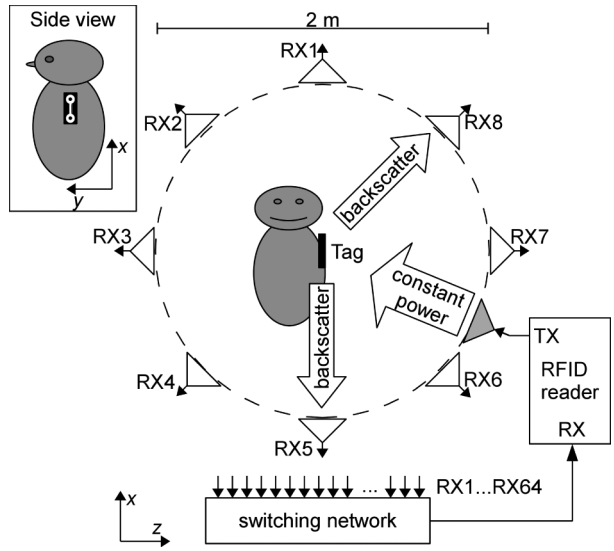

Fig. 2. Measurement setup. The transmitter (TX) transmits carrier, commands, and carrier again, at a constant power. RX1 . . . RX64 are receiving antennas in both vertical and horizontal polarizations, spaced evenly on a spherical surface. Coordinate axis directions are shown at the bottom. Inset shows a side view of the person wearing the tag.

measurements (10 min), and the antenna shape and position are not subject to changes due to breathing, unlike on the collar for example. Although the user can move freely with the tag in real scenarios, the measurement requires the test subject to stay still to allow for the measurement of an instantaneous radiation pattern.

Realized gain in the forward (main lobe) direction was additionally measured using a frequency sweep in an anechoic chamber, using the Tagformance Lite in a monostatic configuration. The tag was again on the upper arm.

A measurement error of less than ± 1 dB is expected in the realized gain, whereas the uncertainty in efficiency is less than ± 0.5 dB. This estimate is based on analyzing the uncertainties of the individual parts of the measurement system as well as the uncertainty in the position of the test subject.

IV. EFFECT OF THE BODY ON THE TAG

The human body affects antennas in two ways: Dielectric loading increases the electrical length of the antenna, and absorption lowers the radiation efficiency. Simply put, dielectric loading detunes the operating frequency and lowers the impedance, and absorption decreases the gain.

Fig. 3 shows the realized gain, i.e., the product of gain and impedance mismatch factor. The peaks correspond to the frequency of best matching. According to simulations, the gain is constant in the measured narrow frequency range. Hence, the variation in realized gain is due to mismatch only.

As seen from Fig. 3, the tested antenna works properly quite close to the body, and its performance at 866 MHz is not sensitive to the variation in the antenna–body separation greater than 8 mm. The realized gain is -7 to -5 dBi, and the theoretical read range with an IC sensitivity of -18 dBm is 6 to 7 m. Even if the antenna is 4 mm away from the body, it can be read from a 3-m distance.

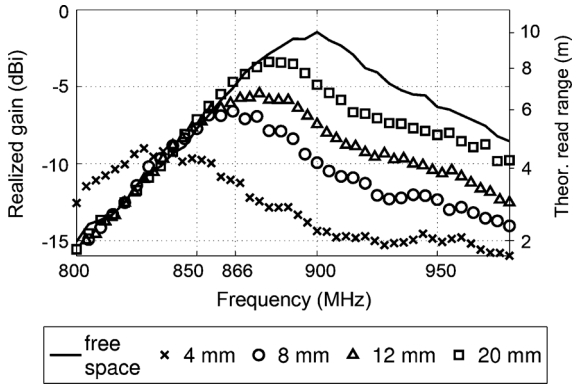

Fig. 3. Realized gains of the tag at different distances from the body. When the antenna is moved away from the body, the operating frequency increases. Theoretical read ranges are also shown; in reality, blind spots appear before the theoretical limit, but occasionally the tag can also be read from further away [9]. Theoretical read ranges have been calculated for 2 W transmitter EIRP power and IC sensitivity −18 dBm. The associated uncertainty is ±1 dB.

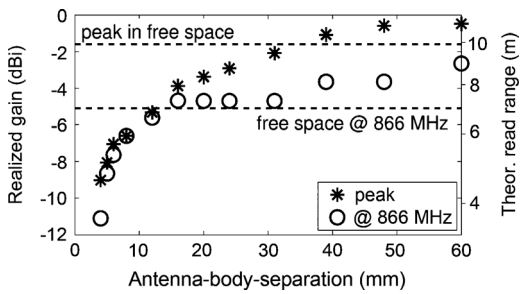

Fig. 4. Measured realized gains at 866 MHz and at peak. Horizontal lines show the peak realized gain and the value at 866 MHz for the tag measured in free space. Theoretical read ranges are also shown.

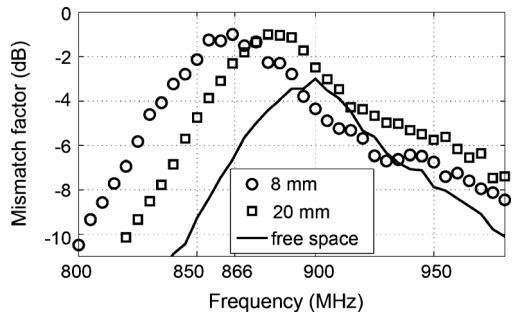

Fig. 5. Impedance mismatch factor (M_2) of the tag worn at different distances from the body. Curves from threshold measurements, peaks aligned with help of simulations. Variation of the IC impedance with frequency is included.

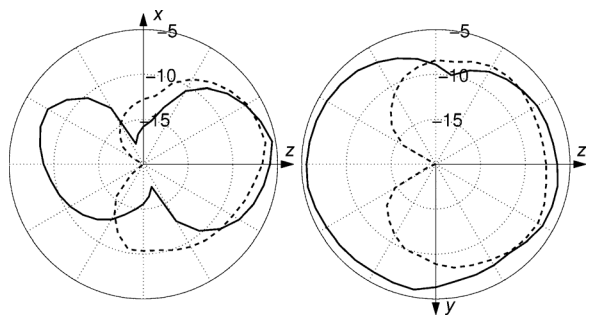

Fig. 6. Measured radiation patterns at 866 MHz. *(left)* E-plane (xz-plane). *(right)* H-plane (yz-plane). (—) In free space. (- - -) Worn with an 8-mm fleece insulation. The radial scale is dBi. Only copolarized component (x) is shown. The E-plane corresponds to Fig. 2 seen from the front, and the H-plane from above. The associated uncertainty is ±1 dB.

Fig. 4 shows how the forward realized gain depends on the spacing between the tag and the body. Both the peak realized gain and the 866-MHz value are shown. When the antenna is far enough from the body, the reflected field starts to add in phase and provides additional gain. At about a distance of 0.1 wavelengths (34 mm), the reflected wave neither cancels nor adds to the direct wave, which is seen in the peak realized gain reaching the free-space value.

Fig. 5 shows the impedance mismatch factor of the tag worn on the body. The free-space impedance has intentionally been designed too high, as indicated by the poor transmission in Fig. 5. Measurements reported in [3, Fig. 4] show that the antenna impedance at 30 mm (0.1 wavelengths) from the body is the same as in free space. Closer, the impedance decreases, resulting in better matching at the target frequency.

It is not possible to read the tag through the body, but the main lobe of the radiation pattern is quite wide, especially in the horizontal plane. Fig. 6 shows the radiation patterns measured in free space and with the tag worn on the upper arm, with an 8-mm-thick textile spacing. The radiation patterns measured with the antenna 20 mm from the body are very similar to the 8-mm case.

In the E-plane, the main lobe on-body is slightly wider than in free space. This would be the vertical (xz) plane if the tag were mounted upright on the user's shoulder as in Fig. 2. The theoretical read range from above is 3 m, from below 4 m, and 6 m in the main lobe. In real-life situations, the readers on the ceiling or on the floor are usually quite near the user, who would be standing directly on top or underneath, so a smaller read range upward and downward is not a problem.

The free-space and on-body H-plane (yz-plane in Fig. 2) patterns coincide in the forward hemisphere. The main lobe is wide, 220°, making the tag practical in use.

Conventional microstrip antennas are often physically wide in the H-plane, which makes their H-plane patterns narrower than that of the presented tag antenna. In the E-plane, the tag is about as long as a quarter-wavelength patch, and indeed their E-plane patterns are alike. A wide main lobe makes the tag easy to read from many directions, which is more convenient in short-range body-worn applications than a narrow main lobe.

According to the measurements, the cross-polar radiation pattern is not significantly affected by the body. The measured cross-polar sidelobe level was about −10 dB in all cases.

The measured antenna efficiencies at 866 MHz are shown in Table III. The table also lists radiation efficiencies, which are estimated with the help of simulated input impedances. At 866 MHz, the antenna efficiencies for both of the measured body-worn cases (8 and 20 mm) coincide, as do the measured patterns and realized gains. We can expect a constant antenna efficiency at 866 MHz for all reasonable antenna–body separations. In free space at 900 MHz (at the best matching), the antenna efficiency is approximated at 39%. The poor free-space efficiency is caused by the free-space input impedance too large

TABLE III
MEASURED ANTENNA EFFICIENCIES AT 866 MHZ, ESTIMATED PEAK ANTENNA EFFICIENCIES, AND ESTIMATED RADIATION EFFICIENCIES OVER THE FREQUENCY BAND. THE ASSOCIATED UNCERTAINTY IS ± 0.5 dB

	antenna eff. (866 MHz)	antenna eff. (peak)	radiation eff. (over band)
Free space	17%	39%	80%
On-body, 8 mm	12%	12%	15%
On-body, 20 mm	12%	16%	20%

to match the IC (as seen in Fig. 5), as well as the small antenna size.

The radiation efficiency of the tag worn 8 mm from the body is approximately 19% of the free-space value, i.e., the *body-worn efficiency* defined in [10, p. 222] is about 19%. For the 20-mm distance, the body-worn efficiency is 25%. If we include the effect of mismatch, the ratio of antenna efficiencies at 866 MHz is 70% for all antenna–body separation distances.

The efficiencies in Table III were measured with the tag mounted on the arm. From [3, Fig. 9], we see that the realized gain of the arm-mounted tag is approximately 1.5 dB greater than of the tag placed on the chest. If the difference is caused by a difference in absorption only, we can estimate that the antenna efficiency of the tag on the chest is 9% at 866 MHz.

Compared to the tags presented in [11], with antenna efficiencies of 33%, 64%, and 60%, the tag presented here seems poor. However, the tags in [11] are four to five times the area of the tag under test. The comparison of published wearable UHF tag antennas in [1] shows that the realized gain of the presented tag is satisfactory, given the antenna size. Gain is mainly set by the antenna size, even in wearable antennas. Moreover, the tag presented in this letter is made of flexible materials, and the metallization is in one layer only.

The effect of antenna position on the body was addressed in [3, Fig. 9]. There, the realized gain in the forward direction was measured in an anechoic chamber with the tag placed on the upper arm, collar, back, and wrist. The effect of arm position was also studied. To achieve the largest realized gain, the upper arm was found to be the best location for the antenna. Attaching the antenna to the collar decreases the realized gain by about 1.5 dB. The pattern of the antenna on the collar is believed to have a narrower main lobe than on the arm due to shadowing, especially in the horizontal plane.

Only the tissue very close to the antenna plays a role in the input impedance. Thus, the body posture and the placement of the antenna on the body do not affect the antenna impedance, as was seen in [3, Fig. 9]. The effect of posture on the radiation pattern is also minor. In the H-plane radiation patterns presented in Fig. 6 (user standing) and [3, Fig. 7] (user sitting), there is only a very small difference in the 3-dB beamwidths. User movements will naturally tilt the main beam. Pattern fragmentation will result if the antenna is covered by a hand. The placement of the tag should be decided based on the application requirements as well as to simplify manufacturing.

V. CONCLUSION

The on-body performance of a small wearable UHF RFID tag has been examined. When the tag is separated from the body by 1 cm, it can be read from a maximum distance of 5–7 m, depending on its location on the body. The measured on-body antenna efficiency, 9%–12%, is good enough for practical use.

The performance of the tag is not very sensitive to the separation from the user, and the tag can be used at any distance (> 5 mm, approximately) from the body. No extra padding is needed because clothes are loose, and there is no need to harden the clothes under the tag. The tag is also usable in free space. The small design (6.8×2.2 cm^2) fits shirt collars and cuffs, or even the button catch between buttonholes, being especially useful when space is limited.

ACKNOWLEDGMENT

The author would like to thank A. Khatun and Dr. J. Toivanen of Aalto University and Dr. J. Tuominen of Voyantic, whose help made the three-dimensional radiation pattern measurement possible.

REFERENCES

[1] T. Kellomäki and L. Ukkonen, "Design approaches for bodyworn RFID tags," in *Proc. ISABEL*, Rome, Italy, Nov. 2010, pp. 1–5.
[2] G. Marrocco, "RFID antennas for the UHF remote monitoring of human subjects," *IEEE Trans. Antennas Propag.*, vol. 55, no. 6, pp. 1862–1870, Jun. 2007.
[3] T. Kellomäki, T. Björninen, L. Ukkonen, and L. Sydänheimo, "Shirt collar tag for wearable UHF RFID systems," in *Proc. Eur. Conf. Antennas Propag.*, Barcelona, Spain, Apr. 2010, pp. 1–5.
[4] Alien Technology, "EPC class 1 gen 2 RFID tag IC," Accessed Jan. 20, 2012 [Online]. Available: http://www.alientechnology.com/docs/products/Alien-Technology-Higgs-3-ALC-360.pdf
[5] G. Marrocco, "The art of UHF RFID antenna design: Impedance-matching and size-reduction techniques," *IEEE Antennas Propag. Mag.*, vol. 50, no. 1, pp. 66–79, Feb. 2008.
[6] *IEEE Standard Definitions of Terms for Antennas*, IEEE Std. 145-1993, 1993.
[7] T. Laitinen, J. Toivanen, C. Icheln, and P. Vainikainen, "Spherical measurement system for determination of complex radiation patterns of mobile terminals," *Electron. Lett.*, vol. 40, no. 22, pp. 1392–1394, 2004.
[8] Voyantic Ltd., "Tagformance Lite," 2011 [Online]. Available: http://www.voyantic.com
[9] M. Taguchi and H. Mizuno, "Analysis of dead zone of RFID system," in *Proc. IEEE Antennas Propag. Soc. Int. Symp.*, Albuquerque, NM, Jul. 2006, pp. 4759–4762.
[10] W. Scanlon and N. Evans, "Antennas and propagation for telemedicine and telecare: On-body systems," in *Antennas and Propagation for Body-Centric Wireless Communications*, P. S. Hall and Y. Hao, Eds. Norwood, MA: Artech House, 2006, ch. 8, pp. 211–239.
[11] M. Švanda and M. Polívka, "Extremely low profile UHF RFID tag antennas for identification of people," in *Proc. Eur. Conf. Antennas Propag.*, Barcelona, Spain, Apr. 2010, pp. 1–4.

Publication [P4]

T. Kellomaki, J. Heikkinen, and M. Kivikoski.
One-layer GPS antennas perform well near a human body.
In *Proc. European Conference on Antennas and Propagation (EuCAP)*,
Edinburgh, UK, November 2007.

ONE-LAYER GPS ANTENNAS PERFORM WELL NEAR A HUMAN BODY

T. Kellomaki, J. Heikkinen, M. Kivikoski

Tampere University of Technology, Institute of Electronics, P.O.Box 692, FI-33101 Tampere, Finland, Tiiti.Kellomaki@tut.fi, fax: +358 3 3115 3394

Keywords: Antenna radiation patterns, Microstrip antennas, Receiving antennas, UHF antennas.

Abstract

The effect of a human body near one-layer GPS antennas has been studied with the help of measurements. In general, to avoid changing the input impedance, the user and the antenna need to be separated by $\lambda/2\pi$. In contrast, antennas with a ground plane may be satisfied with a separation of 1 cm or few millimetres. The radiation efficiencies of the measured antennas at a 3-cm separation are only about 25 % lower than in free space. Outside the reactive near-field region the human body can be modelled as a reflector, thus gain can be increased by proper placement of the antenna. The results presented in this paper are extendable in the region of 1 to 10 GHz. We conclude that one-layer antennas work fine regardless of the human body.

1 Introduction

In the point of view of an antenna at the GPS center frequency, 1575 MHz, the human body is a piece of highly dielectric low-loss material with dimensions comparable to a wavelength (λ). If the antenna and the body are placed very close to each other, the body will detune the antenna and absorb most of the delivered power, which in turn results in high SAR (specific absorption rate) values. To avoid losses, a ground plane is usually employed between the antenna and the user, as in a patch antenna.

One-layer antennas without a shielding ground plane have many advantages compared to two-layer structures. In the manufacturing process, there is no need for precise alignment of the layers. Two-layer antennas usually require the distance between the layers to be constant, which calls for an inconvenient hardening of the cloth substrate. The results presented in this paper show that one-layer antennas need to be placed at a certain minimum distance from the body, but this distance need not be constant.

Most of the earlier research has been focussed on mobile phone antennas near the head. Moreover, the results have been mostly computational. Most of the papers in this field describe the behaviour of complex antennas. The radiation efficiency of a monopole has been studied in [1,2] and the radiation pattern near the head in [3,4].

The purpose of this study is to find out whether one-layer structures without a shielding ground plane can be used as wearable antennas. The return losses and radiation patterns of several antennas have been measured at various separations from the body. It is seen that a gap of $\lambda/2\pi$ between the antenna and the user is sufficient to return the gain to its free-space value. Beyond that distance the human may actually be modelled as a reflector.

In this paper we first describe the antennas under test and the measurement procedures. The results are presented in Section 3 for the input matching, radiation pattern, and radiation efficiency. In Section 4 the results are further discussed and considered from the electromagnetical point of view.

2 Methods

The antennas under test are depicted in Fig. 1. The antenna that this study is mostly focussed on, the inverted-F antenna, has been introduced in [5]. The analysis of the one-layer slot antenna is found in [6], but here the antenna is redesigned for lower frequencies, with a diameter of 13 cm. The remaining

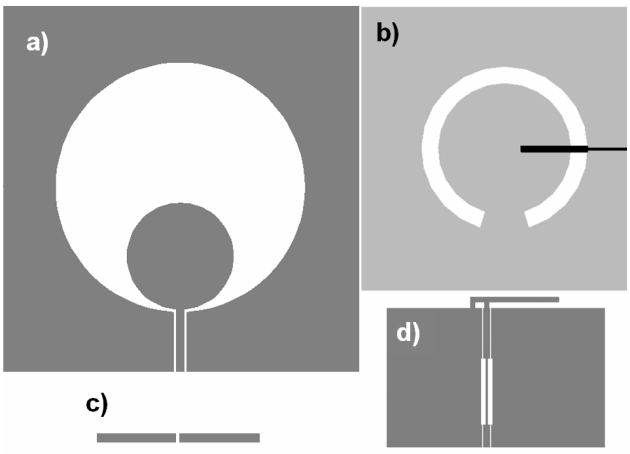

Figure 1: The measured antennas, to scale: a) one-layer slot, b) two-layer slot (black feed line in the lower layer), c) half-wave dipole (length 8.8 cm), d) inverted-F.

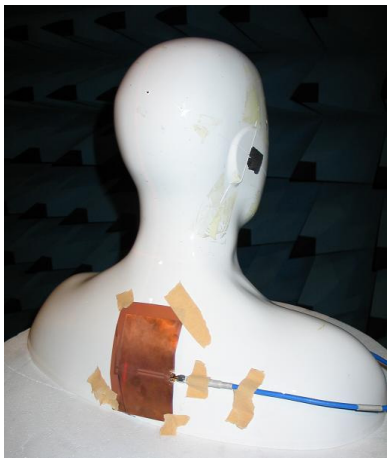

Figure 2: Because of their size, the antennas were mounted on the back of the phantom to allow them to lie flat.

two antennas are a two-layer slot and a half-wave dipole antenna. The inverted-F and two-layer slot antennas exhibit circular polarisation. The antennas have been chosen to represent many different classes of antennas. They have been fabricated on a flexible polyimide substrate, some with additional fabric.

Measurements of return loss and radiation pattern were conducted using a phantom, two human subjects, and a metallic plate for comparison. The SAM phantom comprised of a head and shoulders, and the antennas were mounted on the back, as in Fig. 2, to allow them to lie flat. The main human subject was a 184-cm, 82-kg male. To find out the maximum effect, the antennas were attached to the abdomen where the human is largest.

It was possible to measure the radiation efficiencies only with the phantom model. For the other cases the efficiency can only be roughly estimated. Due to the limitations of the measurement system, only horizontal gain patterns could be recorded with the human subjects.

The antennas were placed at various separations from the user, ranging from 0 mm to 50 mm, and 83 mm (half a wavelength) for curiosity. The gap between the antenna and the user was filled with either styrofoam or bubble wrap. If an antenna is to be integrated into clothing, e.g. fleece fabric could be used as padding.

Antenna	Separation
One-layer slot	30 mm
Two-layer slot	30 mm
Inverted-F	3 mm
Dipole	60 mm

Table 1: The separations between the antenna and the user needed to bring the return loss back to its free-space value.

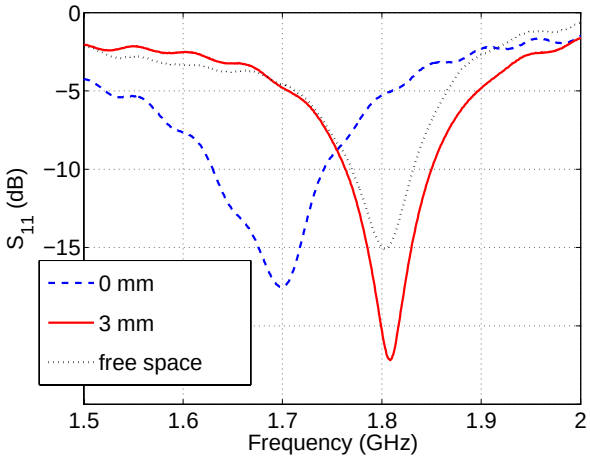

Figure 3: Only by touching the antenna can the user interfere with the return loss of the inverted-F antenna. At distances greater than three millimetres the resonance frequency remains in the free-space value and the curve gradually approaches the free-space curve.

3 Results

The human acts in a twofold way: as an absorber of radiated or reactive power, and a reflector. Located in the reactive near-field of the antenna one takes energy from the field, implicating losses and changes in the input impedance. At larger separations the reflection effect starts to dominate, and the radiation efficiency of the antenna approaches that in free space. The antenna gain may easily exceed the free-space gain by several decibels.

3.1 Return loss

In theory, the antenna input impedance is affected only by objects in the reactive near-field of the antenna. Traditionally, the reactive near-field of an antenna is taken to extend to a distance of $\lambda/2\pi$ from the antenna, here 3 cm. For half-wave dipoles a limit of 2λ is proposed in [7]. Most of the antennas studied here have their reactive fields in a tight gap between an antenna element and a ground plane, and indeed the dipole spreads its fields more than the others.

The input impedance of the inverted-F antenna was affected the least because there is a ground plane in the structure and the reactive fields are concentrated in the gap between the F arm and the ground. Fig. 3 shows the return loss of the inverted-F antenna at different distances from the body. The separations at which the body stops affecting each antenna are summarised in Table 1. The required padding thicknesses of few centimetres are easily realised, as clothes are usually thick and loose.

The dipole antenna is the most sensitive one of the measured antennas. Its return loss at various distances from the body is plotted in Fig. 4. A variation of 100 MHz is recorded in the resonance frequency, though the GPS center frequency is

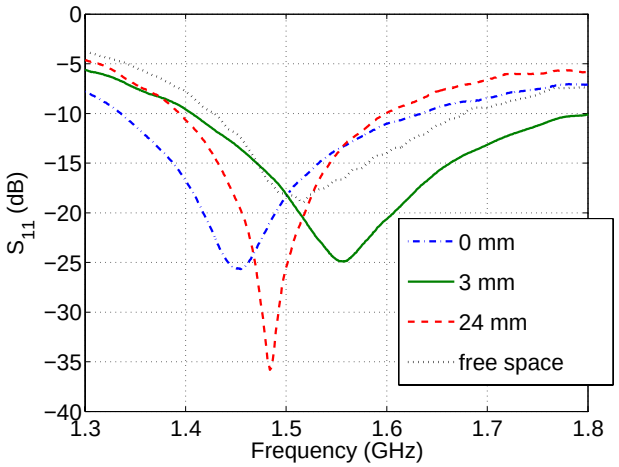

Fig. 4: The return loss of the dipole is significantly affected by a human even 2.4 cm away.

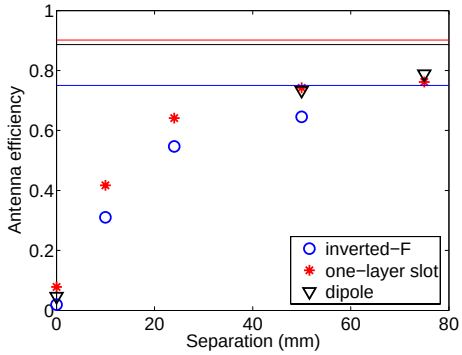

Figure 5: The antenna efficiencies of three antennas, measured using a phantom. Most of the loss is due to absorption and not detuning, thus the points also quite accurately represent the radiation efficiencies. The three horizontal lines represent the free-space efficiencies of (from top to bottom) the slot, the dipole, and the inverted-F.

always inside the –10-dB band as the dipole is relatively broadband. Extra loss introduced by the body is seen in the lowered Q value. The return loss deviates from the free-space curve until the separation is 6 cm (nearly half a wavelength).

For other antennas than dipoles, the shifting of the resonance frequency or other changes in the antenna input impedance due to the presence of a human body are small, predictable, and controllable at the GPS frequency. Thus the impedance presents no problem to the antenna designer.

3.2 Radiation pattern and efficiency

In the vicinity of a human body any GPS antenna will have a radiation pattern similar to a patch antenna. To achieve omnidirectionality, several antennas would need to be placed around the body, because at the GPS frequency the body cannot be penetrated. For the best performance the antenna can be placed on the shoulder facing upward, thus directing the null toward ground.

Antenna	Vertical coax	Horizontal coax
One-layer slot	23 dB	11 dB
Two-layer slot	14 dB	13 dB
Inverted-F	12 dB	9 dB
Dipole	20 dB	13 dB

Table 2: The front-to-back ratios measured with the feeding coaxial cable of the antenna vertically or horizontally oriented. The latter appear smaller, possibly because of the radiation from the feeding cable. The distance between the antenna and the user is 10 mm.

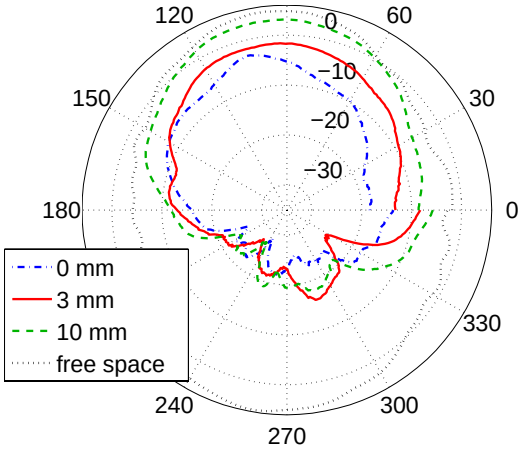

Figure 6: The one-layer slot antenna needs to be placed at 2.5 cm from the body to reach the free-space gain. The radial unit is dBi. The feed line of the antenna is oriented vertically.

When the user is placed in the reactive near-field of the antenna, the radiation efficiency of the antenna becomes very poor. The efficiency increases rapidly with increasing distance in the reactive near-field region, then more slowly. The results in Fig. 5 have been measured using a phantom. At a separation of $\lambda/2\pi$ the measured antennas exhibited radiation efficiencies of about three quarters of the free-space efficiency (e.g. for inverted-F at $\lambda/2\pi$ 60 % and in free space 75 %). Note that these results are not the worst case results with a large amount of tissue behind the antenna but measured with the antenna mounted on the back of the phantom's neck.

The human body acts as a scatterer or an obstacle if the separation between the antenna and the user is greater than $\lambda/2\pi$. The antennas radiate quite well in the forward direction, but the front-to-back ratios are between 10 and 20 dB no matter the separation. Table 2 lists the achieved front-to-back ratios at a separation of 10 mm. The forward radiation patterns will adopt the shape of the free-space pattern. For example, the radiation pattern of any measured antenna except the dipole at a separation of 10 mm will follow the shape of the free-space pattern in a sector of at least 100 degrees.

Some examples of the radiation patterns at various distances are presented in Figs. 6 for the one-layer slot and 7 for the inverted-F antenna. The forward gain is seen to gradually increase whereas the backward radiation is nearly unchanged. As a result of interference between the components radiated from the left and right side of the user, the backward hemisphere is filled with nulls and minor lobes.

The separation where the maximum gain reaches the free-space forward gain is nearly the same at which the user no longer changes the input impedance. If the distance is further increased, the forward gain will grow until a certain limit, as if the antenna was placed near a reflecting ground plane. The separations where the free-space and maximum reachable gains are achieved are tabulated in Table 3.

The forward gains at two interesting separations and the maximum reachable gains are listed in Table 4. At the best, it is possible to obtain a gain as much as three decibels greater than in free space.

Antenna	Separation for free-space gain	Separation for maximum gain
One-layer slot	24 mm	50 mm
Two-layer slot	10 to 20 mm	unknown
Inverted-F	15 mm	37 mm
Dipole	30 mm	50 to 80 mm

Table 3: The separation between the antenna and the user needed to achieve the free-space gain, and the separation which gives the maximum reachable gain.

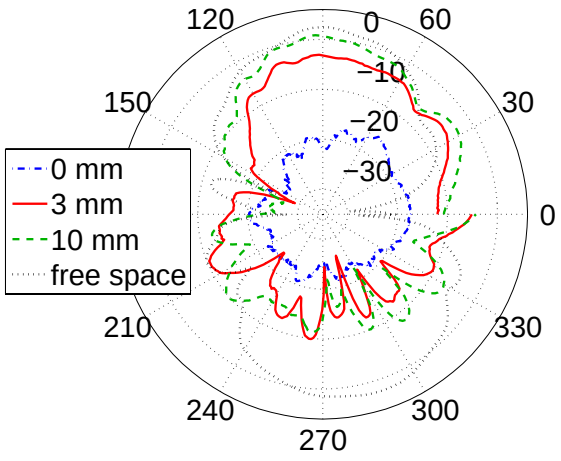

Figure 7: If the inverted-F antenna is placed directly on the clothes of the user, it radiates very poorly, but even a 3-mm gap is sufficient to enhance the radiation efficiency. The radial unit is dBi. The F arm points downward.

To exclude the effect of absorption, the inverted-F antenna was also measured attached to a 38-cm-by-38-cm metallic plate. When the separation is greater than 2.5 cm (again at the boundary of the reactive near-field), the results for the radiation pattern coincide with those measured using a human subject, as seen in Fig. 8. The radiation pattern features such as lobes and nulls are visible even at a separation of 3 or 10 mm, but the levels given by the metallic plate are 5 to 10 dB too strong, as seen in Fig. 8 a.

Antenna	At 10 mm	At 24 mm	At optimum
One-layer slot	–2.4 dB	–0.1 dB	+1 dB
Two-layer slot	0 dB	+3.13 dB	unknown
Inverted-F	–1.5 dB	+0.3 dB	+2.8 dB
Dipole	–3.2 dB	–0.8 dB	unknown

Table 4: Forward gains at separations of 10 mm, 24 mm, and at the optimum separation (as listed in the last column of Table 3). The gains are given in decibels relative to the free-space gain. As the maximum gain of the dipole was measured on the phantom only, it is not listed here. The optimum gain of the two-layer slot is a little more than the 24-mm value.

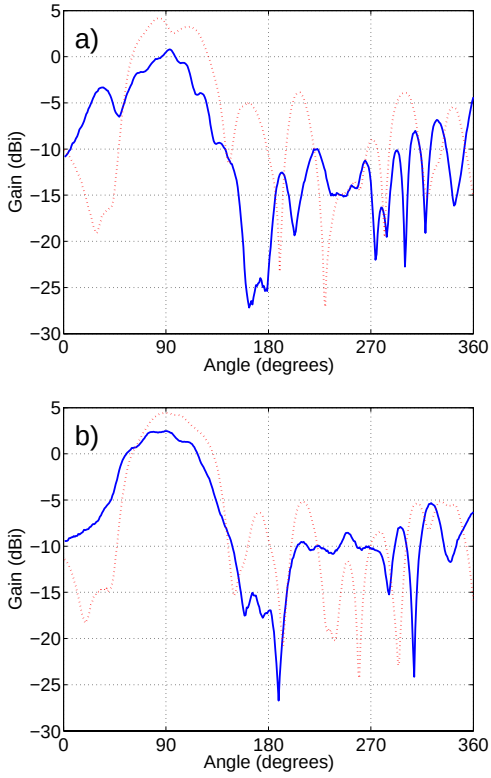

Figure 8: The horizontal plane patterns of the inverted-F antenna attached to either the metallic plate (dotted red) or the human abdomen (solid blue line) at a separation of a) 10 and b) 24 mm.

For the linearly polarised antennas the cross-polarisation (in dBi) remains as low as in free space, whereas the co-polarised component increases with distance. Axial ratios as good as in free space (1 dB) were recorded when the inverted-F antenna was mounted at 1 or 2.5 cm from the user. It is possible that the frequency of the best axial ratio is shifted a little downward, this however was not examined further.

3.3 Only little variation in results

The test setup was varied to find out whether the results can be extended. The user was replaced by a smaller one of the opposite sex. The antenna placement on body was varied to study more likely positions. Last, a statistical measurement was conducted to study the effect of body movements on the antenna performance. The following results were measured for the inverted-F antenna only.

The radiation pattern of the inverted-F antenna was measured using two test subjects: a 184-cm, 82-kg male and a 172-cm, 68-kg female. Measurements with the former one were conducted several times at different times of day, and the acquired results are plotted in Fig. 9. We observed that the variation in the results is random and thus caused mostly by the poor repeatability as the antenna placement on body and the body position vary from measurement to measurement.

In practice, a GPS antenna would surely be placed on the user's shoulder or neck. As the measurement system only allowed the measurement of horizontal radiation patterns, the antenna was mounted on the upper arm instead of the shoulder.

The maximum gain of a wearable antenna depends mostly on the separation between the antenna and the body, regardless of the antenna position on body. If the antenna is placed on the back of the neck, the main lobe becomes wider than in the other cases; otherwise the changes in the radiation pattern are insignificant. Even the front-to-back ratio remains poor no matter the placement.

With the user walking toward the transmitting antenna and the inverted-F antenna mounted on the abdomen, the maximum variation in the received power level is three decibels. If the user turns 80 degrees off the transmitting antenna, shadowing effects are introduced as the arm swings in the line-of-sight path. The variation in the power level is more than 10 dB, even 20 dB, mostly introduced by the moving arm.

4 Discussion

As observed in the results section, the human body may be seen as a reflector of some sort. It is not necessary to shield this reflector out, rather it should be utilised as a part of the antenna system.

Computational results for the radiation efficiency of a monopole close to a head have been reported in [1,2]: 50 %

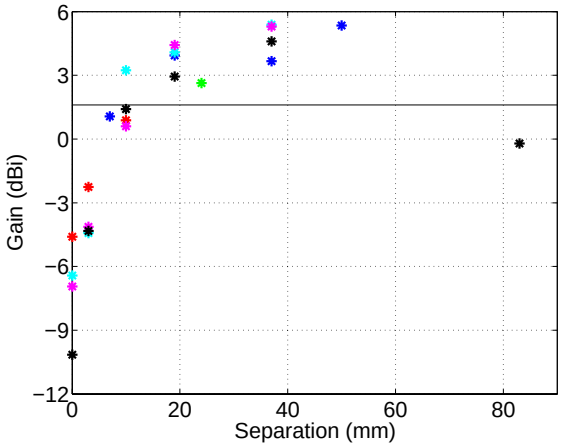

Figure 9: The forward gain of the inverted-F antenna measured at different separations. The horizontal line represents the free-space gain. 40 mm equals roughly a quarter of a wavelength. Different measurements are seen to differ considerably but randomly.

and 60 %, respectively, at a separation of $\lambda/2\pi$. Here the measured results are around 60 %, or three quarters of the free-space efficiency of each antenna, even for the dipole. The increase of the radiation efficiency with increasing distance is rapid, as also reported previously.

The observed shadowing effect and front-to-back ratios are in agreement with those reported earlier: 10 to 20 decibels for a monopole close to a human head at 1800 MHz [3,4]. The shadowing effect is strong although the head is smaller than the trunk.

Although the forward gain may increase dramatically due to the reshaping of the radiation pattern, it is intuitive that the increase in the maximum gain is about three decibels or less. For example, in [3] the forward gain of a monopole increases by about 10 dB but the maximum gain actually decreases compared to the free-space case.

At the GPS frequencies the human body may be treated as a reflector with a reflection coefficient of –0.7, as calculated from the wave impedance in the tissue [8]. When the user is outside the reactive near-field region, the forward radiation pattern may even be calculated using the image source method, assuming the human an infinite ground plane, which results in a good correspondence.

Creeping waves—surface waves that propagate in the shadow region—are insignificant in the scattering case studied. The backward radiation is caused by fringe effects in the boundary of the lit and shadowed regions rather than creeping waves. If creeping waves had a notable effect, the results measured using a human and a metallic plate would differ much more.

A good wearable antenna obviously needs to be small, insensitive to deformation and the presence of the user, and easy to fabricate. Of the measured one-layer antennas the

inverted-F antenna was the best. Moreover, all the results presented here suggest that we can give up the belief that a ground plane must always be employed between the antenna and the user.

Although the measurements were made mostly with the antenna attached to the abdomen of the user, the results can be used to estimate the human effect for antennas placed otherwise as well. Care shall be taken to ensure that the condition "large with respect to the penetration depth" is satisfied. A good place for a GPS antenna would naturally be on the shoulder or integrated into a bicycle helmet, so that the null introduced by the body would be directed toward the ground.

The results presented in this paper have been measured around the GPS center frequency (1.575 GHz) but may be extended to even 10 GHz. The properties of tissues do not change very rapidly in this frequency range [8], and the body may be considered to be of a quasi-optical size. However, extending the results below 1 GHz might be risky. For example, at 100 MHz totally different mechanisms dominate, and the penetration depth is significantly larger.

5 Conclusion

One-layer structures may well be used as wearable antennas. For best performance, structures with a ground plane (as the inverted-F antenna in Fig. 1 d) ought to be favoured over dipole- or monopole-like antennas, because in the former ones the near-field is concentrated in the gap between the radiating element and the ground. This means that there only needs to be a small separation between the user and the antenna to keep the user out of the reactive near-field region. The separations needed for the examined antennas ranged from one to three centimetres.

Attached to a human body, any antenna has a radiation pattern similar to a patch antenna. The radiation efficiency is about 25 % lower than in free space if the antenna is placed at a distance of $\lambda/2\pi$ from the body.

The forward gain can be increased about 3 dB above the free-space gain. Backward radiation, however, is blocked. The human body may be modelled as a reflecting plane with a reflection coefficient of –0.7.

Future plans on this subject include the validation of the model at other frequencies of interest. The model of the human body as a reflector or a poor ground plane gives rise to the interesting thought of using it as a ground for a microstrip line or a microstrip antenna.

Acknowledgements

Many thanks to Mr. Juha Lilja for excellent performance as a test subject.

This work was funded by the Finnish Funding Agency for Technology and Innovation under contract no. 40014/06, and by the Graduate School in Electronics, Telecommunications and Automation (GETA).

References

[1] T. Fukasawa, Y. Nishioka, S. Makino, Y. Sunahara. "Characteristics of a dipole antenna built-in a flip of a portable telephone", *Proc. Vehicular Technology Conference 2002*, vol. 2, pp. 547–551

[2] M. A. Jensen, Y. Rahmat-Samii: "EM interaction of handset antennas and a human in personal communications", *Proc. IEEE*, **83**, 1, pp. 7–17, (1995).

[3] J. T. Rowley, R. B. Waterhouse. "Performance of shorted microstrip patch antennas for mobile communications handsets at 1800 MHz", *IEEE Trans. Antennas Propag.*, **47**, 5, pp. 815–822, (1999).

[4] J. Toftgård, S. Hornsleth, J. B. Andersen: "Effects on portable antennas of the presence of a person", *IEEE Trans. Antennas Propag.*, **41**, 6, pp. 739–746, (1993).

[5] J. Heikkinen, T. Laine-Ma, A. Ruhanen, M. Kivikoski. "Flexible antennas for GPS reception", *Proc. European Conference on Antennas and Propagation*, 2006.

[6] M. A. Habib, T. A. Denidni, G. Y. Delisle. "Design of a new wide-band CPW-fed circular slot antenna," *2005 IEEE Antennas and Propagation Society International Symposium*, vol. 1B, pp. 565–568.

[7] S. Laybros, P. F. Combes. "On radiating-zone boundaries of short, $\lambda/2$, and λ dipoles", *IEEE Antennas Propag. Mag.*, **46**, 5, pp. 53–64, (2004).

[8] Institute for Applied Physics, Italian National Research Council. "An Internet resource for the calculation of the dielectric properties of body tissues". [Online]. Available: http://niremf.ifac.cnr.it/tissprop/

Publication [P5]

T. Kellomäki, W. G. Whittow, J. Heikkinen, and L. Kettunen.
2.4 GHz plaster antennas for health monitoring.
In *Proc. European Conference on Antennas and Propagation (EuCAP)*,
Berlin, Germany, March 2009.

2.4 GHz Plaster Antennas for Health Monitoring

Tiiti Kellomäki [#1], William G. Whittow [*2], Jouko Heikkinen [#3], Lauri Kettunen [#4]

[#] *Department of Electronics, Tampere University of Technology*
P.O.Box 692, FI-33101 Tampere, FINLAND
[1] tiiti.kellomaki@tut.fi, [3] jouko.heikkinen@tut.fi, [4] lauri.kettunen@tut.fi

[*] *Department of Electronic and Electrical Engineering, Loughborough University, Loughborough, Leics, UK, LE11 3TU*
[2] w.g.whittow@lboro.ac.uk

***Abstract*— Commercial plaster material (polyacrylate) is used as an antenna substrate. Two 2.45 GHz patch antennas are introduced, both designed to be attached directly to the skin. Measured efficiencies are 70 % in free space and 60 % on-body. Measured on-body gains of each antenna are 6.2 and 1.4 dBi. Simulated 1 g specific absorption rates (SAR) of the two antennas are 2.3 W/kg and 1.6 W/kg using 1 W input power. 10 g SAR values are 0.6 W/kg and 1.2 W/kg. Antenna feeding using snap-on buttons is investigated and has been found useful.**

***Index Terms*— Antennas, medical services, microstrip antennas.**

I. Introduction

Many medical applications require gathering data of the patient's condition. Examples include heart rate, breath rate, and blood oxygen level. Usually these data are transmitted via a cable, which limits the patient's movements.

Freedom of movement is especially important in home nursing and in monitoring athletes' recovery after training. As an alternative to cables, the patients could carry a belt-worn device which records data and transmits the results wirelessly to the system whenever possible. Plaster-based sensors have been developed in the recent years [1]. As printed electronics evolves, the whole system including the measurement electronics, data gathering, radio transceiver, and antenna could be integrated on a single, disposable plaster.

In this paper, we examine the feasibility of plaster material as an antenna substrate, and present two antenna structures. The antennas are to be attached directly to the skin, like regular wound-care plasters. To minimise the effect of the body on the antennas, a ground plane is used. Slits are cut in the antennas to increase flexibility and breathability.

The antenna structures as well as the electrical properties of the plaster are described in Section II. Section III contains measured results for the regular antenna parameters. Simulated SAR values are presented in Section IV. We describe an alternative feeding method using snap-on buttons and examine the effect of the user sweating on antenna parameters in Section V. Section VI concludes the work.

II. Antenna Structures

The goal of the design process was to design antennas on a plaster substrate that cover the frequency band from 2.4 to 2.5 GHz. Linear polarisation was desired, because circular polarisation characteristics would depend too much on antenna bending, as shown by our ongoing research. The antennas were designed to be flexible and breathable.

TABLE I
Patch Antenna Dimensions (in millimetres)

ground and substrate		patch and feed		slits and strips	
w_g	81	w_p	47	w_c	3
l_g	80	l_p	48	w_b	4
w_s	57	w_f	4.5	w_a	1
l_s	58	l_{in}	15	p	1
h	1.36	g	1	l_1	10
				l_a	5

Commercially available Mölnlycke Mefix [2] plaster material (self-adhesive polyacrylate) was chosen as the substrate. Its dielectric properties were measured at 2.45 GHz. The dielectric constant is about 1.38 and loss tangent 0.02. Compared to a PCB material the dielectric constant is very low but losses are about the same as of a poor PCB.

The conducting material of the antennas was copper tape. In the future, the antennas could e. g. be printed on the plaster. Research is going on to find a suitable conducting material for wearable antennas.

We must use a ground plane, because the antennas operate less than one millimetre from the body. The reactive near-field is then trapped between the radiating element and the ground plane. This reduces the effect of the user on input impedance (resonance frequency) and radiation, and lowers SAR.

Two antennas were designed, one a half-wave patch and the other a quarter-wave antenna short-circuited to the ground. The substrate for both is an 8-layer plaster, which is 1.36 mm thick. The dimensions of the antennas are given in Figs. 1, 2, 3, and 4, and in Tables I and II.

To increase flexibility and breathability, slits were cut both in the antenna elements and ground planes. The x-directional slits do not affect the current flow of the radiating mode, however extra horizontal strips had to be added at the feed point level to allow for y-directional current at the feed. The antenna dimensions are a trade-off between antenna efficiency and breathability.

III. Measured Results

Regular antenna parameters, the input impedance and radiation pattern, were measured both in free space and on-body.

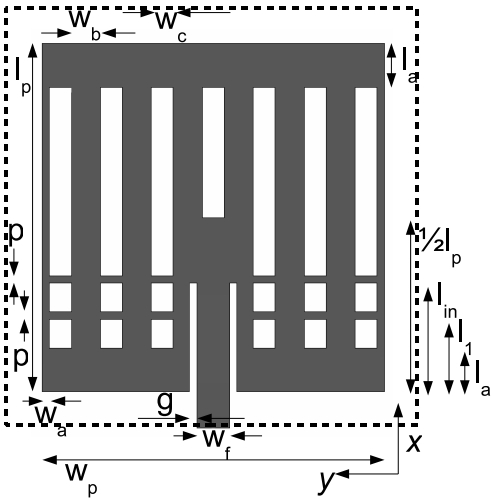

Fig. 1. Dimensions of the patch antenna–the part above substrate. The substrate is shown dashed.

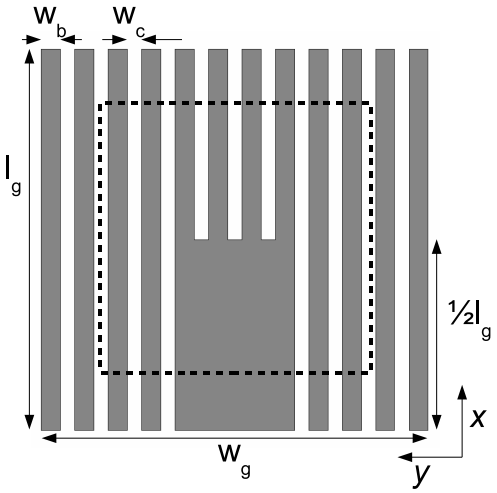

Fig. 2. Dimensions of the patch antenna ground plane. A substrate (shown dashed) of width w_s, length l_s, and height h is placed at the centre of the ground plane. Note that the substrate does not cover all of the ground plane. The whole structure lies on two layers of plaster (thickness about 0.3 mm). The slits in the ground plane and the patch coincide.

TABLE II
QUARTER-WAVE ANTENNA DIMENSIONS (IN MILLIMETRES)

ground and substrate		patch and feed		slits and strips	
w_g	54	w_p	36	w_a	4.5
l_g	59	l_p	25.5	w_b	3.5
l_1	14	w_f	5	w_c	1.5
l_s	28.5	l_{in}	18	w_d	14
w_s	42	l_{sh}	2	l_c	17.5
h	1.36	g	1	p	1

A. Input Matching

The 2.45 GHz ISM band (Industrial–Scientific–Medical) extends from 2.4 to 2.5 GHz, a bandwidth of 4.1 %. This

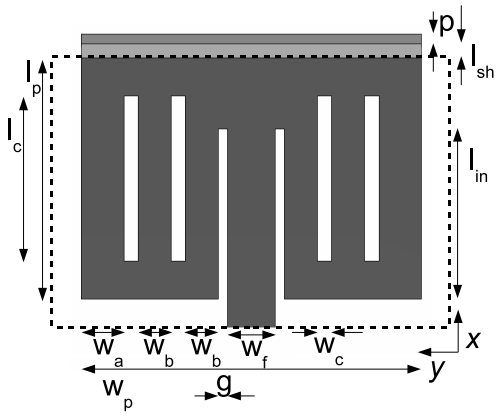

Fig. 3. Dimensions of the quarter-wave antenna–the part above substrate. The light gray part (length l_{sh}) is bent from above the substrate to the ground plane level, so that the uppermost part (length p) is actually a part of the ground plane. The patch is thus short-circuited to the ground. The substrate is shown dashed.

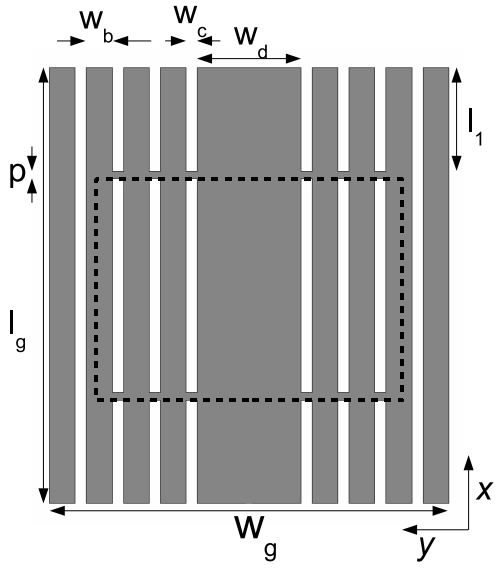

Fig. 4. Dimensions of the quarter-wave antenna ground plane. The parts of width p here (upper one) and in Fig. 3 coincide. A substrate (shown dashed) of width w_s, length l_s, and height h is placed on the ground plane centred in the y direction. The whole structure lies on two layers of plaster (thickness about 0.3 mm). The slits in the ground plane and the patch coincide.

can be covered by the 6-dB band of an antenna with a Q value of less than 28.

We measured the antenna input impedances using a vector network analyser. For on-body measurements the antennas were attached to the abdomen in order to avoid bending which would possibly interfere with the measurement.

The human body lowers the resonance frequencies of both antennas. At the same time the input resistance at resonance frequency is lowered. The Q value decreases when the antenna is placed on the body, indicating losses in the body. Figures 5 and 6 illustrate the change. The values in free space and on-body are listed in Table III.

TABLE III

INPUT IMPEDANCE MEASUREMENT RESULTS

	patch	quarter-wave
input resistance, free space	54 Ω	58 Ω
input resistance, on-body	42 Ω	51 Ω
Q, free space	27	23
Q, on-body	23	19
resonance frequency change between free space and on-body	< 20 MHz	< 5 MHz

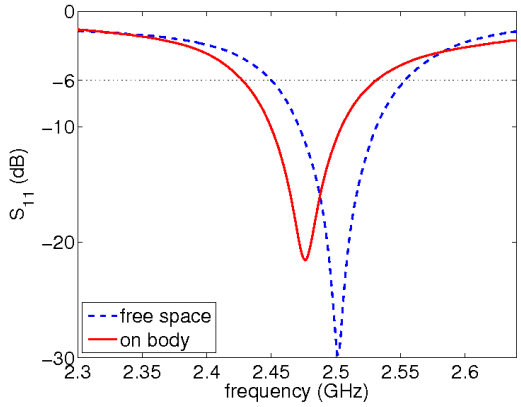

Fig. 5. The S_{11} of the patch antenna. User affects the resonance frequency but the change Q value (bandwidth) is small. Some of the observed frequency change may be due to antenna bending on-body.

Although the antennas are designed to be flexible especially regarding bending about the x axis, they are both sensitive to strong bending. Wrapping the antennas about a styrofoam cylinder of diameter 94 mm caused the resonance frequency to drop by 40 MHz. The prototypes described here may be used only on flat parts of the body, such as on the chest or back. If the antennas are placed on arms or other such places to imply antenna curvature, it is necessary to redesign the element length to attain the desired resonance frequency.

B. On-Body Radiation Patterns

The on-body radiation patterns were measured in an anechoic chamber. The antennas were attached to the abdomen. We only measured the radiation patterns in the yz plane. The inaccuracy associated with the on-body results is about ± 2 dB. The antennas were also measured in free space, using a Satimo StarLab system [3]. From the free-space measurements we get the radiation efficiency, and from the change in Q value between free-space and on-body we can estimate the bodyworn efficiency.

Table IV summarises the measured free-space and on-body results. Example radiation patterns are presented in Figs. 7 and 8, which show the horizontal plane when the antenna feed cable points downwards.

Measurements show that both antennas perform well on-body. The radiation efficiency in free space (about 70 %) is quite large considering that the antennas were made on a plaster substrate. Even a non-uniform ground plane prevents

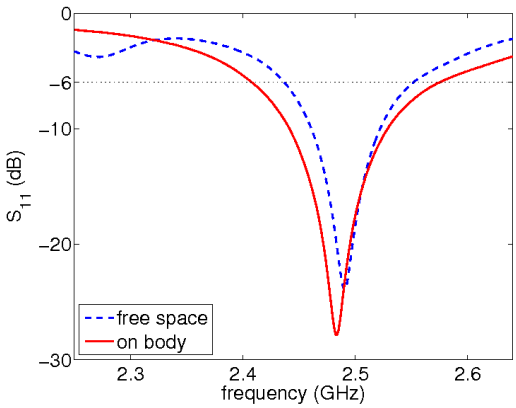

Fig. 6. The S_{11} of the quarter-wave antenna. The resonance frequency does not change significantly but the bandwidth grows.

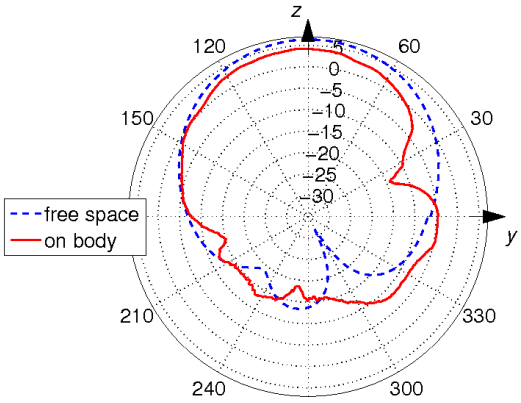

Fig. 7. Patch antenna radiation patterns at 2.5 GHz, in the yz plane, x-directionally polarised. Radial scale is in dBi.

TABLE IV

RADIATION PATTERN MEASUREMENT RESULTS.

	patch	quarter-wave
radiation efficiency in free space	70 %	72 %
maximum gain in free space	6.7 dBi	4.2 dBi
maximum gain when worn	6.2 dBi	1.4 dBi
radiation efficiency on-body (estimate)	60 %	60 %
bodyworn eff. (estimated from Q)	85 %	83 %

the radiation efficiency from dropping too much on the body. The bodyworn efficiency can be calculated from

$$\text{bodyworn efficiency} = \eta_{\text{rad}}^{\text{on-body}} / \eta_{\text{rad}}^{\text{free space}} = Q^{\text{free space}} / Q^{\text{on-body}}$$

where the η_{rad} is the radiation efficiency and Q is the Q value [4]. The right side of the equation assumes that only one mode is present both in free space and on-body and that only the loss Q changes.

IV. SIMULATED SPECIFIC ABSORPTION RATE

This section considers the specific absorption rate (SAR) at 2.4 GHz from the two plaster antennas. SAR is the standard criteria for measuring the amount of electromagnetic energy

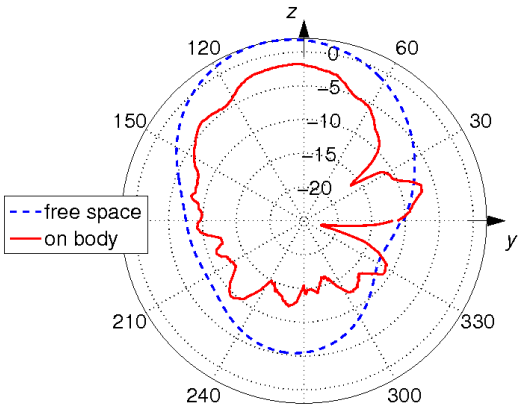

Fig. 8. Quarter-wave antenna radiation patterns at 2.5 GHz, in the yz plane, x-directionally polarised. Radial scale is in dBi.

absorbed in the body and is calculated as

$$\text{SAR} = \frac{\sigma |E|^2}{\rho}$$

where $|E|$ is the rms magnitude of the electric field strength vector, ρ is the mass density of the material in kg/m^3 and σ is the electrical conductivity in S/m. [5]

Note that the maximum 1 g SAR, defined by international ANSI/IEEE standards (used by the FCC in the USA) is 1.6 W/kg [6]. The 10 g SAR is comparable to the European ICNIRP safety standards of 2.0 W/kg [7].

The SAR values in this paper were simulated in CST [8] by placing the antenna next to a digital human body model. The model is from The Visible Human Project [9]. To reduce the memory constraints and improve the computation speed, the body was truncated to leave a section of the torso and also by using one homogenous tissue, see Fig. 9. Homogeneous phantoms are often used for SAR studies as they are well known to give conservative SAR values [5], [10]. SAR measurements and simulations generally agree to within 10 % [5].

The electrical properties of the body simulating tissue were σ = 1.88 S/m, ϵ_r = 37.97, and ρ = 1000 kg/m^3. The Visible Human model was imaged with the subject lying on a flat metallic bench and consequently the phantom has a flat back. The antenna designs in this paper are planar and therefore the centre of the lower back was a convenient place to locate the antenna. In future work, we will bend the antenna so that it can be added to the arm or leg. All results in this section have been calculated with 1 W input power.

To make the SAR simulation easier, the simulated patch antenna model was slightly different from the measured one. The centre slit of the simulated model is 7 mm longer and the metal strips adjacent to it are 1 mm narrower than in the measured one. The effect of this difference on SAR is negligible. The measured and simulated quarter-wave antennas are identical.

The 1 g SAR of the patch antenna was 2.27 W/kg and the 10 g SAR was 0.59 W/kg. Therefore, with a 1 W input power the antenna would be below the limits in Europe but not in the USA. If this antenna were to be used in the USA, the input power would have to be limited to 0.7 W. Fig. 10 shows that the largest 1 g SAR volume is located near the feed of the antenna and this is much larger than other 1 g volumes. Fig. 11 shows that the 10 g SAR distribution is more uniform.

The quarter-wave antenna has a smaller 1 g SAR of 1.58 W/kg, see Fig. 12. This means that this antenna would not breach the IEEE safety standards. However the 10 g SAR of 1.21 W/kg, see Fig. 13, was twice as large as with the patch antenna. The 1 g and 10 g SAR plots of the quarter-wave antenna have a similar pattern to each other.

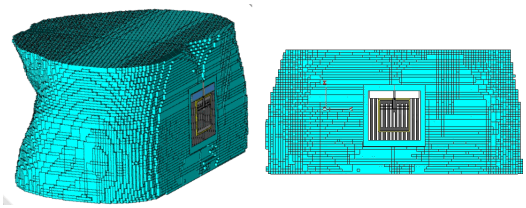

Fig. 9. Patch antenna on the back of the torso model. Feed line points upwards.

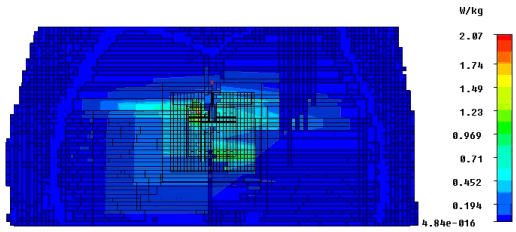

Fig. 10. The 1 g SAR of the patch antenna. Feed line points upwards.

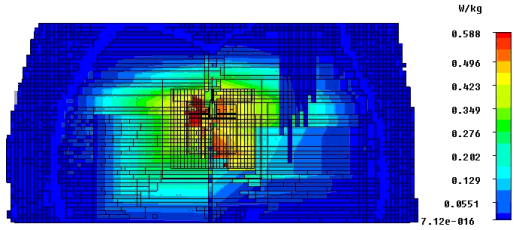

Fig. 11. The 10 g SAR of the patch antenna. Feed line points upwards.

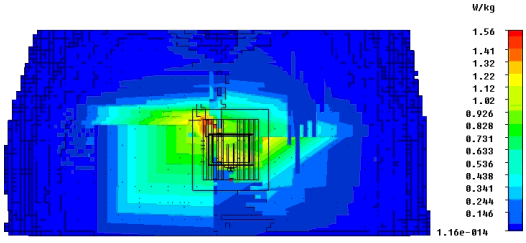

Fig. 12. The 1 g SAR of the quarter-wave antenna. Feed line points downwards.

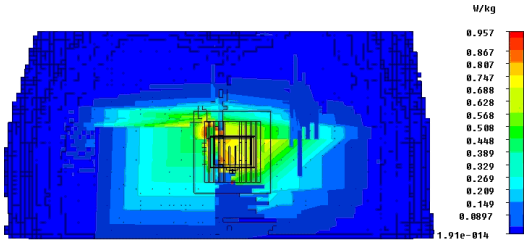

Fig. 13. The 10 g SAR of the quarter-wave antenna. Feed line points downwards.

V. Antennas in Use

Finally, the antennas were tested in real operating conditions. To make the RF connection cheaper, we investigated the usability of snap-on buttons. The antennas were also subjected to a harsh environment, namely a sweating user.

A. Snap-On Buttons in Feed

RF connectors are expensive and thus not suitable for disposable single-use antennas. Instead, we experimented using snap-on buttons, a technique proposed in [11]. In [11], the antennas were fed using a pin through the ground plane. The exact feeding position was found difficult to control.

The antennas proposed in this paper employ an inset microstrip feed line. The snap-on buttons are connected to the microstrip instead of the patch. This gives us more control of the feed impedance, and additionally it is easier to connect the coaxial cable to the edge of the antenna rather than through it. Problems arising from our approach include a very long transition from the coaxial cable to the microstrip, which adds inductance in the feed, and the fact that the coaxial cable may move in use.

We measured the time domain response of a button-fed 50-ohm microstrip line. The reflection from the button was better than –14 dB up to 3 GHz. This indicates that snap-on buttons are suitable for use in cheap commercial devices.

B. Sweating Effects

The product sheet of the plaster material describes the plaster as nonabsorbent, but states that air and water vapour would pass through [2]. Thus it was expected that sweating would not alter the antenna parameters significantly.

We attached the antennas to the back of a male who then jogged for 45 minutes, sweating heavily. No cables were attached to the antennas during the exercise. The radiation patterns and input impedances were measured afterwards. The antennas were not wet to touch after they had been shaken dry. The glue had however partially failed. The user's shirt was dry at the places where the antennas had been.

The radiation patterns were measured right after sweating, and the input impedances about one hour after it.

Sweating reduced the antenna efficiencies by between 2 and 8 %. The radiation patterns were unaffected. The measured resonance frequencies were not changed by sweating. The input impedance decreased by about 8 ohms (patch) or 6 ohms (quarter-wave). The Q value of the quarter-wave antenna reduced from 28 to 24, whereas for the patch antenna the change was smaller than measurement uncertainty.

VI. Conclusion

Antennas made on a plaster substrate have been described. The antennas employ a ground plane between the radiating element and the user to reduce losses. Slits cut in both the elements and the ground planes add flexibility and breathability.

The bandwidth of the plaster antennas covers the 2.4 GHz ISM band. The input impedance is not significantly affected by the body presence. The gain of the half-wave patch antenna is 6.2 dBi and the quarter-wave patch 1.4 dBi, both measured with the antenna attached to the abdomen. Estimated body-worn efficiencies (radiation efficiency on-body compared to the free-space value) of the antennas are 85 %.

The SAR values of the antennas were quite high. Particularly the patch antenna would break the U.S. SAR limits if more than 0.7 W is fed into the antenna. The SAR could be reduced by adding more metal to the antennas, especially in the areas of high current density near the feed point.

Of the two antennas described here, the larger one (patch) was seen to be better, especially in terms of the on-body gain. However, if smaller antennas are desired, the quarter-wave antenna has proven useful as well.

Acknowledgment

Tiiti Kellomäki wishes to thank Timo Kellomäki for excellent performance as a sweating anthropomorphic mannequin. Tiiti Kellomäki's research was funded by The Graduate School in Electronics, Telecommunications and Automation (GETA). William Whittow thanks Shahid Bashir for his CST expertise.

References

[1] T. Vuorela, J. Hännikäinen, and J. Vanhala, "Plaster like Physiological Signal Recorder – Design Process, Lessons Learned," in *Proceedings of the Ambience 08 Smart Textiles – Technology and Design,* p. 89–96. Borås, Sweden, June 2–3, 2008.

[2] Mefix. [Online]. Available: `http://www.molnlycke.com/item.asp?id=924`

[3] SATIMO [Online]. Available: `http://www.satimo.com/`

[4] W. G. Scanlon and N. E. Evans, "Numerical analysis of bodyworn UHF antenna systems," *Electronics & Communication Engineering Journal,* vol. 13, no. 2, p. 53–64, Apr 2001.

[5] W. G. Whittow, C. J. Panagamuwa, R. M. Edwards, and J. C. Vardaxoglou, "On the effects of straight metallic jewellery on the specific absorption rates resulting from face illuminating radio communications devices at popular cellular frequencies," *Physics in Medicine and Biology*, vol. 53, p. 1167–1182, 2008.

[6] ANSI/IEEE 1992 IEEE standard for safety levels with respect to human exposure to radio frequency fields 3 kHz to 300 GHz. *Standard C95.11992.*

[7] ICNIRP 1998 Guidelines for limiting exposure to time-varying electric, magnetic and electromagnetic fields (up to 300 GHz), *Health Phys.,* **74,** 494–522.

[8] CST [Online.] Available: `http://www.cst.com/`

[9] The National Library of Medicine's Visible Human Project [Online]. Available: `http://www.nlm.nih.gov/research/visible/visible_human.html`

[10] O. P. Gandhi and Jin-Yuan Chen, "Electromagnetic absorption in the human head from experimental 6-GHz handheld transceivers," *IEEE Trans. Electromagn. Compat.,* vol. 37, no. 4, p. 547–558, Nov 1995.

[11] I. Belov, M. Chedid, and P. Leisner, "Investigation of snap-on feeding arrangements for a wearable UHF textile patch antenna," in *Proceedings of the Ambience 08 Smart Textiles – Technology and Design.* Borås, Sweden, June 2–3, 2008.

Publication [P6]

T. Kellomäki and W. G. Whittow.
Bendable plaster antenna for 2.45 GHz applications.
In *Proc. Loughborough antennas and propagation conference (LAPC)*,
Loughborough, UK, November 2009.

Bendable Plaster Antenna for 2.45 GHz Applications

Tiiti Kellomäki[#1], William G. Whittow[*2]

[#] *Tampere University of Technology, Department of Electronics, P.O.Box 692, FI-33101 Tampere, Finland*

[1]tiiti.kellomaki@tut.fi

[*]*Department of Electronic and Electrical Engineering, Loughborough University, Loughborough, Leics, UK, LE11 3TU*

[2]w.g.whittow@lboro.ac.uk

***Abstract*— A plaster antenna for 2.45 GHz applications is presented. Measurement results for different use cases are given, and bending effects are examined. The proposed structure exhibits a 6 dBi on-body gain, and covers the 2.4–2.5 GHz ISM band in all use cases. The effect of bending the antenna on the SAR has been investigated by simulations. The antenna is suitable for medical applications.**

I. Introduction

Bodyworn antennas, and especially disposable plaster antennas can prove useful in patient monitoring in e.g. hospitals or home nursing, or in monitoring athletes' recovery after training.

Current technology requires the transmitter to be a belt-carried box, but in the future we may see disposable transmitters printed on plasters, harvesting their transmit power from ambient radio waves. Plaster antennas are also feasible for passive RFID applications such as locating a patient.

In this paper we present a patch antenna with the substrate made of commercially available plaster material. The patch is designed to be flexible. The feed uses snap-on buttons to connect the antenna to a coaxial cable.

Some problems have been encountered with the previous plaster antennas [1]. The resonance frequencies were seen to shift when the antennas were bent. Also the peak SAR values were high. All this was seen to be due to the slits cut in the antennas. In this paper we focus on how these problems can be fixed.

The antenna structure with dimensions is introduced in Section II. In Section III, the measured antenna properties are presented, and the effects of bending and humidity are examined. The simulated SAR values are presented in Section IV, and Section V concludes the work.

II. Antenna Structure

The proposed antenna structure is a conventional rectangular patch, fed with a short microstrip line. Eight layers of commercial Mefix plaster (self-adhesive polyacrylate [2]) form the substrate. Only a part of the ground plane is covered with the substrate plaster; this results in reduced losses compared with a substrate the size of the ground plane.

Small slits are cut in the ground plane, to make it more flexible. The ground plane thus consists of nine separate metal strips. Solid copper foil tape would not stretch but will wrinkle or break, whereas the air gaps allow the ground to stretch and adapt to the body shape.

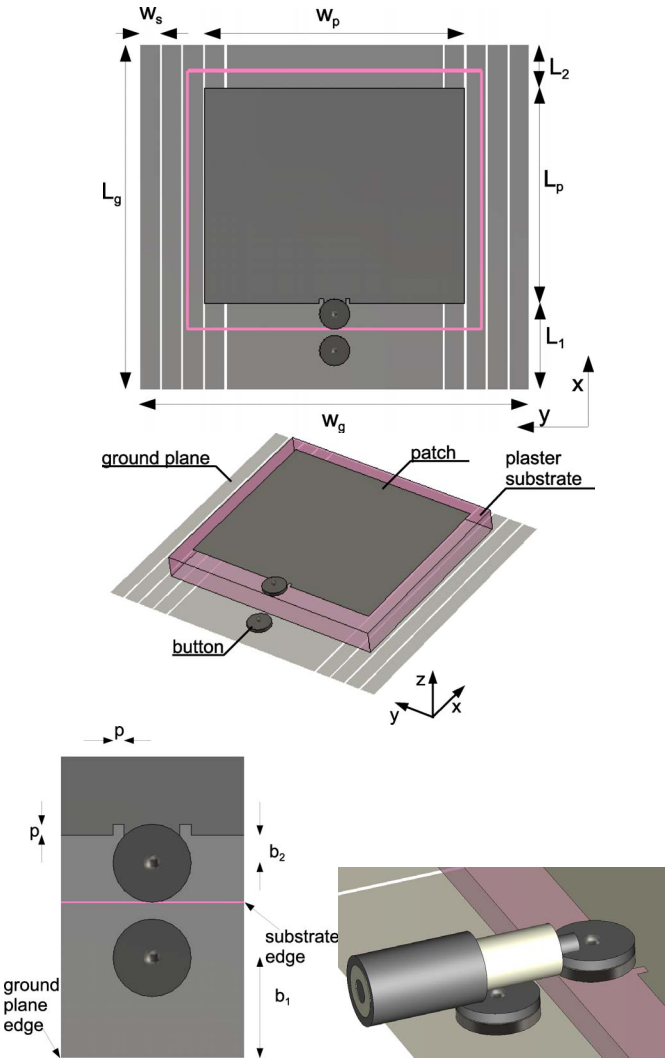

Fig. 1 The antenna structure. Grey: metal; pink: edges of the plaster substrate. The eight slits (white; air) cut in the ground plane are identical, 0.5 to 1 mm wide. The structure lies upon a 10-cm plaster square, which is then attached to the skin. Middle: perspective view of the structure, substrate thickness exaggerated. Bottom: a closeup of the feed point, and a coaxial cable attached to the buttons.

Figure 1 presents the antenna shape, and the dimensions are listed in Table I. The important dimensions are marked with an asterisk, and the rest may be allowed to vary. During tests, the manufacturing tolerance was at least ±0.5 mm.

Commercial snap-on buttons are used to feed the antenna. One male button is punched through the ground plane and

TABLE I
ANTENNA DIMENSIONS IN MILLIMETRES. IMPORTANT DIMENSIONS ARE MARKED WITH AN ASTERISK.

patch length *	L_p	50	patch width *	w_p	60
ground length	L_g	80	ground width	w_g	90
	L_1	20	metal strip width	w_s	4…5
	L_2	10	slit width		0.5…1
feed line width		5.5	feed inset *	p	1
substrate length		60	substrate width		70
substrate thickness *	h	1.36	substr. dielectric constant	ε_r	1.38
button diameter		7	substr. loss tangent	tan δ	0.02
button place 1	b_1	10	button place 2	b_2	2…3

another one through the short microstrip line feeding the patch. A coaxial cable with female buttons is used for measurements. The patch and the substrate are not placed at the centre of the ground plane, to allow some space around the button. The spacing between the buttons is due to the button size (diameter 7 mm). The snap-on button feed is described in detail in [3].

The metallic parts of the tested prototypes were cut out of copper foil tape. In the future and in mass production, the antennas could be e.g. inkjet printed.

As shown in previous research [1], slits can be cut in patch antennas. One must make sure there is a continuous path for the current in both the patch element and the ground plane. Here the slits are vertical, as is the radiating current mode. Cutting slits in the patch increases the input impedance and the Q value. Slits in the ground plane decrease the Q value because the tissue losses increase, and consequently the SAR increases as well. Cutting the antenna makes it more sensitive to bending, i.e. bending a cut antenna changes its resonance frequency more than that of a solid antenna.

Compared to the previous patch antennas [1], this antenna is designed to have a stable resonance frequency even when slightly bent. With no slits under the patch feed point, the SAR value is reduced.

III. MEASURED IMPEDANCE AND RADIATION

Seven prototype antennas were constructed and tested. The input impedances were measured using a vector network analyser. In all the measurements the antennas were fed using a 7-cm coaxial cable with snap-on buttons. The placement of the buttons introduces an uncertainty of 5 to 10 ohms in the resonant resistance and 10 MHz in the resonance frequency.

A Satimo Starlab system with about a 1 dB accuracy [4] was used in all the free-space radiation pattern measurements. The on-body radiation patterns were measured in an anechoic chamber. The set-up allowed only the horizontal pattern measurement. The expected accuracy of the on-body measurements is about 2 dB in the main lobe.

A. Input Impedance On-Body

Plaster antennas are designed to be attached directly to the skin, and thus the free-space performance is of no practical importance. However, it is easy to design, model, and measure antenna prototypes in free space, and apply the predicted body influence to the design process.

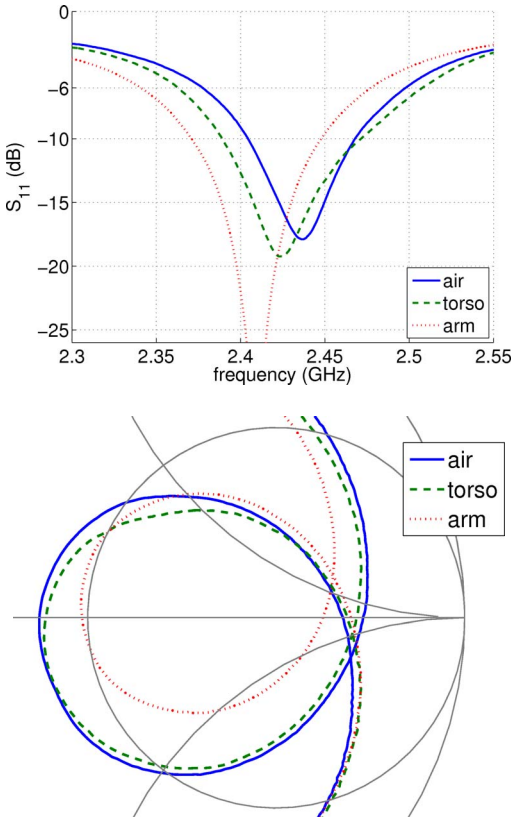

Fig. 2 The measured input impedance. a) Return loss on the dB scale; b) an enlarged view of the Smith chart. On arm, we see that the bending causes the impedance to decrease. The resonance frequency detunes slightly, due to bending in the *xz* (E-plane) as well as the *yz* plane (H-plane), and also due to the inaccuracy associated with the button feed. Because the manufacturing tolerances, the centre frequency is not exactly 2.45 GHz.

Compared to free-space measurements, the body lowers the input impedance by about 5 ohms. There is virtually no detuning effect. The increased losses are seen in the lowered Q value: from about 28 in free space to about 25 on-body. This means that the bandwidth grows by 10 MHz.

It is difficult to isolate the effects of the dielectric body and bending, because the body cannot be made fully flat. Attaching the antenna to the arm, the input impedance is lowered by few ohms compared to on-torso, as further described in section III C.

Figure 2 shows the S_{11} curve of the antenna placed on various places on the body. On the arm, the antenna is curved in the *yz* plane (H-plane, see Fig. 5), but bending also in the *xz* plane (E-plane) is unavoidable. Some detuning is observed, mostly due to the snap-on button feed arrangement, but also because of bending in the *xz* plane. Nevertheless, the usable 6-dB bandwidth is more than 100 MHz, enough to cover the 2.45 GHz ISM band.

The input impedance does not vary from person to person. Variation in the measurement results is mainly caused by the snap-on buttons in the feed (see [3]) and by the deformation of the antenna.

TABLE II
RESULTS OF THE HORIZONTAL PATTERN MEASUREMENT

	torso	**arm**	**air**
max. gain (dBi)	5…7	6…7	7
Front-to-back ratio (dB)	10…15	20	15

B. Radiation Patterns On-Body

In free space, the gain was measured to be 7 dBi and the radiation efficiency 73% (–1.4 dB). The peak on-body gains in the horizontal plane are slightly lower than in free space, as listed in Table II. With a small user, a distinct back lobe is seen when the antenna is placed on the torso; with large users the front-to-back ratio is larger. On the arm, the body shadows the backwards direction by 20 dB, regardless of the user size. Fig. 3 illustrates the effect of different users on the radiation pattern, and free-space and on-body patterns are compared in Fig. 4.

The measurements were repeated using three test subjects, and the results were seen to agree within the measurement inaccuracy, except for the back lobe. Results are also consistent with the earlier experiments on plaster antennas [1].

C. Bending

The effects of bending were examined by attaching the antennas on styrofoam cylinders. The bending radii were 47 mm, 68 mm, and 115 mm, corresponding to arm, thigh, and side of the thorax. Here the *yz* bending refers to 'bending around a cylinder directed along the *x* axis,' or bending in the H-plane. The bent antenna always has the patch on the upwards side, i.e. the antenna is always convex. Fig. 5 illustrates *yz* bending.

If the antenna is bent in the *yz* plane, the input impedance decreases, and as a result the bandwidth narrows. This effect is more pronounced in air than on body: when the antenna is moved from torso to arm, the impedance changes less than due to a similar bending in air. The change in resonance frequency is seemingly random.

Bending the antenna in the *xz* plane (E-plane) alters the current flow paths, and thus the resonance frequency increases. In air, the 68 mm bending radius was seen to increase the resonance frequency by 50 MHz, or half the bandwidth to be covered. The 47 mm radius resulted in 70 MHz detuning. Again, if the antenna is bent on the body, we observe detuning of 5 to 20 MHz, much less than in air. Bending in the *xz* plane does not change the input resistance at resonance.

Table III summarises the measured changes in input impedances and resonance frequencies due to bending.

The radiation patterns were measured with the antennas bent on styrofoam. Bending causes the main lobe to widen, and thus the gain drops by 0.5 dB. The radiation efficiency does not change due to bending.

In use the antennas are simultaneously bent in both planes. The *xz* bending should be minimised when the antennas are attached to the body. The limbs and thorax are the most feasible body parts considering this.

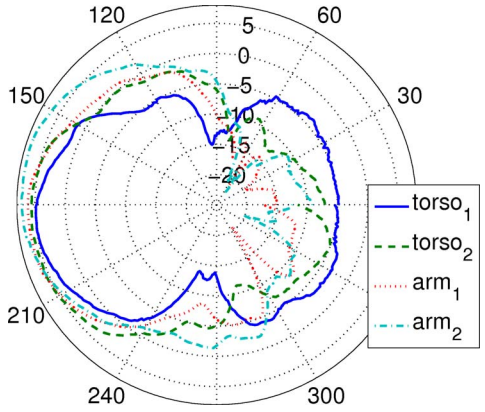

Fig. 3 The measured horizontal plane (*yz* or H-plane) patterns on two test subjects: 1—a 68-kg female, 2—a 88-kg male. There is a strong shadowing effect by the body. The patterns were measured at 2440 MHz (arm) and 2480 MHz (torso). Radial scale in dBi.

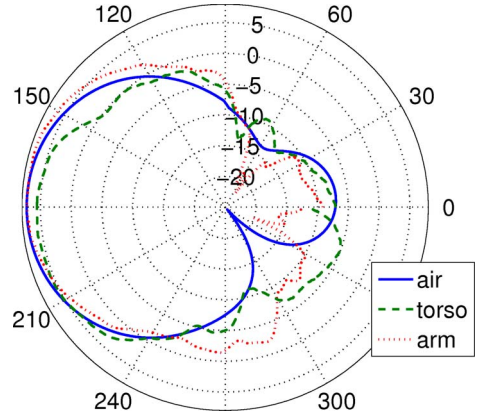

Fig. 4 The measured horizontal plane (*yz* or H-plane) patterns in free space and on body. The test subject is the male in Fig. 3. The patterns were measured at 2440 MHz (arm and free space) and 2480 MHz (torso). Radial scale in dBi.

TABLE III
MEASURED CHANGES IN INPUT IMPEDANCE AND RESONANCE DUE TO BENDING. POSITIVE VALUE: BENDING INCREASES THIS.

	air 47 mm	**arm 47 mm**	**air 68 mm**	**thigh 68 mm**
ΔZ_{in} (*yz* bending, ohms)	–10	–5	–10	–6
Δf_{res} (*xz* bending, MHz)	+70	+5	+50	+20

To make the bent antennas more comfortable, they could also be constructed bent. The eight plaster layers and the associated glue make the substrate quite rigid, which results in the antenna being easily wrinkled. If the layers were attached to each other on a cylinder, the antenna would be easier to bend on the arm. Otherwise there would be no need to change the structure, except perhaps to move the inset feed point.

D. Humidity

Attaching plaster antennas to the body makes them subject to a humid environment. To simulate the effect of humidity, two sample antennas were tested in a climate chamber. The test was a 24-hour run in 37 °C, with a relative humidity of 90%. This corresponds to very heavy use, excluding

showering. After the treatment, the copper foil had changed colour, but the antenna did not seem moist.

The resonance frequency was seen to shift upwards by 10 to 20 MHz, and the 6-dB bandwidth to grow by 10 MHz, indicating increased losses. No significant change was observed in the resonant resistance or radiation parameters. Hence the antenna material seems very stable in the predicted use environment.

Tests with previous plaster antennas have shown that a sweating user does not affect the antenna parameters [1]. The main problem associated to sweating is that sweaty antennas easily come off the skin. Showering is certain to short-circuit the antenna, unless it is somehow protected—and such protection would make the antenna feeding clumsy.

IV. Specific Absorption Rate (SAR)

In this section, the SAR from the antenna will be considered when the antenna is bent around a cylinder. Only *yz* (H-plane) bending was considered. In this work Empire commercial FDTD software [5] has been used.

The SAR was calculated at 2.45 GHz. The phantoms were homogeneous with the following properties: relative permittivity, ε_r = 37.97, conductivity, σ = 1.88 S/m, mass density = 1000 kg/m³. All results in this section are normalized to 1 W input power. It was assumed that the smallest bend radius would have the largest effect, therefore, three geometries were considered: 1) the flat antenna on a 94 mm thick rectangular phantom, 2) the flat antenna on a cylindrical phantom (radius = 47 mm) and 3) the antenna bent around a 47 mm cylindrical phantom (see Figure 5). The results are shown in Table IV.

Table IV shows that the effect on SAR of bending the antenna around a cylinder is relatively small. Only 2% of the power is absorbed in the phantom, showing that the metallic ground plane is effective at shielding the body. In fact the maximum SAR occurs between the strips in the ground plane. With 1 W input power, the IEEE SAR limits are not breached. The 10 g SAR values are always smaller than the 1 g SAR values and will not break the ICNIRP limits in Europe [1]. The SAR from the antenna in this paper is lower than the previous design [1].

V. Conclusion

A patch antenna structure with a plaster substrate has been proposed. The antenna covers the band from 2.4 to 2.5 GHz in all the use cases. The measured on-body gain is 6 dBi, but the backwards radiation is shadowed by 15 dB. The simulated SAR has been considered when the antenna is bent around a cylinder. Bending changes the antenna properties, but the structure is usable on curved body parts if properly placed.

Compared to the previous plaster antennas [1], the proposed structure is much less sensitive to bending. The SAR values were also not substantially affected by bending the antenna. This antenna produces a lower SAR than in [1] and the ground plane means that relatively little energy will be absorbed in the body.

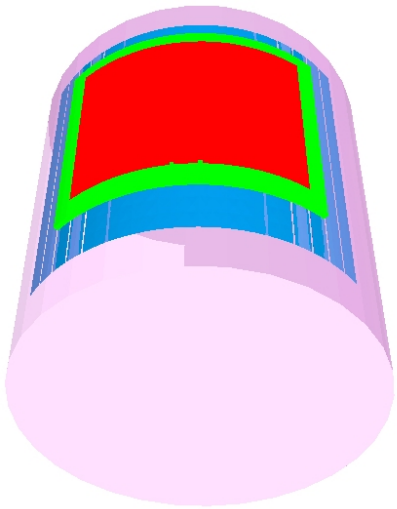

Fig. 5 The patch antenna bent around a cylindrical phantom with a 47 mm radius. This '*yz* bending' (H-plane bending) is the desired bending direction in use.

Table IV
Simulated SAR Normalised to 1 W.

Antenna	Phantom	1 g SAR (W/kg)	Power absorbed (W)
Flat	Flat	0.87	0.023
Flat	Cylinder: 47 mm radius	0.62	0.024
47 mm bend radius	Cylinder: 47 mm radius	0.87	0.019

The proposed plaster antenna is applicable for all kinds of patient monitoring systems, or it can be modified for RFID use.

Acknowledgment

Sincere thanks to Mr. Joel Salmi and B.Sc.(Econ.) Timo Kellomäki who lent their bodies for the measurements, and to M.Sc. Janne Kiilunen and M.Sc. Kirsi Saarinen who helped with the climate chamber measurements. Many thanks to Dr. Benoit Derat for his outstanding Empire support and his consi**derat**ion. Tiiti Kellomäki's work was funded by the Graduate School in Electronics, Telecommunication and Automation (GETA).

References

[1] T. Kellomäki, W. G. Whittow, J. Heikkinen, and L. Kettunen: "2.4 GHz plaster antennas for health monitoring," in *Proc. European conference on antennas and propagation, 2009,* p. 211–215.

[2] Mefix. [Online]. Available: http://www.molnlycke.com/item.asp?id=924

[3] T. Kellomäki: "Snap-on buttons in a coaxial-to-microstrip transition," in *Proc. LAPC 2009,* Loughborough, UK, 2009.

[4] SATIMO [Online]. Available: http://www.satimo.com/

[5] EMPIRE [Online]. Available: http://www.empire.de/

Publication [P7]

T. Kellomäki, J. Heikkinen, and M. Kivikoski.

Effects of bending GPS antennas.

In *Proc. Asia-Pacific Microwave Conference (APMC)*, pages 1597–1600, Yokohama, Japan, December 2006.

Proceedings of Asia-Pacific Microwave Conference 2006

Effects of Bending GPS Antennas

Tiiti Kellomäki, Jouko Heikkinen, and Markku Kivikoski

Institute of Electronics, Tampere University of Technology, 33101 Tampere, Finland

Tel: +358-3-3115 2931, Fax: +358-3-3115 3394, E-mail: Tiiti.Kellomaki@tut.fi

***Abstract* — The effect of antenna bending on return loss, impedance bandwidth, and radiation pattern is studied, taking four antennas as examples. These include a patch, slot, inverted-F, and dipole antenna. Some of them exhibit circular polarization and one is broadband. Impedance is seen to be fairly constant regardless of bending, though if circular polarization is excited by careful antenna shaping, the circular polarization and corresponding resonance are easily lost. The axial ratios of all examined antennas degrade quickly with decreasing bend radius. Linearly polarized antennas are more tolerant to bending effects, though their polarization may twist and main lobe direction change.**

***Index Terms* — Antenna radiation patterns, antennas, microstrip antennas, slot antennas, strain.**

I. Introduction

A new trend in antenna design is to make antennas wearable and thus integrable into clothing. For convenience, wearable antennas are made flexible by e.g. using a special-purpose PCB or fabric as the antenna substrate. However, little has been done to investigate the effect of antenna bending on bandwidth or radiation pattern.

In this study we examine four antennas. They include a microstrip-fed corner-truncated patch antenna, a coplanar-fed inverted-F antenna, a broadband coplanar-fed slot antenna, and a half-wave dipole for reference. The antennas represent a wide range of antenna types and are thus hoped to give information on which types suffer the least effects of bending.

II. Antennas under test

All the examined antennas except the patch antenna are etched on a flexible polyimide substrate. The complex-shaped antennas are depicted in Fig. 1.

The patch antenna is printed on Gore-Tex fabric thickened with Flexprint thermoweldable plastic. Silver-carbon mixture paste is used as the conducting material. The paste is sensitive to bending as it breaks easily, severing the electrical connection between antenna parts. It is crucial to ensure that the feed line is not broken when the antenna is bent.

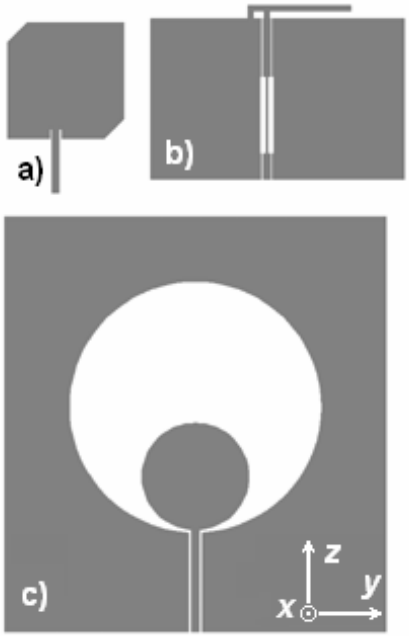

Fig. 1. The antennas under investigation: a) patch (ground plane not shown), b) planar inverted-F, and c) broadband slot antenna. The chosen coordinates apply to all antennas.

To excite circular polarization, two opposite corners of the square patch are cut off and the feed point is slightly displaced from the center. The antenna is fed by a microstrip line, to which an SMA connector is soldered. Two resonances are found at 1.62 and 1.69 GHz, corresponding to the two orthogonal polarization components.

One example of planar antennas is the inverted-F antenna. It consists of a radiating element that is short-circuited to a ground plane at one end. The coplanar feed structure includes an impedance transformer, and an SMA connector is soldered in the end. The antenna exhibits elliptical polarization near its resonance frequency.

Another planar antenna is a broadband circular slot antenna [1]. The fabricated antenna is scaled up

so that the diameter of the circular slot is 128 mm. The antenna shows similar return loss characteristics to the originally proposed antenna: the impedance bandwidth ranges from 860 MHz to 15 GHz.

A half-wave dipole is used for reference. One arm of the dipole is 44 mm long and 5.3 mm wide. There is a 0.5 mm gap between the arms. The dipole is fed by a coaxial line. No balun is used, because in this study we are primarily interested in changes due to bending rather than absolute values.

All the examined antennas are used near the GPS frequency range (around 1.6 GHz). The patch and inverted-F antennas exhibit circular or elliptical polarization whereas the others are linearly polarized.

III. Measurements

The impedance bandwidths were measured using a HP 8722D vector network analyzer, and the radiation patterns in an anechoic chamber equipped with a signal generator, a spectrum analyzer, and a transmitting horn antenna.

To ensure a constant bending radius, the antennas were bent about circular cylinders of EPS (styrofoam) with a dielectric constant close to that of air. The bending radii were 47 mm, 52 mm, 68 mm, and 115 mm, thus ranging from 0.25λ to 0.6λ at the GPS center frequency. For the radiation pattern measurements, only one radius was used: for the slot and inverted-F antennas 47 mm to examine the worst case, and for the microstrip antenna 68 mm to avoid breaking. The radiation pattern of the dipole was measured at all bending radii. The antennas were bent in two principal planes. Thus the feed line was always either parallel or perpendicular to the cylinder axis. The dipole, being nearly one-dimensional, was bent only in the *xy* plane, with its feed line parallel to the cylinder axis.

The radiation patterns of the inverted-F and dipole antenna were measured at their resonance frequencies. The patch antenna was measured at the frequency of the optimal axial ratio, which happened to be at the upper resonance. All these frequencies are close to the GPS center frequency, 1575 MHz. The radiation pattern of the broadband slot antenna was measured at 1.5, 2.5, and 5 GHz.

IV. Results

A. Bandwidth and resonance

The coplanar-fed antennas, i.e. the inverted-F and slot antennas, suffer the least effects of bending.

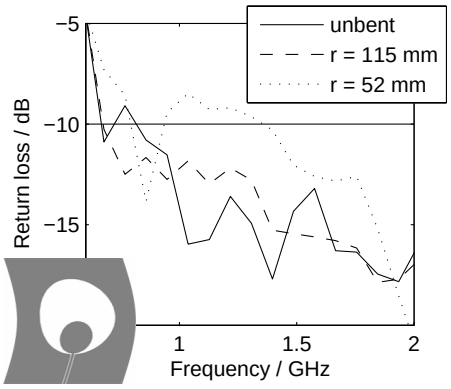

Fig. 2. Return loss of the slot antenna at low frequencies. The antenna is bent in the *xz* plane, and return loss is worsened.

This is due to their planar nature. Bending the inverted-F antenna in either of the planes does not change the resonance frequency at all. The return loss at the resonance frequency changes less than 4 dB, and the effect on bandwidth is negligible. In all, the inverted-F antenna is seen to be immune to the effects of bending.

The properties of the broadband slot antenna do not change almost at all when bending it in the *xy* plane. Bending in the other plane causes the return loss at low frequencies to rise, thus moving the start frequency of the impedance bandwidth from 860 MHz to 1400 MHz, as seen in Fig. 2. This happens because bending the antenna widens the small gap in the feed point, between the two circles. Capacitive loading is reduced, and the impedance band breaks in two. The same effect has been observed in [1], when the gap width has been altered in a simulation model. Otherwise, changes introduced by bending in the *xz* plane are insignificant.

The circularly polarized patch antenna exhibits two resonances in its impedance bandwidth, corresponding to two orthogonal polarization components. Bending the antenna in the *xy* plane causes the lower resonance to disappear, indicating a change from circular to linear polarization. The resonance vanishes even at the largest bending radius. At the same time, the upper resonance frequency is lowered slightly (from 1.69 to 1.6 GHz). Similarly, the upper resonance vanishes when the antenna is bent in the *xz* plane, and this also causes the lower resonance frequency to move downward from 1.62 GHz to 1.59 GHz. The two resonances and the vanishing effect are seen in Fig. 3. The loss of one resonance obviously lowers

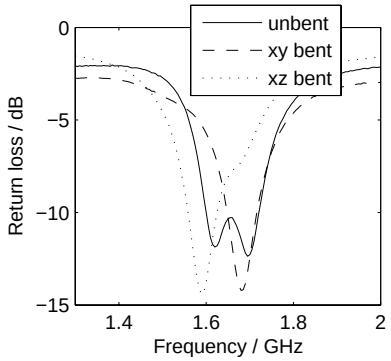

Fig. 3. Return loss of the patch antenna. When the patch is bent in the *xy* plane, the lower resonance is lost, and vice versa.

the bandwidth, here from 9 % to 5 % when stepping from straight to the largest bending radius.

The change from circular to linear polarization and the loss of one resonance are reported also in [2], where the conducting element was made of a flexible non-breaking material. Thus the phenomenon is caused by the deformation of the antenna shape, rather than the breaking of the conducting paste.

Surprisingly, the properties of the simplest examined antenna, the half-wave dipole, change significantly when the antenna is bent. The resonance frequency moves up and down in the range of 1.49 to 1.54 GHz. A more notable effect is that the return loss at the resonance frequency increases from 17 dB to 31 dB and bandwidth decreases from 20 % to 18 % as the bending radius is reduced. This indicates an increase in the antenna *Q* value, which agrees with the theory stating that *Q* value increases when the volume of the sphere surrounding the antenna is reduced [3].

B. Radiation pattern

The major axis of the polarization ellipse of the inverted-F antenna lies ten degrees counterclockwise from the long F arm. The antenna is elliptically polarized, with an axial ratio of 6 dB. When the antenna is bent in the *xy* plane, the radiation characteristics in the convex direction remain nearly unchanged. Bending in the *xz* plane causes the lobe in the convex direction to widen slightly, and the gain to grow 2 dB. All the minima and maxima can be found in the pattern, and therefore it can be said that the pattern is not heavily distorted.

The concave direction pattern is more affected by the bending than the convex one. When the inverted-F antenna is bent in the *xy* plane, the gain in the concave direction increases in both vertical and horizontal polarizations, and thus the radiated power seems to be concentrated in the concave direction. Bent in the *xz* plane, the antenna radiation increases in the vertical and decreases in the horizontal polarization, compared to the unbent antenna.

The axial ratio of the inverted-F antenna degrades from 6 dB to over 10 dB when bending the antenna in either plane.

The slot antenna is linearly polarized with a high cross-polarization level. We take the H-plane to be the one where the antenna is rotated about its feed line. The radiation pattern was measured in both principal planes, and bent in both *xy* and *xz* planes. The H-plane radiation pattern shows bidirectional characteristics in co-polarization, and the cross-polarization pattern resembles a four-leaf clover.

At 1.5 GHz, the polarization of the slot antenna turns towards the vertical direction when the antenna is bent in the *xy* plane, and towards the horizontal when bending in the *xz* plane. This corresponds to a decrease in radiation in the direction of the bending. For example, when the antenna is bent in the *xy* plane, the vertical (*z*) shape of the antenna is unchanged, and thus the vertical behavior remains as it was. In this bending direction, the antenna is deformed horizontally, and thus the horizontally radiated power decreases. The antenna radiates more in the convex direction than the concave, the difference being 5 to 10 dB.

At 2.5 GHz, bending the slot antenna in the *xy* plane makes it radiate vertical polarization almost omnidirectionally in the H-plane. The other bending direction again promotes the horizontal polarization, though the effect is not as distinct as at 1.5 GHz.

Bending in either of the planes degrades radiation in nearly every direction at 5 GHz. At peak gains, the straight antenna dominates the bent ones by 5 dB. Therefore it can be concluded that the slot antenna is most sensitive to deformation at high frequencies, where a slight change in the shape is large with respect to wavelength.

As expected, the polarization of the patch antenna changes from circular to linear (or highly elliptical, with an axial ratio of 8 dB), when the antenna is bent in the *xy* plane. This is illustrated in Fig. 4. For the straight antenna, the major axis of the nearly-circular polarization ellipse is tilted by approximately 45 degrees. However, the bent antenna exhibits completely vertical polarization. The bent patch behaves like a regular half-wave patch antenna with the electric field parallel to the feed line.

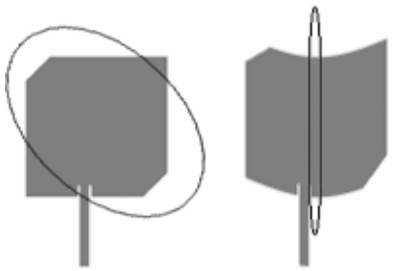

Fig. 4. Polarization ellipses of the patch antenna: the unbent antenna exhibits circular polarization whereas the *xy* bent antenna is vertically polarized.

After investigating the two circularly polarized antennas, we can draw the conclusion that the polarization of circularly polarized antennas quickly degrades into elliptical or linear when the antenna is bent.

Having responded significantly to bending in terms of return loss, the dipole is seen to be quite immune to bending effects in the sense of radiation pattern. The measurements show that only one minimum is filled and shifted slightly off its original location, whereas the other remains unchanged. The coaxial center conductor fed arm points to the filled minimum. In the E-plane pattern, neither lobe becomes larger than the other. This can be surprising, as one might hypothesize both the nulls to fill and the lobe on the concave side to grow. Filling of nulls is reported in [4], where a folded dipole antenna is bent at one point only. However, it occurred only at large bending angles.

The cross-polarization levels of the dipole antenna grow slightly, at most 3 dB. This is due to an increase in radiation by the coaxial feed line. However, the change is insignificant.

V. Conclusion

In terms of return loss, planar antennas are quite immune to bending effects. The resonance frequency of the resonant inverted-F antenna remained constant in bending, as did the impedance bandwidth of the broadband slot antenna. The patch antenna exhibited two resonances, one of which vanished when bending the antenna in either plane. This indicates loss of circular polarization. Additionally, bending shifted the remaining resonance frequency a little lower. This has been reported for other patch antennas as well.

Circular polarization requires the antenna to be of a certain shape, and deformation results in a loss of one polarization component. This is seen clearly in the case of the patch antenna: originally less than 3 dB, the axial ratio degraded to 8 dB when the antenna was bent about a cylinder with a 68 mm radius. Also the elliptical polarization of the inverted-F antenna turned towards linear, from AR 6 dB to over 10 dB.

One interesting effect of bending was that the radiation of the slot antenna was enhanced in the direction which was unbent, i.e. when bending in the *xy* direction, the *z*-polarized component aka the vertical polarization increased.

We conclude that most planar antennas are fairly insensitive to bending effects. The effect on resonance frequency can be approximated as negligible, or in the case of patch antennas, a slight lowering can be predicted. The effect on bandwidth is also insignificant, provided that no resonances are lost. Specifically designed dual-resonances producing circular polarization may vanish at the slightest bending. Thus circularly polarized antennas are most likely to suffer from bending.

For wearable antennas, linearly polarized antennas ought to be favored over circular, as their characteristics are more predictable. If circularly polarized antennas are needed, for example in a GPS receiver, the antenna substrate has to be hardened so that the antenna is not deformed in use.

Acknowledgement

The authors wish to thank Ms. Teija Laine-Ma for fabricating all the measured antennas, and Mr. Juha Lilja for helping measure the radiation patterns.

This work was funded by the Finnish Funding Agency for Technology and Innovation under contract no. 40014/06.

References

[1] M. A. Habib, T. A. Denidni, and G. Y. Delisle, "Design of a new wide-band CPW-fed circular slot antenna," *2005 IEEE Antennas and Propagation Society International Symposium*, vol. 1B, pp. 565-568, July 2005.

[2] A. Tronquo, H. Rogier, C. Hertleer, and L. Van Langenhove, "Robust planar textile antenna for wireless body LANs operating in 2.45 GHz ISM band," *Electron. Lett.*, vol. 42, no. 3, pp. 142-143, February 2006.

[3] R. C. Hansen, "Fundamental limitations in antennas," *Proc. of the IEEE*, vol. 69, no. 2, pp. 170-182, February 1981.

[4] J. Siden, P. Jonsson, T. Olsson, and G. Wang, "Performance degradation of RFID system due to the distortion in RFID tag antenna," *International Conference on Microwave and Telecommunication Technology, 2001*, pp. 371-373.

Publication [P8]

T. Kellomäki.

Snap-on buttons in a coaxial-to-microstrip transition.

In *Proc. Loughborough antennas and propagation conference (LAPC)*, Loughborough, UK, November 2009.

Snap-On Buttons in a Coaxial-to-Microstrip Transition

Tiiti Kellomäki

Tampere University of Technology, Department of Electronics, P.O.Box 692, FI-33101 Tampere, Finland

tiiti.kellomaki@tut.fi

***Abstract*— Commercial snap-on buttons are used in a coaxial-to-microstrip transition. The reflection properties of the transition are examined in time and frequency domains. Snap-on buttons are usable in wearable antenna connections in a frequency range up to three gigahertz.**

I. Introduction

Wearable antennas, and, most of all, disposable, single-use antennas, cannot employ expensive connectors like the SMA. One possible solution is to use snap-on buttons to connect the antenna to a coaxial cable. The expensive cable can be used multiple times, although the antenna is changed daily. Snap-on buttons are an easy solution for end-user applications. The concept of snap-on buttons was first proposed in [1], and antennas fed using snap-on buttons have been examined also in [2].

In this paper we examine the usability of commercial snap-on buttons as RF connectors. The transition from a coaxial to a microstrip line via buttons is measured and simulated, and the results are analysed in both the frequency and time domains. It will be shown that the snap-on button arrangement can be used up to 3 GHz.

The coaxial-to-microstrip transition structure is described in Section II. Measurement and simulation results are given in Sections III and IV. Some problems arising from the use of buttons are discussed in Section V, and Section VI concludes the work.

II. Transition Structure

Two pairs of commercial snap-on buttons are needed for a coaxial-to-microstrip transition: one pair for the signal line and another one for the ground. The male buttons are thinner than the female, and therefore a natural choice is to embed the male buttons into the microstrip line.

Male snap-on buttons are punched through the microstrip line and the ground plane, as shown in Fig. 1. No soldering is required. Punching through the metal works especially well with structures made of copper foil tape. If the metallic parts were e.g. screen or inkjet printed, conducting glue would be required to secure the connection. The buttons can also be sewn onto the substrate.

The coaxial counterpart to the male buttons is shown in Figs. 1 and 2. Two female snap-on buttons are connected to the inner and the outer conductors by twisting the metallic threads around the holes of the button. To avoid short-circuiting, the dielectric insulator of the coaxial cable is left to protect the inner conductor. Again, the connection may be secured by sewing, soldering, or gluing.

Fig. 1 Male buttons are punched through the copper foil tape, and female buttons connected by twisting the metal threads of the coaxial cable through the holes in the buttons. Loose male and female buttons are shown at the bottom.

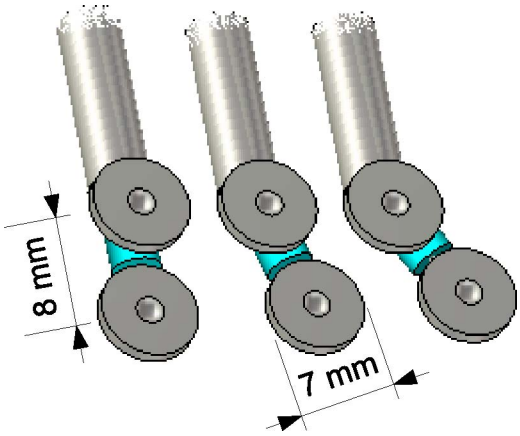

Fig. 2 Female snap-on buttons connected to the coaxial cable. The inner conductor and the associated button may twist in use, as illustrated.

The protruding inner coaxial conductor adds a series inductance to the transition. Similarly to traditional transitions between lines, this structure may be modelled as a low-pass filter.

III. Measured results

The transition structrure was measured in the time domain, which makes it possible to separate reflections from multiple sources. Here the possible reflections include the RF connectors and the termination of the microstrip line, in addition to the button transition itself. A wide frequency range gives a detailed response and makes it easier to distinguish discontinuities, but the transition is also more reflective at higher frequencies.

To examine the response of the transition, five coaxial cables with female buttons and three microstrip lines with male buttons were constructed. The measurement was conducted in the time domain using a vector network analyser with the FFT option.

The measurement set-up was as follows (also see Fig. 3): The reflection measurement was calibrated at the end of the VNA cable. To feed the button transition, a thin PTFE (Teflon) coaxial cable was used. The cable had an SMA connector at one end and buttons at the other end. The buttons connected the coaxial cable to a microstrip line, which was either terminated with 50 ohms or left open.

The network analyser was calibrated for a reflection measurement in the frequency ranges from 50 MHz to 3 GHz, and from 50 MHz to 6 GHz. The time domain response was calculated from the frequency-domain measurement using FFT. Hence the results show the response of the buttons to a bandlimited pulse.

In the time domain result presented in Fig. 4, all the expected discontinuities are visible. Near 0 ns, there is a small reflection at the SMA connector. The reflection magnitude from the buttons, at 1.4 ns, is less than –10 dB within the frequency range up to 3 GHz. If the microstip line is unterminated, a large reflection is seen, but the 50-ohm termination is invisible in the time domain. In the frequency range up to 6 GHz, the button connection shows a reflection magnitude of –7 dB.

Compared to a soldered transition, the reflection from the buttons is about 2 dB larger for the 3-GHz pulse, and 8 dB larger for the 6-GHz one. Figure 5 illustrates the comparison between the buttons and a soldered transition with a 1-mm protrusion of the inner conductor.

Traditionally, a –10 dB reflection magnitude is the upper limit for an 'acceptable' connection. The snap-on buttons thus provide a usable connection up to three gigahertz.

The connection via buttons is not as repeatable as provided by traditional RF connectors. The main reason for this is the series inductance caused by the inner coaxial conductor. The inner conductor easily bends during connection, as shown in Fig. 2, causing the inductance to change. Repeatability was studied by connecting and disconnecting the transition while monitoring the time domain response. The reflection magnitude was seen to differ by less than one decibel between the 10 measurements.

To test the transition in a real application, the input impedances of some 50-ohm antennas were measured using the snap-on buttons at 2.5 GHz. Using one cable and repeating the connection ten times, the input resonant resistance

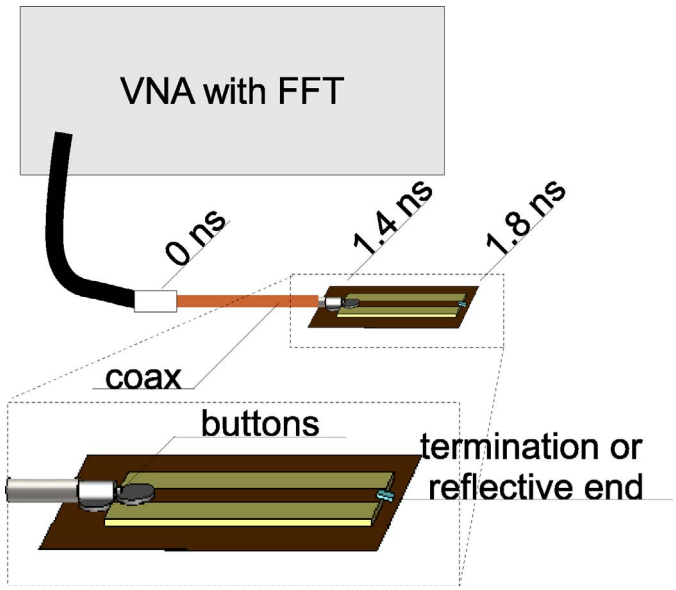

Fig. 3 Set-up for the reflection measurements. The calibration plane is at an SMA connector (or an SMA-SMB adapter) at 0 ns.

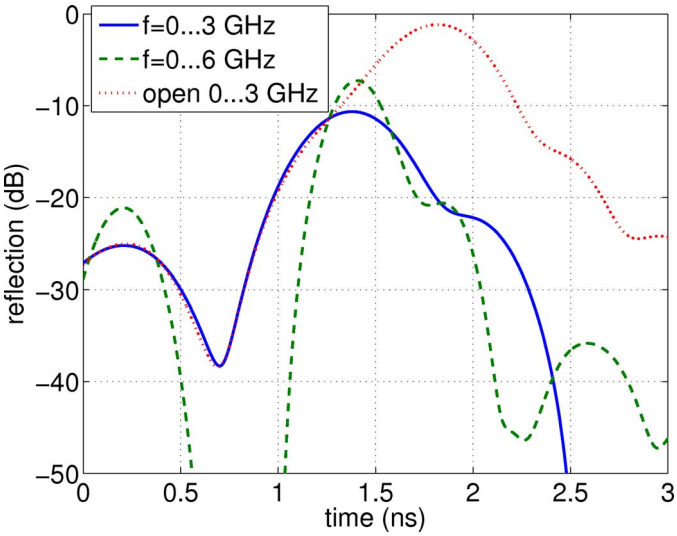

Fig. 4 Measured time domain results for two pulses (solid and dashed curves). Near 0 ns: an SMA-SMB adapter; at 1.4 ns: the button transition; at 1.8 ns: microstrip termination by a resistor. For comparison: open-ended microstrip line measured at the lower frequency range (dotted curve).

TABLE I
Measured and Simulated Results

	0 to 3 GHz	0 to 6 GHz
measured reflection	–10 dB	–7 dB
simulated reflection	–10 dB	–8 dB
repeatability of antenna impedance	±4 ohms	
repeatability of resonance frequency	±10 MHz	
difference betw. cables (measured antenna resonant resistance ~50 Ω)	5…10 ohms	
difference betw. cables (measured antenna resonance ~2.5 GHz)	15 MHz	

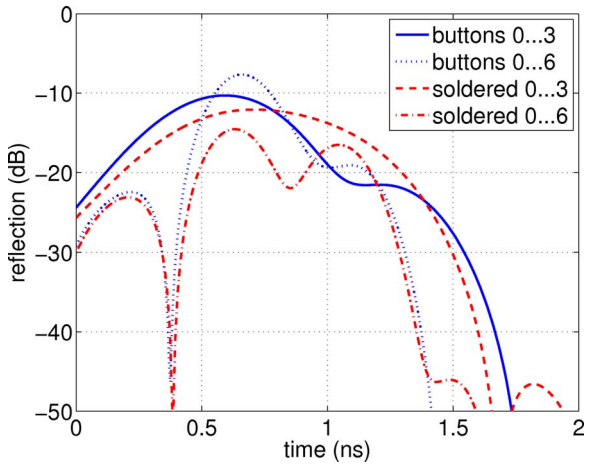

Fig. 5 Measured time domain results for two transitions: snap-on buttons and a coaxial cable soldered to place. Measurement frequency range is from 50 MHz to either 3 or 6 GHz. Button transition is seen at 0.7 ns.

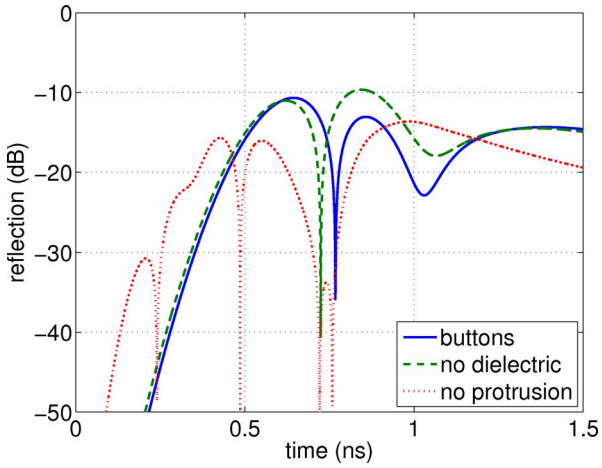

Fig. 6 Simulated time domain responses: the proposed button transition (—), a button transition with no insulator around the protruding inner conductor (--), and a good transition with no protrusion and no buttons (···). The simulated frequency range is from 0 to 3 GHz. The coaxial was shorter in the simulation than in the measurements, hence the time scale is shifted.

measurement could be repeated at a ±4 ohms accuracy. The measured resonance frequency was within 10 MHz in all the iterations.

In the antenna measurements it was also seen that the measured input impedance could change by 5…10 ohms if the coaxial cable was changed. The resonance frequency fluctuation between cables was 15 MHz. This is again caused by the inductance of the protruding inner conductor, the length of which varies between coaxial cables. Machine assembling the buttoned cables is expected to alleviate the problem.

The measured and simulated values are listed in Table I.

IV. Simulated Results

The transition from a coaxial cable to a microstrip line via buttons was simulated using CST Microwave Studio [3]. The transient solver produces a time domain response to a pulse consisting of the desired frequencies. The frequency-domain response (S_{11}) can be acquired using FFT.

In the simulation, the buttons were assumed perfect conductors, and also the connection between the male and the female buttons was assumed perfect. Thus only the structural discontinuity and the series inductance were modelled. However, the simulations agree with the measurement results, leading to the conclusion that the electrical connection causes no problem in the button transition.

The time domain response of the proposed coaxial-to-microstrip transition is shown in Fig. 6 along with two other transition structures. The buttons are seen to produce a reflection of magnitude –10 dB to a pulse limited to 3 GHz. This is in accordance with the measured results. For a frequency range from 0 to 6 GHz, the reflection magnitude is –8 dB.

The simulated electric field amplitude in various planes along the conductor is illustrated in Fig. 7. At the transition region, with the inner conductor covered only by the dielectric, we see a smooth change from a coaxial to a microstrip mode. At the second button, the mode is already a microstrip mode.

V. Problems Associated with Buttons

Repeatability of the connection is a major problem associated to the snap-on button transition. The buttons may twist in use, adding a random series inductance to the feed. This causes the measured input impedance and antenna resonance frequency to differ from the real value. However, the changes in the measured impedance are small, and the button transition has practical value in end-user applications.

When the coaxial cable bends in use, the torsion affects mainly the button transition point. It was seen that bending easily rips the copper foil tape off the substrate, dramatically changing the transition impedance. Another pair of snap-on buttons is needed to keep the cable stable during use. The buttons may also be sewn firmly onto the substrate fabric.

Dirt and wear limit the lifetime of a snap-on button connection. The buttons may break in use after a number of connections—although they are designed for much heavier use than regular RF connectors. The electrical connection between the buttons deteriorates with accumulating dust, grease, or rust, resulting in a larger reflection coefficient. Short-circuiting is expected if water enters the transition. However, if the snap-on buttons are used in a clothing antenna, they can be washed and dried with the garment.

The snap-on buttons cannot be placed directly at the antenna feed point. In order to achieve the desired impedance, manufacturing tolerances of the order of 0.2 mm are required for the feed point. Compared to a typical probe-feed at one point, the snap-on button is large, and thus the actual connection point between the antenna and the cable is uncertain [1]. To overcome this, the snap-on buttons can be connected to a regular transmission line, such as a microstrip or a coplanar line, which in turn feeds the antenna at the desired point.

VI. Conclusion

Snap-on buttons have been used in a coaxial-to-microstrip line transition. This type of a transition is applicable for wearable and disposable antennas. The reflection magnitude from the transition is better than –10 dB for a frequency range up to 3 GHz, and –7 dB up to 6 GHz. The usable frequency range of the transition thus extends to 3 GHz, covering the important 2.45 GHz ISM band.

The repeatability of a snap-on button connection is good enough for wearable antenna applications. The input impedance of an antenna, measured through a button connection, varies by less than 10 ohms between different cables. If manufacturing tolerances are reduced, the repeatability is expected to improve.

A connection relying only on snap-on buttons is not mechanically stable. Additional reinforcing, e.g. extra buttons, must be used to secure the connection. The connection must be protected from water.

The snap-on button connection is especially suitable for telemedicine applications and feeding single-use antennas. If the connection is used in military or search-and-rescue applications, additional care must be taken to protect the connection from rain. For rugged use, robust buttons can be used.

Snap-on buttons provide a cheap, easy, and reasonably reliable connection for wearable antennas, especially for end-user applications.

Acknowledgment

This work was funded by the Graduate School in Electronics, Telecommunication and Automation (GETA).

References

[1] I. Belov, M. Chedid, and P. Leisner, “Investigation of snap-on feeding arrangements for a wearable UHF textile patch antenna,” in *Proceedings of the Ambience 08 Smart Textiles—Technology and Design*. Borås, Sweden, June 2—3, 2008.

[2] T. Kellomäki, W. G. Whittow, J. Heikkinen, and L. Kettunen: ”2.4 GHz plaster antennas for health monitoring,” in *Proc. European conference on antennas and propagation, 2009,* p. 211–215.

[3] CST [Online.] Available: http://www.cst.com/

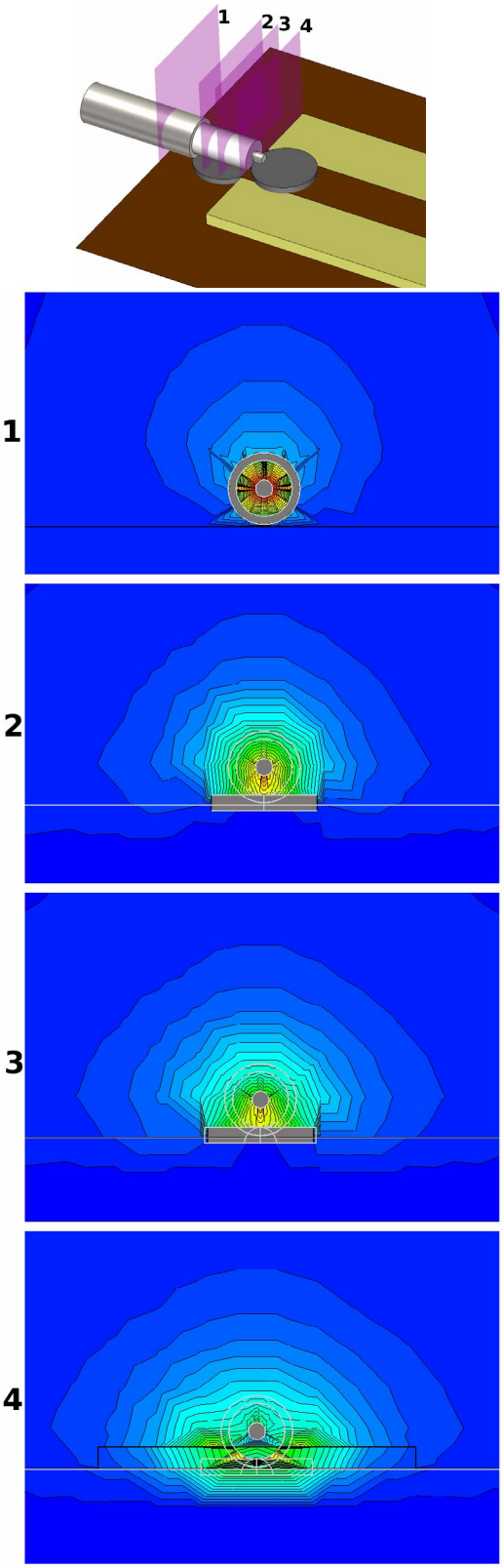

Fig. 7 Electric fields in the button transition, in planes perpendicular to the transmission line, at 3 GHz. The same scale is used in all the figures. From above: 1. Coaxial mode with the outer conductor present. 2. In dielectric only, just after the end of the outer conductor. 3. As previous, but further towards the microstrip. 4. At the beginning of the microstrip line.

Publication [P9]

T. Kellomäki and L. Ukkonen.
Design approaches for bodyworn RFID tags.
In *Proc. International Symposium on Applied Sciences in Biomedical and Communication Technologies (ISABEL)*,
Rome, Italy, November 2010.

Design Approaches for Bodyworn RFID Tags

(Invited Paper)

Tiiti Kellomäki
Tampere University of Technology,
Department of Electronics,
P.O.Box 692, 33101 Tampere, Finland
Email: tiiti.kellomaki@tut.fi

Leena Ukkonen
Tampere University of Technology,
Rauma Research Unit,
Kalliokatu 2, 26100 Rauma, Finland

***Abstract*—Bodyworn tags are a challenging application for radio frequency identification (RFID) systems. The importance of this application will increase in the future due to emerging novel wireless identification and sensor systems. In this paper, a literature survey of wearable RFID tag antennas is presented. One-layer and multilayer tags are compared. The body effect on antenna parameters is analysed. Based on the findings, guidelines for wearable tag antenna design are given. As an example of a bodyworn tag, a meandered dipole is presented.**

I. Introduction

RFID (radio frequency identification) tags integrated into clothing make it possible to monitor people without their conscious effort. Access control using wearable tags is especially useful for example in dementia care. Also, a person's activity can be monitored using a bodyworn RFID tag. Wearable sensors are an emerging technology that can also be combined with RFID tags.

Patients are very commonly identified by a barcode wristband at bedside before giving away drugs. RFID tags require no line-of-sight, and can be read for example through bed sheets. Thus sleeping or unconscious patients can be easily identified without having to disturb them.

This paper begins with a survey of published wearable tags, their applications, and wearable antennas in general. Building on the literature review and experience-based designer intuition, guidelines for wearable tag and antenna design are given in Sec. III. As an example of bodyworn tags with no ground plane, Sec. IV presents a wearable dipole tag. Sec. V concludes the work.

II. Literature Review

A. Applications of Bodyworn Tags

Most person-monitoring UHF RFID tags are integrated into wristbands or name badges. Several case studies of patient or personnel location applications have been reported. Lahtela [1] provides a comprehensive literature review of RFID technology in healthcare. While many applications use 125/135 kHz or 13.56 MHz, some UHF tags have also been tested in real life situations. Unfortunately, many application descriptions fail to state the frequency band or technology used.

Active UHF wristband tags have been used in a Taiwanese hospital to track the position of SARS infected patients [2]. The tags were to be equipped with thermometres, but in the end the system had to be reduced to tracking only. In addition, an extensive reader infrastructure was built. Positive results gave rise to new plans of extending the system to precious equipment tracking and newborn baby identification.

In another study in Taiwan, patients have been identified with the help of UHF wristband tags [3]. The aim of the project was to improve drug safety. Medication was pre-packed in doses, marked with barcodes. The nurses would scan both the patient and the dose before giving away the drug.

B. Bodyworn Tags

Many name badge tags, wristband tags, and wearable textile tags have been published in the recent years. All of these are used in a tricky environment, with the presence of a highly lossy dielectric—the human body. Table I summarises the published results of bodyworn tags, listing the antenna size, total height from the skin, and realised gain. The measurements have been made against the complex IC impedance, and the listed gains are thus realised gains, including the mismatch loss. In the following, all the antennas operate in the 865 MHz or 920 MHz UHF band, unless otherwise stated.

Marrocco [4] conducted an extensive parametric study of a one-layer square antenna with a nested slot. By varying the structure parameters of this antenna, a range of antennas from a dipole to a loop are obtainable. Impedance matching charts and gains are presented. To prevent the antenna from being short-circuited by the body, Marrocco uses a 4 mm thick silicone slab with an ε_r (dielectric constant) of 11.9. When worn on the body, the antennas provide a gain of –8.5…–7 dBi. Examined antenna dimensions range from 30 mm × 30 mm to 50 mm × 50 mm, the smallest of which are easily fitted on a wristband.

A tag antenna for detecting human body movements was presented by Occhiuzzi and Marrocco [5], [6]. The antenna design is a series-fed L-patch that can also be seen as a short-circuited patch antenna. Because the ground plane is almost equal to the patch element, the antenna may also be seen as a shorted parallel-plate antenna. Measuring 49 mm × 60 mm × 4 mm, the antenna gives a gain of –4…–1 dBi on the body. PTFE is used as the substrate material as well as an insulator between the antenna and the body.

In [7], Švanda and Polívka present a patch antenna (165 mm × 74 mm × 4.8 mm) and a dualband patch (155 mm × 74 mm

× 4.8 mm), both weighing about 20 g. Dielectric foam with ε_r = 1.29 is used as the substrate. The ground plane is only about twice the area of the patch, and the structure can again be seen as a parallel plate antenna. The human body lowers the gain by about 1 dB, even if it is touching the antenna.

Another design by Švanda and Polívka [8] is a three-layer structure with dipoles over patches over a ground plane. The dimensions are 95 mm × 65 mm × 1 mm, with the patches virtually the same size as the ground plane. The substrate ε_r is 3.2. As measured, the radiation efficiency increases from 61% to 82% when the antenna is brought from free space to touching an agar phantom, and realised gain increases from 1.3 to 1.7 dBi [9]. This phenomenon is not further explained. Detuning is also observed: the resonant frequency moves upwards by about 5 MHz. Both the real and the imaginary parts of input impedance decrease by about one-half.

In the same paper [8], Švanda and Polívka report a two-layer patch or parallel-plate design with dimensions 100 mm × 60 mm × 0.76 mm on the same ε_r = 3.2 substrate. Introduction of the agar phantom increases the radiation efficiency from 55% to 80% and realised gain from 1.0 to 1.6 dBi [9]. Less resonant frequency detuning is observed than for the previous antenna. The real and imaginary parts of the input impedance on phantom are about 0.6 times the free-space values.

Švanda and Polívka [10] present another three-layer structure with a loop over patches over a ground plane. The dimensions are 105 mm × 70 mm × 1.8 mm, with ε_r of 10, and again the four patches cover the whole ground plane. The structure can also be seen as a parallel-plate antenna or even a slot antenna excited with the loop. The antenna has been measured next to an agar phantom, and no detuning has been observed. The antenna efficiency falls from 38% in free space to 33% on phantom, and gain from 0.8 dBi to 0.6 dBi. Next to the phantom, the real and imaginary parts of the input impedance are 0.7 times the free-space values [9].

Rajagopalan and Rahmat-Samii show a dual-patch, or a slot antenna with a ground plane [11]. The structure is a metal strip wrapped around a piece of FR4 measuring 116 mm × 40 mm × 0.4 mm. When a 1.4 mm thick foam was placed between the tag and the user, the read range was measured 3.5 m, corresponding to a realised gain of –6 dBi. The tag also works when bent. An interesting comparison between identification of metal and human is presented: although the input resistance of the tag is lower on metal than on body, the read ranges for metallic objects are about 20% larger. This means that the effect of absorption by the body is greater than the additional mismatch loss introduced by the metal.

A 2.45 GHz folded dipole with a reflector, embedded into a wristband, was suggested by Takahashi *et al.* [12]. The antenna, measuring 40 mm × 2 mm × 2 mm, is inherently designed to be used bent around a cylinder. The reflector is stated to improve gain by 5 dB, and a realised gain of –6.7 dBi is thus achieved. Detuning is reported when the antenna is moved away from the wrist, but the operating frequency is stable when the antenna-body spacing is more than 1 mm. Naturally, spacing also increases gain.

TABLE I
WEARABLE TAGS ON HUMAN BODY. ANTENNA SIZE IS GIVEN IN WAVELENGTHS. S DENOTES ANTENNA–BODY SPACING AND H ANTENNA THICKNESS, GIVING TOTAL HEIGHT S+H.

Size (λ)	Real. gain (dBi)	S (mm)	S+H (mm)	Description
0.12…0.2	–8.5…–7	4	4	1-layer: dipole/loop [4]
0.21	–11 –6	4 10	4 10	1-layer: dipole [13]
0.22	–4…–1	2	6	2-layer: patchlike [5] [6]
0.33	–7	0	2	2-layer: dipole + reflector (2.45 GHz) [12]
0.34	+1.6	0	0.76	2-layer: patch [8] [9]
0.35	–6	1.4	1.8	2-layer: patches or slot [11]
0.36	+0.6	0	1.8	3-layer: patch + loop [10]
0.36	+1.7	0	1	3-layer: patch + dipole [8] [9]
0.50	+3…+5	0	4.8	2-layer: patch, dualband [7]
0.52	+5	0	4.8	2-layer: patch, single-band [7]

The usage of a one-layer dipole structure as a bodyworn RFID tag antenna was examined by Kellomäki *et al.* [13]. The meandered dipole structure of 68 mm × 22 mm was designed on a normal textile substrate with the ε_r between 1 and 1.5. Detuning as well as realised gain were measured with a range of antenna–body spacings. A reasonable spacing of 10 mm would give a –6 dBi realised gain. The tag is further described in Sec. IV.

Švanda and Polívka briefly addressed meandered dipole antennas in [7], and concluded that the detuning effect of the human body was too large for the tag to be practical. A 10-mm spacing resulted in about 70 MHz of detuning, and 20 mm in 30 MHz. The measurement was made in a 50-ohm system.

Several commercial tags have been reported to operate on the human body or a metallic object [14, Table III]. The sizes range from 200 mm × 160 mm × 17 mm to 50 mm × 40 mm × 3 mm. Most of the listed antennas are thicker than 4 mm, and some even exceed 10 mm, indicating the use of a ground plane. Even commercial UHF RFID wristbands with a 1.9-m average read range are available [15].

C. Wearable Antennas

Wearable antenna research has been more or less concentrated on patch-like antennas with a ground plane between the antenna element and the user. Also electromagnetic band-gap (EBG) structures have been utilised in preventing the body from affecting the antenna, but it is worth noting that most of the EBG structures include a ground plane. The following gives examples of one-layer wearable antennas.

Matthews *et al.* constructed a spiral antenna for the frequency band from 200 MHz to 500 MHz [16]. Although operated a few centimetres from the body, the antenna exhibited a gain of 0 to +5 dBi. The structure is very large, covering the whole backside of a shirt.

Narrowband bodyworn dipoles at 100 MHz have been measured [16], [17] and modelled [18]. At that frequency, the

length of the human body is comparable to a wavelength, and a very simple phantom can be used to model the body effect. Severe detuning is observed, and moreover, the body posture affects the resonant frequency.

Various one-layer GPS antennas (1.5 GHz) near the body were studied in [19]. The structures included an inverted-F, a dipole, and slot antennas. The dipole was the most sensitive of the studied antennas and instead, it is advisable to use structures with a gap: In dipoles, the reactive near-field spreads in a large volume. For example in the inverted-F antenna the near-field is concentrated between the F and the ground plane, both in the same layer. It was concluded that a spacing of 60 mm ($\lambda/2\pi$) resulted in 75% bodyworn efficiency and no detuning for any of the antennas. In some cases there was no detuning unless the user was touching the antenna.

Attempts to use the human body as a ground plane for the antenna have been made by Fukasawa *et al.* [20]. The antenna was mounted on a handheld device, where a naked metal part would touch the user's hand and thus allow for RF currents to flow in the hand. The test frequencies ranged from 300 MHz to 2 GHz. A similar structure may prove useful in wristband antennas. In textile antennas, however, a stable contact point between the antenna and the body would be too cumbersome.

III. Guidelines for Wearable Tag Design

Designing a wearable tag antenna begins with three choices: Will a ground plane be used or does the tag use the body as a reflector? Will the antenna be integrated into clothing or worn separately, like a nameplate? Which materials are allowed?

Compared to single-layer antennas such as dipoles or loops, two-layer antennas provide one important advantage: the ground plane can effectively prevent the user from affecting input impedance and absorbing power. Patches work even when touching the body. On the other hand, multilayer antennas are sensitive to thickness change, and for example fleece fabric squeezes very easily. Thus the antenna must be somewhat rigid.

One-layer antennas can use the body as a reflector, but a certain spacing between the antenna and the body is always required. Consequently, even if the antenna itself is very thin, the spacing will be about the same as the total thickness of a two-layer antenna. One-layer antennas are in general easier to fabricate than multilayer antennas, and may be less sensitive to deformation.

Wristband antennas are presently cheaper than clothing-integrated antennas. They can also be replaced more easily. However, they can be irritating both physically and mentally. From the point of view of an antenna designer, the wrist provides a relatively low-loss location, and if the wristband is fixed on the arm, the impedance will also be quite stable.

Clothing antennas, on the other hand, can be less obtrusive and more easily hidden. There is also much more space for the antenna in the garments than on a wristband. Antenna–body spacing is unpredictable. There is also the risk that the user absent-mindedly takes off his shirt and thus also the tag.

Truly wearable antennas should only utilise normal textile materials, conductive threads, and perhaps flexible silicone or plastic slabs and coatings. The dielectric constant of textiles ranges from 1 to 1.7, whereas for silicone it is as high as 12. Coating or waterproof laminates like Gore-Tex can protect the IC as well as the metallic layer in washing. The antenna should be as flexible as possible, and its performance should also be tested when it is bent or otherwise deformed.

We believe that conventional textile and electronics can be integrated, first in the form of separate badges sewn onto a finished garment. Later on, electronics will be integrated into the textile as a regular part of the cutting and sewing process.

Based on the application requirements, a wearable tag designer can decide the desired read range or realised gain, and the antenna–body spacing. Hospital applications are often satisfied with a relatively small read range. If the patient is to be identified at bedside, half a meter could be enough. If necessary, the antenna can be off-tuned in free space and with too large an input impedance, which will then be compensated by the body effects.

The body affects antennas similarly to a metallic plate. The forward gain of electric antennas such as dipoles decreases comparably to $\sin(2\pi \times \text{distance/wavelength})$ [21]. On the contrary, the gain of magnetic antennas is comparable to the cosine, implying that the antennas benefit from nearly touching the body. Magnetic antennas in the sense of [21] are however not low profile, but for example loops perpendicular to the body.

The presence of the dielectric body lowers the resonant frequency of antennas, especially those with no shielding between the user and the antenna. This detuning depends on the spacing between the antenna and the user, but when UHF frequencies are considered, not on the body posture. Operating frequency and impedance are also quite insensitive to the location of the antenna on the body.

Loss resistance increases and radiation resistance decreases when an antenna is brought near a human. Mutual capacitance between the antenna and the body causes energy to be stored in the electric field, overriding the inductance that is often wanted in the input impedance. The input resistance and reactance can decrease by one-half as judged by experiments [9], [13].

If possible, the reactive near-field should be spatially limited, for example in a slot between two elements. This is used in an inverted-F antenna with the ground plane in the same layer as the F [19]: there is a strong electric field between the F and the ground, in a small slot. The meandered dipole tags presented in [7] and Sec. IV exhibit strong electric fields between the meandered parts, but the fields decay rapidly compared to a half-wave dipole.

Small antennas usually exhibit a large Q value, meaning a large reactive near-field strength. Thus the impedance changes very easily when the body enters the near-field. Detuning is especially harmful since a large Q also means a narrow bandwidth. This could be helped if the antenna was placed over a ground plane, but that basically means increasing the antenna size.

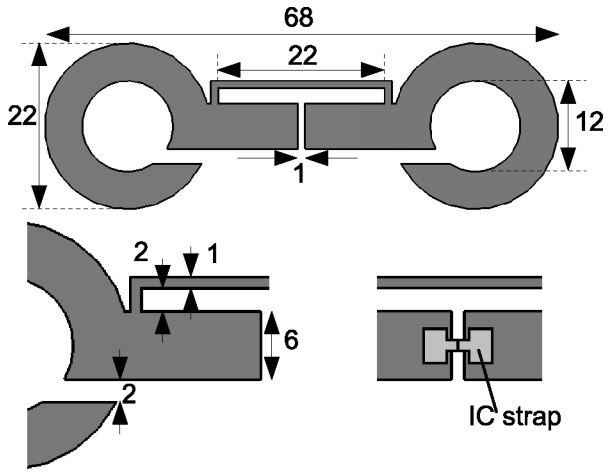

Fig. 1. The proposed tag antenna dimensions and two close-up views. The structure is completely in one layer, and rests on any fabric substrate available. The IC is located at the centre of the strap.

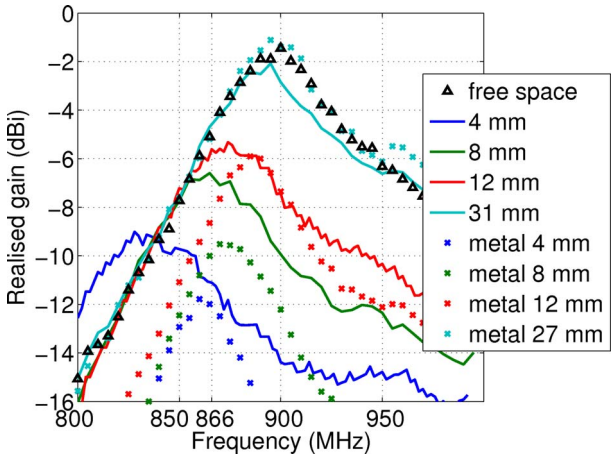

Fig. 2. Realised gain of the tag: in free space, worn on upper arm with various antenna–body spacings, and on metal with various spacings. The tag will be used at 866 MHz. Note for monochrome prints: the peaks from left to right correspond to the legend entries from top to down.

It is worth noting that if an antenna is designed to be used on a human body, this does not guarantee operation on metal, or vice versa!

IV. Shirt Collar Tag Antenna

As an example of an RFID tag designed for integration into clothing, a shirt collar tag is presented. The structure has previously been discussed in [13]. The small one-layer design, 68 mm by 22 mm, can easily be integrated on the collar or the button catch of a dress shirt. The tag is passive, that is, it contains no internal power source. The tag is designed for the Alien H3 strap, the impedance of which is (16-j150) Ω at 866 MHz [22].

The dimensions of this meandered dipole antenna are presented in Fig. 1. The one-layer design can easily be integrated into clothing. Because there is no ground plane, the antenna has to be separated from the body by at least 5 mm—a separation easily realised in clothing. Normal fabric (ε_r = 1 to 1.5) can be used as the substrate. Note that [13] erroneously gives L_t = 12 mm for the T-match length, while the correct value 22 mm is given here.

The operating frequency is mainly set by the total length of the antenna, including the length of the ring sections. The T-match (the parallel thin line) controls the inductance: the longer the T-match, the larger the inductance. Wider metal strips make the tag more broadband. This antenna has been deliberately designed off-tuned in free space, so that detuning by dielectric loading would bring the operating frequency to 866 MHz.

Close to the body, both the resonant frequency and impedance of the antenna decrease. Dielectric loading decreases the operating frequency. On the other hand, the decrease in impedance acts in the opposite way: the frequency of the best impedance matching increases. This is due to the fact that the antenna is matched to a complex and non-constant impedance. The two combined, the operating frequency of the tag decreases only slightly.

The tag antenna is designed to operate at a 1-cm spacing from the body. However, when the antenna is attached to loose clothing, the spacing may vary from 0.5 to 5 cm, or even more. Such a variation can completely detune some antenna designs. The behaviour of the tag antenna was measured with spacings 4 to 60 mm from the body, as well as in free space. It is worth noting that the smallest spacing is only 1 percent of the free-space wavelength.

The antenna was seen to work well with any spacing greater than 1 cm from the body, and sufficiently well even closer to the body. Fig. 2 shows the realised gain when the tag is placed at various distances from the body. Despite detuning and absorption, the antenna performance at 866 MHz is quite stable. There is no need to thicken the clothes for the antenna to work properly.

Varying the tag position on the body causes a ±2 dB variation in realised gain. Tag position has no effect on the frequency of best matching, that is, on the antenna impedance.

The measured radiation pattern with the tag worn on body is presented in Fig. 3. Because of inevitable and strong shadowing by the body, the tag can only be read from one hemisphere. The 3-dB beamwidth in the H-plane (vertical polarization, tag mounted on torso) is greater than 180°.

The performance of the tag was also measured near a metallic plate. From Fig. 2 we see that metal causes less detuning than the body. There is no dielectric loading that would bring the operating frequency further down. Metal apparently decreases input impedance more than the body, resulting in severe mismatching. The tag is somewhat applicable to identifying metallic objects, but the performance near metal is poor.

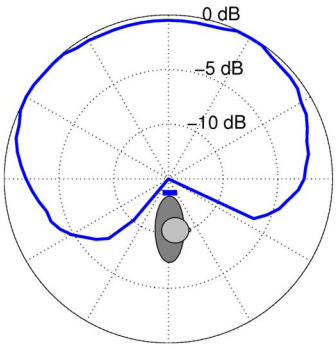

Fig. 3. Measured normalised H-plane radiation pattern of the tag antenna worn on the upper arm, with 8 mm spacing between antenna and body. In the figure, the wearer faces right and the antenna is on the upwards pointing arm.

V. Conclusion

In this paper, we presented a literature review of bodyworn RFID tags and analyzed different tag antenna design approaches.

Bodyworn UHF RFID tags have been used in many hospital applications for person identification. Even commercial wristband tags are available. Wristband antennas can be used in person monitoring, as well as clothing antennas. Wristband antennas are an easier solution, but textile integrated antennas will eventually become practical.

Most bodyworn antennas use a ground plane to prevent the user's body from absorbing power and affecting the input impedance. Research on one-layer antennas has also been conducted. Realised gains ranging from –10 to +5 dBi have been reported. The choice between an antenna with or without ground plane can be made based on the requirements of a specific application.

As an example, a wearable tag antenna with dimensions 68 mm by 22 mm was presented. The body effect on tags was illustrated using this shirt collar tag. Body lowers the input impedance, decreases the resonant frequency, and reduces the radiation efficiency. The effects can be compensated by proper tag design.

Bodyworn tags are a challenging RFID application. Design of bodyworn tag antennas requires knowledge of the effects of human body on the functioning of different antenna types. Based on this knowledge, the most suitable tag antenna type for the specific application can be chosen and further developed.

Acknowledgment

Tiiti Kellomäki's work was funded by the Graduate School in Electronics, Telecommunications and Automation (GETA). Leena Ukkonen was funded by the Academy of Finland and the Finnish Funding Agency for Technology and Innovation.

References

[1] A. Lahtela, "A short overview of the RFID technology in healthcare," in *4th Int. Conf. Systems and Networks Communications*, 2009.

[2] S.-W. Wang, W.-H. Chen, C.-S. Ong, L. Liu, and Y.-W. Chuang, "RFID application in hospitals: A case study on a demonstration RFID project in a Taiwan hospital," in *Proc. 39th Hawaii Int. Conf. System Sciences, vol. 8*, 2006, p. 184a.

[3] F. Wu, F. Kuo, and L.-W. Liu, "The application of RFID on drug safety of inpatient nursing healthcare," in *ICEC 05: Proc. 7th Int. Conf. Electronic commerce*, New York, NY, 2005, pp. 85–92.

[4] G. Marrocco, "RFID antennas for the UHF remote monitoring of human subjects," *IEEE Trans. Antennas Propagat.*, vol. 55, pp. 1862–1870, June 2007.

[5] C. Occhiuzzi and G. Marrocco, "RFID detection of human body movements," in *Proc. 39th European Microwave Conf.*, 2009, pp. 17–20.

[6] C. Occhiuzzi, S. Cippitelli, and G. Marrocco, "Modeling, design, and experimentation of wearable RFID sensor tag," *IEEE Trans. Antennas Propagat.*, vol. 58, pp. 2490–2498, Aug. 2010.

[7] M. Svanda and M. Polivka, "Dualband wearable UHF RFID antenna," in *Proc. European Conf. on Antennas and Propagation*, Edinburgh, UK, Nov. 2007.

[8] M. Švanda and M. Polívka, "Two novel extremely low-profile slot-coupled two-element patch antennas for UHF RFID of people," *Microwave Opt. Technol. Lett.*, vol. 52, pp. 249–252, Feb. 2010.

[9] ——, "Extremely low profile UHF RFID tag antennas for identification of people," in *Proc. European Conf. on Antennas and Propagation*, Barcelona, Spain, Apr. 2010.

[10] ——, "Novel dual-loop antenna placed over patch array surface for UHF RFID of dielectric and metallic objects," *Microwave Opt. Technol. Lett.*, vol. 51, pp. 709–713, Mar. 2009.

[11] H. Rajagopalan and Y. Rahmat-Samii, "Conformal RFID antenna design suitable for human monitoring and metallic platforms," in *Proc. European Conf. on Antennas and Propagation*, Barcelona, Spain, Apr. 2010.

[12] M. Takahashi, T. Nakajima, K. Saito, and K. Ito, "Characteristics of wristband type RFID antenna," in *Proc. European Conf. on Antennas and Propagation*, Barcelona, Spain, Apr. 2010.

[13] T. Kellomäki, T. Björninen, L. Ukkonen, and L. Sydänheimo, "Shirt collar tag for wearable UHF RFID systems," in *Proc. European Conf. on Antennas and Propagation*, Barcelona, Spain, Apr. 2010.

[14] M. Polívka, M. Švanda, P. Hudec, and S. Zvánovec, "UHF RF identification of people in indoor and open areas," *IEEE Trans. Microwave Theory Tech.*, vol. 57, pp. 1341–1347, May 2009.

[15] Daily RFID. (2010, Aug.). [Online]. Available: http://www.rfid-in-china.com/2008-11-30/products_detail_2187.html, http://www.rfid-in-china.com/2008-08-20/products_detail_1992.html

[16] J. C. G. Matthews, B. P. Pirollo, A. J. Tyler, and G. Pettitt, "Wideband body wearable antennas," in *IET Seminar on Wideband, Multiband Arrays for Defence or Civil Applications*, Mar. 2008.

[17] T. Kellomaki, J. Heikkinen, and M. Kivikoski, "Wearable antennas for FM reception," in *Proc. European Conf. on Antennas and Propagation*, Nice, France, Nov. 2006.

[18] Z. H. Hu, M. Gallo, Q. Bai, Y. I. Nechayev, P. S. Hall, and M. Bozzetti, "Measurements and simulations for on-body antenna design and propagation studies," in *Proc. European Conf. on Antennas and Propagation*, Edinburgh, UK, Nov. 2007.

[19] T. Kellomaki, J. Heikkinen, and M. Kivikoski, "One-layer GPS antennas perform well near a human body," in *Proc. European Conf. on Antennas and Propagation*, Edinburgh, UK, Nov. 2007.

[20] T. Fukasawa, M. Ohtsuka, Y. Sunahara, and S. Makino, "A wide bandwidth monopole antenna using a human body as a ground plane," in *Proc. IEEE Antennas and Propagation Society Int. Symp.*, 2004.

[21] W. Scanlon and N. Evans, "Antennas and propagation for telemedicine and telecare: on-body systems," in *Antennas and propagation for body-centric wireless communications*, P. S. Hall and Y. Hao, Eds. Artech House, 2006, ch. 8, p. 220.

[22] Alien Technology. (2009, Dec.) Higgs-3 product overview. [Online]. Available: http://www.alientechnology.com/docs/products/DS_H3.pdf

Tampereen teknillinen yliopisto
PL 527
33101 Tampere

Tampere University of Technology
P.O.B. 527
FI-33101 Tampere, Finland

ISBN 978-952-15-2778-4
ISSN 1459-2045